bioRxiv preprint doi: https://doi.org/10.1101/2021.04.18.440372; this version posted September 29, 2021. The copyright holder for this preprint (which was not certified by peer review) is the author/funder, who has granted bioRxiv a license to display the preprint in perpetuity. It is made available under aCC-BY-NC-ND 4.0 International license.

Stabilisation of Antithetic Control via Molecular Buffering

Edward J. Hancock[1, 2] and Diego A. Oyarzún[3, 4]

[1)] *School of Mathematics and Statistics, The University of Sydney, NSW, 2006, Australia*

[2)] *Charles Perkins Centre, The University of Sydney, NSW, 2006, Australia*

[3)] *School of Informatics, The University of Edinburgh, United Kingdom*

[4)] *School of Biological Sciences, The University of Edinburgh, United Kingdom*

(Dated: 29 September 2021)

A key goal in synthetic biology is the construction of molecular circuits that robustly adapt to perturbations. Although many natural systems display perfect adaptation, whereby stationary molecular concentrations are insensitive to perturbations, its *de novo* engineering has proven elusive. The discovery of the antithetic control motif was a significant step toward a universal mechanism for engineering perfect adaptation. Antithetic control provides perfect adaptation in a wide range of systems, but it can lead to oscillatory dynamics due to loss of stability, and moreover, it can lose perfect adaptation in fast growing cultures. Here, we introduce an extended antithetic control motif that resolves these limitations. We show that molecular buffering, a widely conserved mechanism for homeostatic control in nature, stabilises oscillations and allows for near-perfect adaptation during rapid growth. We study multiple buffering topologies and compare their performance in terms of their stability and adaptation properties. We illustrate the benefits of our proposed strategy in exemplar models for biofuel production and growth rate control in bacterial cultures. Our results provide an improved circuit for robust control of biomolecular systems.

I. INTRODUCTION

Synthetic biology promises to revolutionise many sectors such as healthcare, chemical manufacture and materials engineering[7]. A number of such applications require precise control of biomolecular processes in face of environmental perturbations and process variability[22]. An important requirement in such control systems is *perfect adaptation*, a property whereby chemical concentrations remain insensitive to perturbations[20,23]. The molecular mechanisms that can produce perfect adaptation has been extensively studied in natural systems[3,14,20,23]. In these systems, perfect adaptation can be produced by a range of feedforward and feedback mechanisms[3,20]. Such natural systems have been shaped by evolutionary processes, but it remains unclear if they are sufficiently robust and tuneable for *de novo* engineering of perfect adaptation in synthetic circuits.

One approach to engineer perfect adaptation relies on the use of feedback control. As illustrated in Figure 1A, this strategy requires circuits that sense the output and act upon the inputs of a biomolecular process. The groundbreaking work by Briat and colleagues[1,4] identified *antithetic feedback* as a promising candidate for engineering perfect adaptation in living systems. Antithetic control involves a feedback mechanism with two molecular components that sequester and annihilate each other (see Figure 1B). It enables a system output to robustly follow an input signal and remain insensitive to various types of perturbations, akin to what integral feedback achieves in classic control engineering strategies[2].

The original antithetic control motif, however, has two weaknesses that can limit its applicability: it is often not effective when cells are growing rapidly, and the feedback mechanism can cause unwanted oscillations under a range of conditions[27]. Specifically, dilution effects caused by cell growth cause "leaky integration" - so called because integration is a form of memory and dilution causes that memory to leak over time[29]. This prevents perfect adaptation from occurring during rapid growth. Although in some motif configurations, the loss of perfect adaptation can be partly mitigated with a stronger feedback[29], in general the use of strong feedback results in the loss of stability and undesirable oscillations[27]. Such oscillations can be stabilised in specific motifs[15], and in more general cases the combination of antithetic control with classic Proportional-Integral-Derivative (PID) control has been shown to improve temporal regulation[5,9]. Yet to date, there is no general strategy to avoid oscillations and prevent the loss of adaptation during rapid growth.

Here we propose an extended antithetic control system that resolves the above limitations. We show that the addition of molecular buffers improves stability and suppresses undesirable oscillations, and moreover it can allow for near-perfect adaptation in fast growth regimes. Molecular buffering is a widespread regulatory mechanism in nature (e.g. ATP, calcium & pH buffers[17,21,32]) that has received modest attention in the literature as compared to other regulatory mechanisms. Recent work found that the combination of buffering and feedback is often critical for robust regulation[16,17]. Buffering has the ability to attenuate fast disturbances and stabilise feedback control[17], and can also be essential for the control of multiple coupled outputs[18]. Here, we first show that a number of buffering topologies can stabilise the original antithetic control system and preserve perfect adaptation. We then show that buffering can allow in-

bioRxiv preprint doi: https://doi.org/10.1101/2021.04.18.440372; this version posted September 29, 2021. The copyright holder for this preprint (which was not certified by peer review) is the author/funder, who has granted bioRxiv a license to display the preprint in perpetuity. It is made available under aCC-BY-NC-ND 4.0 International license.

creased feedback strength or 'gain' without producing oscillations, which in turn reduces the steady state error even in fast growth conditions. To illustrate the utility of this new antithetic control strategy, we examine two case studies that involve the control of biofuel production and growth rate in microbes.

II. BACKGROUND

A. Perfect adaptation and antithetic control

Antithetic control employs a feedback mechanism with two molecular components that sequester and annihilate each other (see Figure 1B). In its most basic formulation, an antithetic system contains a two-species molecular process to be controlled, and a two-species antithetic controller. The two species of the controlled process (x_1 and x_2) can represent a variety of molecular systems, including e.g. mRNA and protein as in Figure 1A. The goal of the antithetic control system is to desensitise the steady state concentration of x_2 with respect to external perturbations. Such perturbations include, for example, insults of molecular species coming from upstream or downstream processes, changes in cellular growth conditions, or alterations to binding affinities between species.

In the absence of stochastic effects, the feedback system can be modelled by the ODEs:

$$\begin{aligned} \dot{x}_1 &= \theta_1 z_1 - \gamma_p x_1, \\ \dot{x}_2 &= k x_1 - \gamma_p x_2, \\ \dot{z}_1 &= \mu - \eta z_1 z_2 - \gamma_c z_1, \\ \dot{z}_2 &= \theta_2 x_2 - \eta z_1 z_2 - \gamma_c z_2, \end{aligned} \tag{1}$$

where z_1 and z_2 are the concentrations of species in the antithetic controller, and θ_1, k, and θ_2 are positive parameters representing first-order kinetic rate constants. The parameter μ describes a zero-order influx of controller species z_1, while η is a second-order kinetic rate constant. We further assume that molecular species are diluted by cellular growth, degraded by other molecular components, or consumed by downstream cellular processes, all of which we model as a first-order clearance with rate constant γ_p. The controller species z_1 and z_2, on the other hand, are assumed to be diluted by cellular growth with a rate constant γ_c.

In the absence of dilution effects ($\gamma_c = 0$), from the model in (1) we can write:

$$\dot{z}_1 - \dot{z}_2 = \mu - \theta_2 x_2,$$

which after integration becomes

$$z_1(t) - z_2(t) = \theta_2 \int_0^t \left(\frac{\mu}{\theta_2} - x_2(t') \right) dt'.$$

The above equation means that, if the system has a stable equilibrium, the steady state concentration of x_2 is

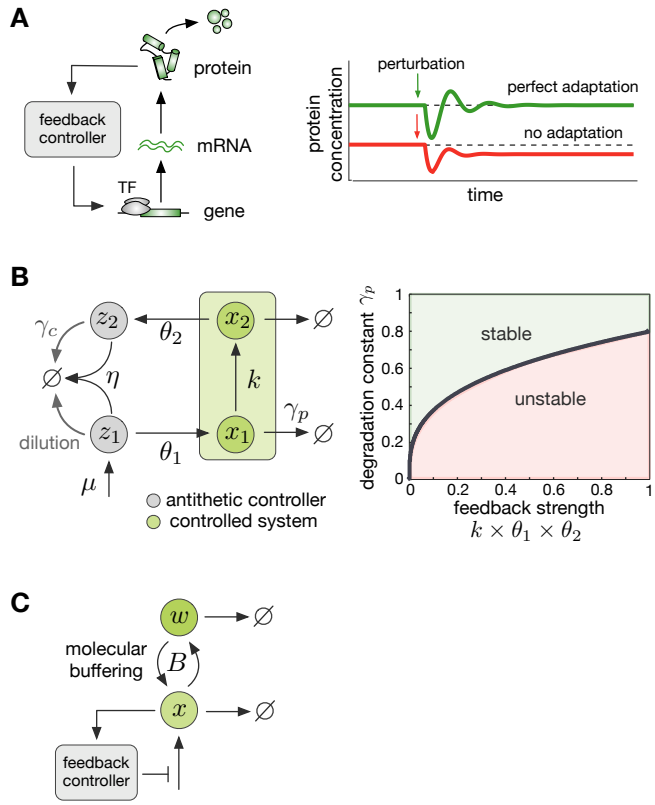

FIG. 1. Perfect adaptation and feedback control. **(A)** Schematic of a feedback system designed to achieve perfect adaptation in protein expression. Based on readouts of protein concentration, the controller modifies the activity of a transcription factor (TF). If the controller achieves perfect adaptation, steady state protein concentrations are robust to perturbations. **(B)** Left: the antithetic feedback controller, first proposed Briat *et al* in[4], can achieve perfect adaptation. In the presence of dilution ($\gamma_c \neq 0$), the antithetic controller does not achieve perfect adaptation. Right: conditions for stability in the case of a two-species system. The stability boundary is the condition in (2); the example was computed with fixed parameters $k = \theta_2 = \gamma_p = 1$. **(C)** In the example, molecular buffering provides a general mechanism to stabilize feedback control systems[17]. The buffer reversibly sequesters molecules of species x into an inactive form w.

$x_2 = \mu/\theta_2$, and hence independent of all model parameters except μ and θ_2. Therefore the antithetic control system displays perfect adaptation because the steady state of x_2 is robust to perturbations in parameters k, θ_1, θ_2 and η.

A caveat of antithetic feedback is that it can have a destabilising effect. When the controller species are not diluted ($\gamma_c = 0$), it can be shown that a parametric condition for stability is[27]:

$$\gamma_p^3 > \frac{k\theta_1\theta_2}{2}. \tag{2}$$

As shown by the stability diagram in Figure 1B, strong antithetic feedback can cause the system to lose perfect

bioRxiv preprint doi: https://doi.org/10.1101/2021.04.18.440372; this version posted September 29, 2021. The copyright holder for this preprint (which was not certified by peer review) is the author/funder, who has granted bioRxiv a license to display the preprint in perpetuity. It is made available under aCC-BY-NC-ND 4.0 International license.

adaptation and display oscillatory dynamics. Moreover, in the presence of dilution of the controller species ($\gamma_c > 0$), the antithetic controller is unable to produce perfect adaptation[27]. The adaptation error can be reduced with stronger feedback, for example by increasing the rate constants θ_1, k, or θ_2. Yet as mentioned above, stronger feedback can cause unwanted oscillations[27]. These caveats are particularly relevant in bioproduction applications that require fast culture growth[10,35].

B. Molecular buffering

Buffering is the use of molecular reservoirs to maintain the concentration of chemical species[17]. It is a widespread regulatory mechanism found across all domains of life, with common examples including pH, ATP and calcium buffering[21,32]. Molecular buffering can have a number of regulatory roles[17,18], including acting as a stabilising mechanism for other molecular feedback systems[17].

To provide a background on buffering models, we consider the simple case of a chemical species (x) that is subject to feedback regulation, as shown in Figure 1C. A general model for such process is:

$$\begin{aligned} \dot{x} &= \underbrace{p(x)}_{\substack{\text{production}\\ \text{with feedback}}} - \underbrace{\gamma_x x}_{\text{removal}} + \underbrace{g_w(w) - g_x(x)}_{\text{buffering}}, \\ \dot{w} &= \underbrace{g_x(x) - g_w(w)}_{\text{buffering}} - \underbrace{\gamma_w w}_{\text{removal}}, \end{aligned} \tag{3}$$

where w is a molecular buffer for the regulated species x, and $p(x)$ is a feedback-regulated production rate of x. The parameters γ_x and γ_w are first-order clearance rate constants of x and w, respectively. The terms g_w and g_x describe the reversible binding of species x and the buffer w. The steady state $(\bar{x}, \bar{w})$ occurs when production matches degradation (i.e. $p(\bar{x}) = \gamma_x \bar{x} + \gamma_w \bar{w}$) and conversion from x to w matches the reverse conversion plus removal (i.e. $g_w(\bar{w}) = g_x(\bar{x}) + \gamma_w \bar{w}$).

It can be shown that after linearisation and assuming that the buffering reactions rapidly reach quasi-equilibrium, the model (3) can be simplified to (see SI1):

$$(1+B)\Delta\dot{x} = -\underbrace{h\Delta x}_{\text{feedback}} - \underbrace{(\gamma_x + B\gamma_w)\Delta x}_{\text{removal}} \tag{4}$$

where $\Delta x = x - \bar{x}$ is the deviation of x from the steady state $\bar{x}$, $h = -\partial p/\partial x$ is the linearised feedback gain and B is the buffer equilibrium ratio:

$$B = \frac{\Delta w}{\Delta x}, \tag{5}$$

where $\Delta w = w - \bar{w}$ is the deviation of w from the steady state $\bar{w}$. The parameter B is buffer-specific and quantifies the change in the concentration of a regulated species (x) to the change in the concentration of a buffering species (w) when the buffering reactions are at quasi-equilibrium[17,18].

From (4) we observe that buffering slows down the rate of change of the output x by a factor of $(1+B)$. It can be shown[17] that this slowed rate generally helps to attenuate fast disturbances and stabilise unwanted oscillations (see SI1). More generally, the stabilisation effect of buffering results from two properties. First, the buffering reactions counteract changes to a target molecular species by acting directly on the species and not via indirect or complex feedback loops[16,17]. Second, buffering can be shown to be mathematically equivalent to popular feedback strategies known to have useful stabilisation properties[2]. In particular, rapid buffering without degradation ($\gamma_w = 0$) is equivalent to negative derivative feedback[17]:

$$\Delta\dot{x} = \underbrace{-B\Delta\dot{x}}_{\substack{\text{derivative}\\ \text{feedback}}} - \underbrace{h\Delta x}_{\substack{\text{proportional}\\ \text{feedback}}} - \gamma_x \Delta x,$$

where the buffer equilibrium ratio B corresponds to the derivative feedback gain commonly employed in control engineering. Likewise, the general case of non-rapid buffering with degradation is mathematically equivalent to the so-called "lead" controller employed in control engineering[16]. In the next section, we study the ability of buffering to stabilise oscillations in antithetic control systems.

III. BUFFERING CAN STABILISE ANTITHETIC INTEGRAL FEEDBACK

In this section we study a modified version of the antithetic feedback controller that includes buffering of its molecular components. We consider a number of architectures (Figure 2A) and identify those that suppress oscillations caused by the instability illustrated in Figure 1B. We show that rapid buffering without degradation does not improve stability, while non-rapid buffering and rapid buffering with degradation are highly effective stabilisers.

A. Rapid Buffering

To study the impact of buffering on the antithetic controller, we consider mathematical models for the topologies in Figure 2A, in which species z_1, z_2, and x_2 are buffered by molecules w_1, w_2, and w_x, respectively. For simplicity, we use linear buffering reaction rates in order to focus on the nonlinearity due to the mutual annihilation of controller species z_1 and z_2[9]. As in Eq. (4), we assume that the buffers rapidly reach quasi-equilibrium

bioRxiv preprint doi: https://doi.org/10.1101/2021.04.18.440372; this version posted September 29, 2021. The copyright holder for this preprint (which was not certified by peer review) is the author/funder, who has granted bioRxiv a license to display the preprint in perpetuity. It is made available under aCC-BY-NC-ND 4.0 International license.

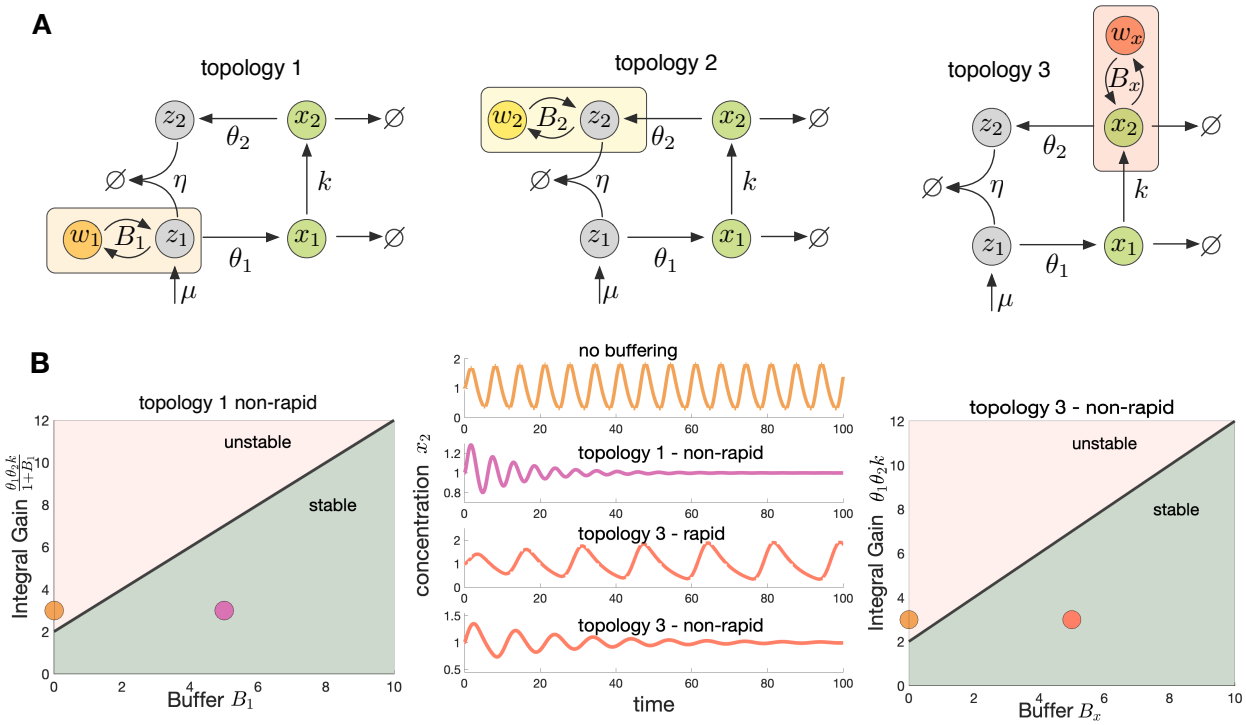

FIG. 2. **Buffering stabilizes antithetic feedback . (A)** Schematics of three buffered antithetic systems, without dilution ($\gamma_c = 0$); each topology includes buffering a specific molecular species. **(B)** Stability diagram for buffered topologies 1 and 3. The stability boundary on the left corresponds to the condition in (10) and the boundary on the right to (11). The time courses show simulations of the output species (x_2) for different topologies. Parameters are $\mu = 1$, $\theta_1 = 3$, $\theta_2 = 1$, $\gamma_p = 1$, $\eta = 100$ and $k = 1$. With topology 1, parameters are $B_1 = 5$, $\theta_1 = 18$ and $b_{wz} = 1$ (non-rapid). With topology 3, parameters are $B_x = 5$, $\theta_1 = 3$, $b_{wx} = 1$ (non-rapid) and $b_{wx} = 20$ (rapid).

to obtain the following extended model (see SI2.1):

$$\begin{aligned} \dot{x}_1 &= \theta_1 z_1 - \gamma_p x_1 \\ (1+B_x)\dot{x}_2 &= k x_1 - (\gamma_p + B_x \gamma_x) x_2 \\ (1+B_1)\dot{z}_1 &= \mu - \eta z_1 z_2 \\ (1+B_2)\dot{z}_2 &= \theta_2 x_2 - \eta z_1 z_2, \end{aligned} \tag{6}$$

where B_x, B_1 and B_2 are the equilibrium ratios for each buffer, and γ_x represents the degradation rate of buffer w_x. The extended model in (6) reduces to the original antithetic system in (1) if $B_x = 0$, $B_1 = 0$ and $B_2 = 0$.

In the extended antithetic controller with rapid buffering, the parameters $(B_x, B_1, B_2, \gamma_x)$ are additional tuning knobs that can be used to shape the closed-loop dynamics. In Figure 2A we show the three considered buffering architectures.

We first show that buffered antithetic feedback preserves perfect adaptation. From (6) we write

$$(1+B_1)\dot{z}_1 - (1+B_2)\dot{z}_2 = \mu - \theta_2 x_2,$$

which after integrating becomes:

$$(1+B_1)z_1(t) - (1+B_2)z_2(t) = \theta_2 \int_0^t \left(\frac{\mu}{\theta_2} - x_2(t') \right) dt'.$$

The above integral ensures that if the system is stable then the steady state of x_2 is $x_2 = \mu/\theta_2$, hence independent of all parameters except μ and θ_2. The steady state of x_2 is thus robust to perturbations in the original parameters k, θ_1, θ_2, and η, as well as the additional parameters introduced by the buffering mechanism B_x, B_1, B_2, and γ_x. This means that the buffered antithetic feedback displays perfect adaptation as in the original formulation in Eq. (1).

Assuming strong integral binding (large η) then z_2 is small and so with rapid buffering we have the antithetic input in to the controlled system (see Figure 1B and SI4.1)

$$\theta_1 z_1 = \underbrace{\frac{\theta_1 \theta_2}{(1+B_1)}}_{\substack{\text{integral} \\ \text{feedback gain}}} \underbrace{\int_0^t \left(\frac{\mu}{\theta_2} - x_2(t') \right) dt'}_{\substack{\text{negative} \\ \text{integral feedback}}}, \tag{7}$$

where $\theta_1 z_1$ represents the control of x_1 production in (6) and we can observe that the integral gain is dependent upon B_1. This changes the gain because rapid buffers tend to slow down the dynamics of z_1 in (6) and for integral feedback the gain is inversely proportional to the time scale of z_1.

As shown by the stability condition in (2), the origi-

bioRxiv preprint doi: https://doi.org/10.1101/2021.04.18.440372; this version posted September 29, 2021. The copyright holder for this preprint (which was not certified by peer review) is the author/funder, who has granted bioRxiv a license to display the preprint in perpetuity. It is made available under aCC-BY-NC-ND 4.0 International license.

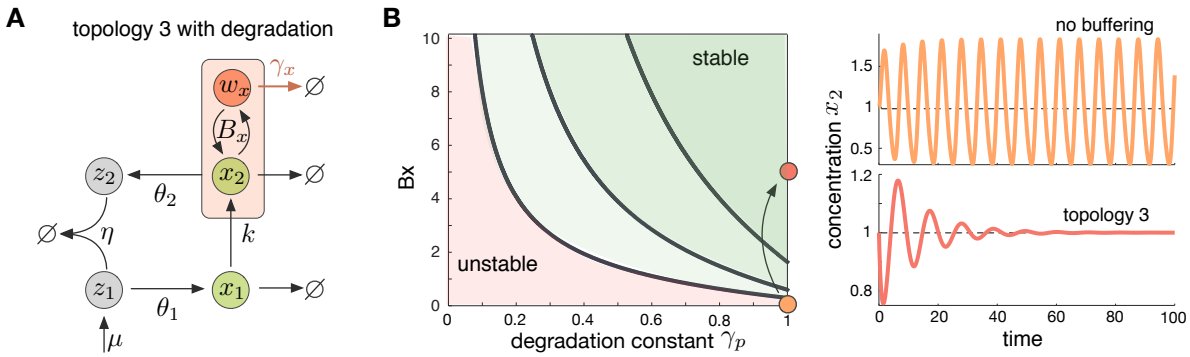

FIG. 3. **Stabilizing effect of topology 3 with degradation. (A)** We revisit topology 3 with degradation of the buffer with degradation rate constant γ_x. **(B)** Stability diagram for increasing values of the degradation rate constant $\gamma_x = \{0.5, 1, 2\}$; the stability boundary corresponds to the condition in (12). Time courses are simulations of the output species (x_2) for two representative cases. Parameter values are $\mu = 1$, $\theta_1 = 2$, $\theta_2 = 1$, $\gamma_p = 1$, $\eta = 100$ and $k = 1$. For the case of buffering $B_x = 20$ and $\gamma_x = 1$.

nal antithetic control system becomes oscillatory when the feedback gain is too strong or the degradation of x_1 and x_2 is too slow[27]. To analyse the stabilising role of buffering, we first consider the system in the absence of degradation of the w_x buffer (i. e. $\gamma_x = 0$). Assuming rapid buffering and strong integral binding (large η), we find that the system is stable when (see SI2.1):

$$\gamma_p^3 > \underbrace{\frac{\theta_1\theta_2 k}{(1+B_1)}}_{\substack{\text{integral}\\ \text{feedback}\\ \text{gain}}} \underbrace{\frac{1+B_x}{2+B_x}}_{\substack{\text{stabilisation}\\ \text{effect}}} . \tag{8}$$

From the condition (8) we observe that increasing B_1 reduces the lower bound for γ_p and improves stability. However, from (7) we also observe that such effect is equivalent to a reduction in the feedback gain by a factor $(1 + B_1)$. Therefore a similar effect can be obtained simply by changing the gain $\theta_1\theta_2$ without the additional complexity of buffering z_1. Moreover, the condition in (8) also shows that rapid buffering of z_2 has no impact on stability, because the stability boundary is independent of B_2, whereas rapid buffering of x_2 can destabilise the system and produce oscillations, because the stability boundary becomes more stringent for large B_x.

B. Non-Rapid Buffering in Topologies 1 and 3

We next sought to determine the stabilisation properties of non-rapid buffering, i. e. implemented with buffers that do not satisfy the rapid equilibrium assumption. We show that non-rapid buffering can be a highly effective stabilisation strategy for Topologies 1 and 3, and this stabilisation effect is greater than the effect attributed to the change in feedback gain alone.

To model the effect of non-rapid buffering, we replace the model for $\dot{x}_2$ and $\dot{z}_1$ in (6) by

$$\begin{aligned} \dot{x}_2 &= kx_1 - \gamma_p x_2 - b_x x_2 + b_{wx} w_x \\ \dot{w}_x &= b_x x_2 - b_{wx} w_x \\ \dot{z}_1 &= \mu - \eta z_1 z_2 - b_z z_1 + b_{wz} w_z \\ \dot{w}_z &= b_z z_1 - b_{wz} w_z, \end{aligned} \tag{9}$$

and keep the models for $\dot{x}_1$ and $\dot{z}_2$ identical as in (6). Given that in the previous section we found that topology 2 does not alter stability, from here onward we set $B_2 = 0$. For topologies 1 and 3, the buffer equilibrium ratios (B_1, B_x) determine the concentration of the buffering species at equilibrium and the reverse reaction rate constants (b_{wz}, b_{wx}) determine the speed at which the buffers reach equilibrium. These four parameters can be regarded as tuning knobs for modifying the closed-loop dynamics, akin to the role of B_1 and B_x in the rapid buffering case of the previous section.

For Topology 1 (i.e. $b_x = b_{wx} = 0$) and assuming strong antithetic binding (large η), the stability condition is:

$$\gamma_p^3 > \underbrace{\frac{\theta_1\theta_2 k}{(1+B_1)}}_{\substack{\text{integral}\\ \text{feedback}\\ \text{gain}}} \underbrace{\frac{1}{(2+B_1)}}_{\substack{\text{stabilisation}\\ \text{effect}}} \tag{10}$$

whereas for Topology 3 (i.e. $b_z = b_{wz} = 0$) the stability condition becomes:

$$\gamma_p^3 > \frac{\theta_1\theta_2 k}{2+B_x}. \tag{11}$$

To derive both conditions (10)–(11) we have assumed for simplicity that $b_{wz} = \gamma_p$ and $b_{wx} = \gamma_p$, respectively. The general stability condition for other values of b_{wz} and b_{wx} can be found in SI2.2–2.3.

As shown by the stability diagrams in Figure 2, the conditions in (10)–(11) reveal that increases to the buffering ratios B_1 and B_x relax the upper bound for integral

bioRxiv preprint doi: https://doi.org/10.1101/2021.04.18.440372; this version posted September 29, 2021. The copyright holder for this preprint (which was not certified by peer review) is the author/funder, who has granted bioRxiv a license to display the preprint in perpetuity. It is made available under aCC-BY-NC-ND 4.0 International license.

feedback gain and thus improve stability; this suggests that non-rapid buffering of both z_1 and x_2 provide an effective route to suppress oscillations. As shown in SI2.2–2.3, this stabilisation effect is stronger for $b_{wz} > \gamma_p$ in Topology 1 and $b_{wx} < \gamma_p$ in Topology 3.

C. Rapid Buffering with Degradation

So far we have assumed that the buffers are not subject to degradation. To establish the impact of buffer degradation on stability, here we show that buffer degradation in Topology 3 can suppress oscillations and preserve perfect adaptation; this new topology is shown in Figure 3A. Under the same assumptions as condition (8) (rapid buffering and strong binding rate constant η), the stability conditions are (see SI2.1):

$$\gamma_p^3 > \frac{\theta_1\theta_2 k}{2+\left(1+\frac{\gamma_x}{\gamma_p}\right)B_x}\frac{1+B_x}{1+\frac{\gamma_x}{\gamma_p}B_x}. \tag{12}$$

Condition (12) reduces to the one in (8) if $\gamma_x = 0$ and there is no buffering of z_1, i.e. $B_1 = 0$.

As shown by the stability diagram in Figure 3B, topology 3 with degradation provides an effective solution to stabilise the closed-loop. The condition in (12) suggests that the ratio γ_x/γ_p has a key role in stability. Buffers with shorter half-lives (larger γ_x) tend to almost completely remove the instability, even for low buffer equilibrium ratios B_x. As we show in SI2.4, under the condition $\gamma_x/\gamma_p > 1/3$, increases in B_x tend to stabilise the closed-loop. This includes the important case where both x_2 and its buffer are degraded at the same rate, i.e. $\gamma_x = \gamma_p$. For large values of B_x, the stabilisation effect is even stronger and becomes independent of the half-life of w_x. We found a similar stabilisation effect in systems with x_1 buffering that include degradation of the buffer (see SI2.5).

IV. ACHIEVING NEAR PERFECT ADAPTATION IN FAST GROWTH

It is well-known that dilution by cell growth can disrupt perfect adaptation in the original antithetic control system[1]. Thus here we explore the impact of dilution in the proposed topologies with molecular buffering. To study the effect of dilution, we modify (9) to include dilution terms for the control species z_1 and z_2, as well as the buffer for z_1:

$$\begin{aligned}
\dot{x}_1 &= \theta_1 z_1 - \gamma_p x_1\\
\dot{x}_2 &= k x_1 - \gamma_p x_2 - b_x x_2 + b_{wx} w_x\\
\dot{w}_x &= b_x x_2 - b_{wx} w_x - \gamma_x w_x\\
\dot{z}_1 &= \mu - \eta z_1 z_2 - \gamma_c z_1 - b_z z_1 + b_{wz} w_z\\
\dot{w}_z &= b_z z_1 - b_{wz} w_z - \gamma_c w_z\\
\dot{z}_2 &= \theta_2 x_2 - \eta z_1 z_2 - \gamma_c z_2.
\end{aligned} \tag{13}$$

where γ_c represents the dilution rate constant of the control species z_1, z_2 and buffer species at z_1. We assume that dilution of x_1 and x_2 and the buffer at x_2 can be lumped into their first-order degradation rates. As in the previous section, the model (13) can be further simplified for the rapid buffering case (see SI3.1).

A. Topology 3 with dilution

We found that buffering at x_2 can reduce steady state error by enabling an increase to the feedback gain without causing oscillations. For the case of dilution with a single buffer at x_2, we set $b_z = b_{wz} = 0$ in (13). The resulting steady state is (see SI3.1):

$$x_2 = \left(\frac{\mu}{\theta_2}\right) \times \left(\frac{1}{1+\Omega_x^{-1}}\right), \tag{14}$$

where

$$\Omega_x = \frac{\alpha}{\gamma_c\left(1+B_x\frac{\gamma_x}{\gamma_p}\right)} \tag{15}$$

and $\alpha = \theta_1\theta_2 k/\gamma_p^2$. The second term on the right hand side of (14) is always smaller than unity. Therefore the steady state of the output is $x_2 < \mu/\theta_2$ and the system loses perfect adaptation. Moreover, the deviation of the steady state of x_2 from the reference point μ/θ_2 is (see SI3.1):

$$\frac{x_{2n} - x_2}{x_{2n}} = \frac{1}{1+\Omega_x} \tag{16}$$

where $x_{2n} = \mu/\theta_2$ is the reference input. Increases to B_x, γ_c or γ_x in (16) thus amplify the steady state error, while increases to the feedback strength $k\theta_1\theta_2$ brings the system closer to perfect adaptation.

We first obtained conditions for stability in Topology 3 with dilution and non-rapid buffering (see SI3.2). Setting $\gamma_x = \gamma_c$ in (13) we get:

$$\Omega_x < \frac{\gamma_p}{\gamma_c}\frac{2+B_x}{1+B_x\frac{\gamma_c}{\gamma_p}}\left(\left(1+\frac{\gamma_c}{\gamma_p}\right)^2 + 2B_x\frac{\gamma_c}{\gamma_p}\right), \tag{17}$$

where for simplicity we have set $b_{wx} = \gamma_p - \gamma_c$. The stability conditions for general choices of b_w can be found in SI3.2.

Taken together, the relations in (16)–(17) define an upper bound for the best possible steady state error. Specifically, in (16) we see that stronger feedback gain can increase Ω_x and so reduce the steady state error. Buffering of x_2 tends to stabilise the oscillations and, at the same time, allows the steady state error to be reduced by stronger feedback gain, without the risk of instability observed in the original antithetic mechanism. This phenomenon is illustrated in Figure 4A, which shows the stability condition (17).

bioRxiv preprint doi: https://doi.org/10.1101/2021.04.18.440372; this version posted September 29, 2021. The copyright holder for this preprint (which was not certified by peer review) is the author/funder, who has granted bioRxiv a license to display the preprint in perpetuity. It is made available under aCC-BY-NC-ND 4.0 International license.

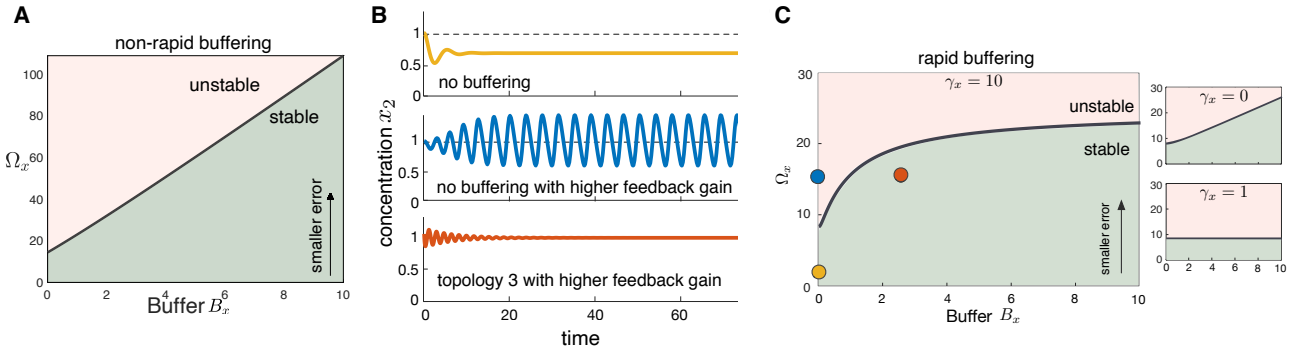

FIG. 4. **Adaptation in Topology 3 with dilution.** **(A)** Stability condition in (17) for non-rapid buffering with rate constants $\gamma_c/\gamma_p = 0.2$. **(B)** Simulation with varying feedback gain $\theta_1 = \{2, 15, 400\}$ (from top) and buffer constant ($B_x = \{0, 2.5\}$). In all simulations the model parameters are $k = 1$, $\theta_2 = 1$, and $\gamma_p = 1$, $\gamma_c = 1$ and $\gamma_x = 10$. **(C)** Stability condition in (18) for rapid buffering with rate constants $\gamma_c = 1$ and $\gamma_p = 1$.

In the case of rapid buffering, the condition for stability becomes (see SI3.1):

$$\begin{aligned} \Omega_x &< \left(1 + \frac{\gamma_c}{\gamma_p}\right)(1 + A)\left(\frac{\gamma_p}{\gamma_c} + A^{-1}\right) \\ A &= \frac{1 + B_x \frac{\gamma_x}{\gamma_p}}{1 + B_x}. \end{aligned} \tag{18}$$

As in the non-rapid case, the relations in (16) and (18) define an upper bound for the best possible steady state error. This phenomenon is illustrated in Figure 4C, which shows the stability condition (18). Notably, we observe that increasing B_x improves stability only in regions for low and high values of γ_x, and not intermediate values. Figure 4B shows simulations of the stabilising effect of molecular buffering for the case of $\gamma_x = 10$, which enables a decrease of steady state error by means of stronger feedback gain. We also found that topology 3 improves stability even without buffer degradation ($\gamma_x = 0$), which can be observed in Figure 4B. This improvement differs from the case when there is no dilution in (8).

B. Topology 1 with dilution

We found that non-rapid buffering at z_1 can similarly reduce steady state error via increases to the feedback gain. To examine this result in detail, we set $B_x = 0$ in (13) and compute the resulting steady state (see SI3.4):

$$x_2 = \left(\frac{\mu}{\theta_2}\right) \times \left(\frac{1}{1 + \Omega_1^{-1}}\right) \tag{19}$$

where

$$\Omega_1 = \frac{\alpha}{\gamma_c(1 + B_1)} \tag{20}$$

and $\alpha = \theta_1\theta_2 k/\gamma_p^2$. As in the previous case, the steady state satisfies $x_2 < \mu/\theta_2$ and thus the system loses perfect adaptation (see Figure 5). Moreover, in this case the steady state error is (see SI3.4):

$$\frac{x_{2n} - x_2}{x_{2n}} = \frac{1}{1 + \Omega_1} \tag{21}$$

where $x_{2n} = \mu/\theta_2$ is the reference input. Increasing B_1 or γ_c in (21) increases the steady state error, while increasing the feedback strength $k\theta_1\theta_2$ brings the system closer to perfect adaptation. If for simplicity we assume that $b_{wz} = \gamma_p - \gamma_c$, the condition for stability is (see SI3.5):

$$\Omega_1 < \frac{\gamma_p}{\gamma_c}\frac{(2 + B_1)}{(1 + B_1)}\left(1 + B_1 + \frac{\gamma_c}{\gamma_p}\right)\left(1 + \frac{\gamma_c}{\gamma_p}\right). \tag{22}$$

The general case for other choices of b_w can be found in SI3.5. Non-rapid buffering thus enables a reduction of the steady state error via increased feedback gain without unwanted oscillations. This phenomenon is illustrated in Figure 5A, which shows simulations and the stability condition (22) that describes the upper bound on the steady state error. In contrast, rapid buffering does not improve the stability condition and so does not enable a decrease in the adaptation error (see SI3.4); we have illustrated this phenomenon in Figure 5B via numerical simulations.

While the benefit of buffering described here are for a simple network and a steady state error (adaptation) tradeoff, control theory can be use to mathematically quantify this benefit for more general networks and more general tradeoffs involving both steady state and temporal dynamics (see SI4.3).

V. CASE STUDIES

A. Model for biofuel production

To illustrate the potential of the proposed control topologies, here we employ an existing model for biofuel production that incorporates antithetic control[6] (see

bioRxiv preprint doi: https://doi.org/10.1101/2021.04.18.440372; this version posted September 29, 2021. The copyright holder for this preprint (which was not certified by peer review) is the author/funder, who has granted bioRxiv a license to display the preprint in perpetuity. It is made available under aCC-BY-NC-ND 4.0 International license.

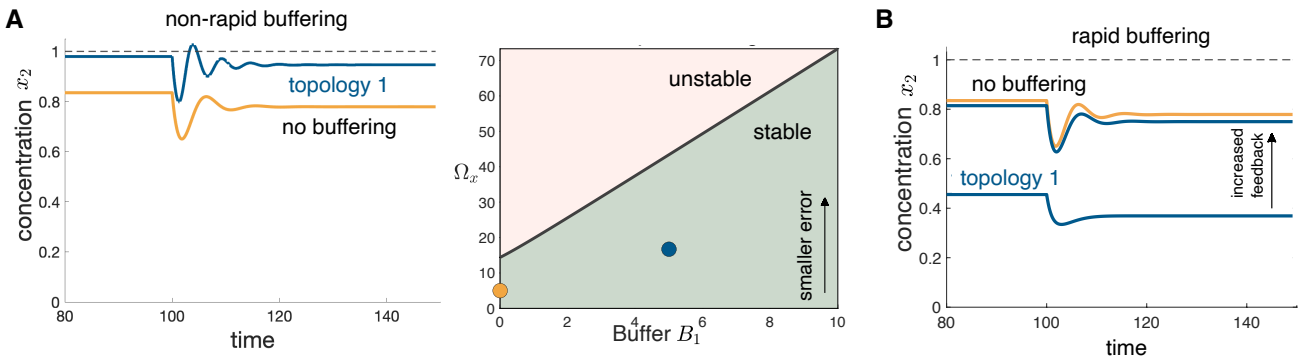

FIG. 5. **Adaptation in Topology 1 with dilution. (A)** Non-rapid buffering with stronger feedback reduces the adaptation error. (Left) In simulations the model parameters are $\theta_2 = 1$, $\gamma_p = 1$, $\eta = 100$, $\mu = 1$, $\gamma_c = 0.2$, and $k = 1$ changes to $k = 0.7$ at $t = 100$. (Right) The stability condition in (22) for non-rapid buffering with dilution rate constant in the ratio $\gamma_c/\gamma_p = 0.2$. **(B)** Rapid buffering increases the adaptation error while rapid buffering with stronger feedback is identical to no buffering with weaker feedback. Parameter values for the non-rapid case are $\theta_1 = \{1, 15\}$, $B_1 = \{0, 5\}$ and $b_{w1} = \{0, 0.8\}$; parameters for the rapid case are $\theta_1 = \{1, 5\}$ and $B_1 = \{0, 5\}$.

also[12]), shown in Figure 6A. The synthetic system produces biofuel from sugars through a metabolic pathway. The biofuel product can be toxic to the cell and so efflux pump proteins are expressed to remove the toxic metabolic product. However, at large concentrations the efflux protein pump can also be toxic. A feedback mechanism can help robustly regulate these two competing toxic products. The antithetic feedback mechanism senses the biofuel concentration to control the expression of efflux pump protein. An increase in the pump protein then reduces the biofuel concentration, completing the loop. Stability is known to be a major issue for the system, as it susceptible to oscillation for large η, which is the typical design case[6].

The extended model of the biofuel circuit with antithetic feedback and the addition of a protein buffer is:

$$
\begin{aligned}
\dot{n} &= \alpha_n n(1-n) - \delta_n b_i n - \frac{\alpha_n n p}{p + \gamma_p} \\
\dot{b}_i &= \alpha_b n - \delta_b p b_i \\
\dot{p} &= k z_2 - \beta_p p \\
\dot{b}_e &= V \delta_b p b_i n \\
\dot{z}_1 &= \mu - \eta z_1 z_2 \\
\dot{z}_2 &= \theta b_i - \eta z_1 z_2 - I r_p p + r_w w \\
\dot{w} &= I r_p z_2 - r_w w
\end{aligned}
$$

where n is the normalized cell density, which is assumed to follow logistic growth with additional death rates due to toxicity of intracellular biofuel concentration b_i and efflux protein pump p. The variables z_1 and z_2 are the controller species, while the production of the protein pump p is assumed to be proportional to controller species z_2. The variable w is the buffering species which buffers z_2 through a reversible reaction via chemical species I that inhibits z_2 sequestering when bound to z_2. The variable b_e is the extracellular concentration of biofuel.

Buffering of z_2 can be seen to stabilise the process in the simulations of the model (see Figure 6A). These simulations show that the oscillations, which occur when η is too large, quickly settle to the steady state when buffering is introduced. This stabilising effect is equivalent to the impact of buffering in Topology 1 in Section III. Buffering removes the stability limit on η and so a large antithetic binding rate η is possible without oscillations. This example thus illustrates that the stabilising effect of buffering also occurs in more complex systems than for the simple case presented above.

B. Model for growth control

For the synthetic growth control case study, we use an existing model of the synthetic growth control circuit, which includes the new addition of buffering[27] (see Figure 6B). The variable N represents the population size and is assumed to follow logistic growth, with an additional death rate due to toxicity that is proportional to the concentration of $CcdB$ per cell. $Ccdb$ is a protein that is toxic to the cell. $mRNA$ is messenger RNA while $asRNA$ is a short antisense RNA that has a complementary sequence to the mRNA, which enables sequestration between the two. $mRNA$ and $asRNA$ form the antithetic integral controller. The transcription of mRNA is induced by a quorum-sensing ligand. The term G_a represents the gain between N and mRNA induction resulting from the quorum-sensing molecule AHL. W represents a buffer of Ccdb, which consists of an inactivated form of Ccdb that can reversibly bind to an inhibitor molecule I. The adapted model of the genetic

bioRxiv preprint doi: https://doi.org/10.1101/2021.04.18.440372; this version posted September 29, 2021. The copyright holder for this preprint (which was not certified by peer review) is the author/funder, who has granted bioRxiv a license to display the preprint in perpetuity. It is made available under aCC-BY-NC-ND 4.0 International license.

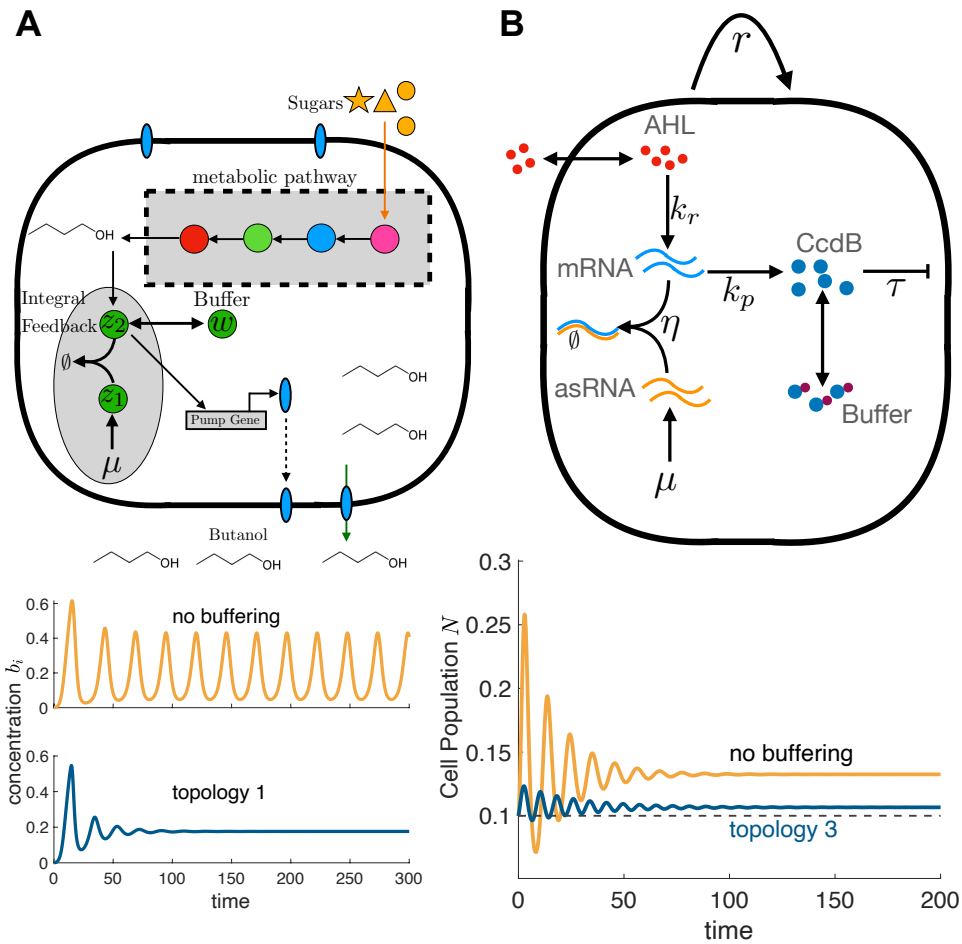

FIG. 6. Case studies of molecular buffering coupled with antithetic control showing improved stabilisation and adaptation. **(A)** Biofuel production system adapted from[6] to include buffering of species z_2. Simulations show the stabilising effect of buffering. Model parameters for simulations are $\alpha_n = 0.66$, $\delta_n = 0.5$, $\gamma_p = 0.14$, $\alpha_b = 0.1$, $\delta_b = 0.5$, $\beta_p = 0.66$, $V = 1$, $\eta = 100$, $\mu = 0.1762$, $\theta = 1$, $I = 1$, $r_p = 0, 1.25$, $r_w = 0, 0.25$, $k = 0.5, 3$. k is increased with buffering to compensate for the reduced integral feedback gain from buffering **(B)** Synthetic growth control circuit[27] adapted to include buffering of CcdB. Simulations show the ability of buffering to decrease the steady state error via stronger feedback without oscillations. Model parameters for simulations with and without buffering are $\gamma_p = 3$, $r = 1$, $\tau = 4 \times 10^{-3}$, $k_R = 10^{-1}$, $G = 10^{-6}$, $\eta = 20$, $\gamma_r = 0.1$, $\mu = 10$, $N_m = 10^9$, $\gamma_w = 10^{-2}$, $k_p = \{20, 200\}$, $b_c = \{0, 7\}$ and $b_w = \{0, 7 \times 10^{-2}\}$.

circuit with the new addition of a protein buffer is

$$\begin{aligned}
\frac{d}{dt}[CcdB] &= k_p[mRNA] - (\gamma_p + b_C I)[CcdB] + b_w[W] \\
\frac{d}{dt}[mRNA] &= k_R G_a N - (\eta[asRNA] - \gamma_R)\,[mRNA] \\
\frac{d}{dt}[asRNA] &= \mu - \eta[asRNA][mRNA] - \gamma_R[asRNA] \\
\frac{d}{dt}N &= rN\left(1 - \frac{N}{N_m}\right) - \tau[CcdB]N \\
\frac{d}{dt}[W] &= b_C I[CcdB] - b_w[W] - \gamma_w[W]
\end{aligned}$$

where $[\cdot]$ represents intracellular concentrations for each species and the last line indicating the rate of change of W is new to the model.

The buffering of $CcdB$ as shown above is equivalent to x_1 buffering in the model (6) and Figure 2, as N is the output and equivalent to x_2. Buffering at x_1 provides a similar benefit as buffering at x_2 and so can also enable near-perfect adaptation.

Buffering of $CcdB$ in conjuction with increased feedback gain can be shown to reduce steady state error in the simulations in Figure 6. Increased feedback gain is implemented in these simulations by increasing the translation rate of $CcdB$.

VI. DISCUSSION

Perfect adaptation has been subject of intense study in the synthetic biology community. Although perfectly adapting systems are ubiquituous in nature, their im-

bioRxiv preprint doi: https://doi.org/10.1101/2021.04.18.440372; this version posted September 29, 2021. The copyright holder for this preprint (which was not certified by peer review) is the author/funder, who has granted bioRxiv a license to display the preprint in perpetuity. It is made available under aCC-BY-NC-ND 4.0 International license.

plementation has proven particularly elusive. The antithetic control motif, first discovered by Briat et al[4] and implemented by Aoki et al[1], provides a new molecular mechanism to build perfect adaptation into a wide range of synthetic gene circuits. A number of works have sought to find alternative circuits that provide adaptation properties similar to antithetic control. For example, several authors have shown that ultrasensitive feedback can display some of the features of perfect adaptation[25,28], and the idea was recently extended in great detail for synthetic gene circuits[30]. Other works have sought to devise molecular implementations of Proportional-Integral-Derivative control[9], as this is a widely adopted strategy for perfect adaptation in engineered control systems.

Here we have addressed caveats of the original antithetic control system with an extended architecture that has improved stability properties. The proposed circuit combines an antithetic motif with a molecular buffering mechanism. Molecular buffering is widely conserved in natural systems, and common examples include the ATP buffering by creatine phosphate, pH buffering and calcium buffering. In all these examples, a molecular buffer sequesters a target molecule into an inactive form, resulting in a system with improved ability to mitigate fast perturbations. In the case of antithetic control, the addition of buffering results in the stabilisation of unwanted oscillations and, moreover, provides near-perfect adaptation even in rapid growth conditions where the performance of antithetic control is known to be particularly poor.

After detailed examination of mathematical models for various circuit architectures (Fig. 2) with rapid and non-rapid buffers, we found two candidate systems with improved stability properties, either by buffering species of the antithetic motif itself, or by buffering a target species to be controlled. The first circuit, called Topology 1 in Fig. 2, under non-rapid buffering provides stability over a larger range of parameters values than classic antithetic control and can generally stabilise unwanted oscillations. Moreover, Topology 1 requires buffering of a molecular species of the antithetic motif itself, and therefore it provides a promising strategy to stabilise variables that are not easily buffered directly, such as population size or metabolite species as illustrated by the example in Fig 6A.

The second circuit, termed Topology 3 in Fig. 2, requires buffering the molecular output of the process to be controlled. We found that when x_2 buffering is either non-rapid or rapid and coupled with degradation, it mitigates oscillations in fast growth regimes. Interestingly, there is a similar effect when applied to intermediate species instead of the output species in the controlled process, such as x_1 in the original circuit shown in Fig. 2 or CcdB in the growth control case study in Fig. 6. Buffering an intermediate species also provides additional design flexibility when the output species cannot be easily buffered.

Although our results indicate that both buffering and degradation can act as stabilisers of antithetic control, designs with increased buffering and reduced degradation can provide substantial benefits. Increased degradation requires a higher production rate to achieve a particular steady state concentration. If the degradation mechanism requires expression of heterologous proteins, an increase in their production rate imposes a heavier genetic burden on the host cell[8,26]. Moreover, in applications, protein production rates are subject to upper limits depending on the genetic machinery of the host[36], and so increasing degradation can also limit the maximum set point concentration. Tuning of degradation can also be difficult to implement given the limited number of degradation tags available.

The effect of buffering on adaptation is strikingly similar to a strategy employed in industrial process control, where buffer tanks are employed to regulate and smooth out the impact of disturbances[13]. In our case, the specific implementation of the molecular buffers is a subject of future study, as this will largely depend on the type of biomolecular process to be controlled (see[18] for quantification of different buffering reaction forms). For example, buffers for gene expression may require gene products to be sequestered, which can be achieved through several mechanisms such as reversible protein-protein binding[24], phosphorylation[19], small molecule inhibitors[11], or DNA decoy sites[34]. In metabolism and signalling systems, ubiquitous examples are the interconversion between a target species and a buffer (e. g. reversible catalysis between ATP and creatine phosphate[17,32]) or sequestering by dedicated proteins (e. g. Ca^{2+} or H^{+} ions[17,21,32]).

Our main goal in this paper was to show that molecular buffering can improve perfect adaptation in the antithetic control motif. Since buffering is known to stabilise a much wider range of molecular networks[16], it also has the potential to improve other circuits implementing perfect adaptation, e. g. those that rely on ultrasensitive behaviour[30]. Further, its properties may be used to instead improve transient response or disturbance rejection of a circuit, rather than only adaptation[16,17]. A key future step is the study of design rules for buffering and antithetic feedback. A useful starting point in this direction are the rules from lead-lag and PID controller tuning from control engineering[16] (see SI4.2). Unlike technological controllers, however, the stabilisation properties of buffering are tied to its synergy with feedback regulation[16,17] and the location of the buffer in a network is important, which introduces new challenges for controller design.

For simplicity, here we have focused exclusively on deterministic dynamics, but the analysis of stochastic effects emerging from the interplay between molecular buffering and antithetic control are particularly attractive, as it is known that buffering does not amplify stochastic fluctuations[17] yet some phenomena are

bioRxiv preprint doi: https://doi.org/10.1101/2021.04.18.440372; this version posted September 29, 2021. The copyright holder for this preprint (which was not certified by peer review) is the author/funder, who has granted bioRxiv a license to display the preprint in perpetuity. It is made available under aCC-BY-NC-ND 4.0 International license.

known to emerge only in the presence of molecular noise[4,31,33].

As synthetic gene circuits grow in size and complexity, there is a growing need for mechanisms that can enhance their robustness in a range of operational conditions. In the longer term, this will require the availability of a catalogue of gene circuits that can produce perfect adaptation in response to perturbations. In this work we have presented one such architecture, and thus laid theoretical groundwork for the discovery of biomolecular systems with improved functionality.

METHODS

All mathematical models are based on systems of ordinary differential equations. The stability conditions in Eqs. (8), (12), (18) and (22) were obtained using frequency domain transformations (Laplace and Fourier) of the linearised models, along with detailed examination of the magnitude and phase equations of the resulting characteristic polynomials for the closed-loop systems[27]. Simulations were carried out using standard ODE solvers in MATLAB. All calculations and model descriptions can be found in the Supplementary Material.

AUTHOR CONTRIBUTIONS

Conceptualization, E.J.H.; Methodology, E.J.H.; Formal Analysis: E.J.H., and D.A.O.; Investigation, E.J.H., and D.A.O.; Writing - Original Draft, E.J.H. ; Writing - Review & Editing, E.J.H., and D.A.O. ; Funding Acquisition, E.J.H.; Supervision, E.J.H., and D.A.O.

ACKNOWLEDGEMENTS

The authors would like to thank Morgan Kelly for her assistance. EJH was would like to thank the contribution of Judith and David Coffey.

The authors declare that there are no competing interests.

REFERENCES

[1] S.K. Aoki, G. Lillacci ans A. Gupta, A. Baumschlager, D. Schweingruber, and M. Khammash. A universal biomolecular integral feedback controller for robust perfect adaptation. *Nature*, 570:533–537, 2019.

[2] K. J. Aström and R. M. Murray. *Feedback Systems*. Princeton University Press, 2008.

[3] N. Barkai and S. Leibler. Robustness in simple biochemical networks. *Nature*, 387:913–917, 1997.

[4] C. Briat, A. Gupta, and M. Khammash. Antithetic integral feedback ensures robust perfect adaptation in noisy biomolecular networks. *Cell Syst.*, 2(1):15–26, 2016.

[5] C. Briat, A. Gupta, and M. Khammash. Antithetic proportional-integral feedback for reduced variance and improved control performance of stochastic reaction networks. *Royal Society Interface*, 15, 2018.

[6] C. Briat and M. Khammash. Perfect adaptation and optimal equilibrium productivity in a simple microbial biofuel metabolic pathway using dynamic integral control. *ACS Synthetic Biology*, 7(2):419–431, 2018.

[7] D. E. Cameron, C.J. Bashor, and J. J. Collins. A brief history of synthetic biology. *Nat. Rev. Microbiol.*, 12(5):381–390, 2014.

[8] F. Ceroni, R. Algar, G. B. Stan, and T. Ellis. Quantifying cellular capacity identifies gene expression designs with reduced burden. *Nature Methods*, 12(5):415–418, apr 2015.

[9] M. Chevalier, M. Gomez-Schiavon, A.H. Ng, and H. El-Samad. Design and analysis of a proportional-integral- derivative controller with biological molecules. *Cell Systems*, 9:338–353, 2019.

[10] V. Chubukov, A. Mukhopadhyay, C.J. Petzold, J.D. Keasling, and H.G. Martin. Synthetic and systems biology for microbial production of commodity chemicals. *npj systems biology and applications*, 2(16009), 2016.

[11] C. Denison and T. Kodadek. Small-molecule-based strategies for controlling gene expression. *Chemistry & Biology*, 5:129–145, 1998.

[12] M. J. Dunlop, J.D. Keasling, and A. Mukhopadhyay. A model for improving microbial biofuel production usinga synthetic feedback loop. *Syst Synth Biol*, 4:95=104, 2010.

[13] A. Faanes and S. Skogestad. Buffer tank design for acceptable control performance. *Ind. Eng. Chem. Res.*, 42(10):2198–2208, 2003.

[14] T. Friedlander and N. Brenner. Adaptive response by state-dependent inactivation. *Proc. Natl. Acad. Sci.*, 106(52):22558–22563, 2009.

[15] A. Gupta and M. Khammash. An antithetic integral rein controller for bio-molecular networks. *IEEE 58th Conference on Decision and Control (CDC), Nice, France,*, pages 2808–2813, 2019.

[16] E.J. Hancock and J.Ang. Frequency domain properties and fundamental limits of buffer–feedback regulation in biochemical systems. *Automatica*, 103:330–336, 2019.

[17] E.J. Hancock, J.Ang, A.Papachristodoulou, and G-B.Stan. The interplay between feedback and buffering in cellular homeostasis. *Cell Systems*, 5(5):498–508, 2017.

[18] E.J. Hancock, J.R. Krycer, and J. Ang. Metabolic buffer analysis reveals the simultaneous, independent control of atp and adenylate energy ratios. *Royal Society Interface*, in press, 2021.

[19] H. Harada, B. Becknell, M. Wilm, M. Mann, L.J. Huang, S.S. Taylor, J.D. Scott, and S.J. Korsmeyer. Phosphorylation and inactivation of bad by mitochondria-anchored protein kinase a. *Mol Cell*, 3(4):413–22, 1999.

[20] J.E. Ferrell Jr. Perfect and near-perfect adaptation in cell signaling. *Cell Systems*, 2:62–67, 2016.

[21] J. Keener and J. Sneyd. *Mathematical Physiology*. Springer-Verlag, 1998.

[22] D. Liu, A.A. Mannan, Y. Han, D.A. Oyarzún, and F. Zhang. Dynamic metabolic control: towards precision engineering of metabolism. *J Ind Microbiol Biotechnology*, 45(7):535–543, 2018.

[23] W. Ma, A. Trusina, H. El-Samad, W.A. Lim, , and C. Tang. Defining network topologies that can achieve biochemical adaptation. *Cell*, 138(4):760–73, 2009.

[24] J. De Melo, L. He, and D. Tang. The protein-protein interaction-mediated inactivation of pten. *Curr Mol Med*, 14(1):22–33, 2014.

[25] F. Montefusco, E.O. Akman, S.O. Soyer, and D. G. Bates. Ultrasensitive negative feedback control: A natural approach for the design of synthetic controllers. *PLOS One*, 11(8), 2016.

[26] E. M. Nikolados, A. Y. Weiße, F. Ceroni, and D. A. Oyarzún. Growth Defects and Loss-of-Function in Synthetic Gene Circuits. *ACS Synthetic Biology*, 8(6):1231–1240, 2019.

[27] N. Olsman, A-A. Baetica, F. Xiao, Y.P. Leong, R.M. Murray, and J.C. Doyle. Hard limits and performance tradeoffs in a class of antithetic integral feedback networks. *Cell Systems*, 9, 2019.

[28] D. A. Oyarzún and G.-B. Stan. Synthetic gene circuits for metabolic control: design trade-offs and constraints. *Journal of the Royal Society, Interface / the Royal Society*, 10(78), oct 2013.

bioRxiv preprint doi: https://doi.org/10.1101/2021.04.18.440372; this version posted September 29, 2021. The copyright holder for this preprint (which was not certified by peer review) is the author/funder, who has granted bioRxiv a license to display the preprint in perpetuity. It is made available under aCC-BY-NC-ND 4.0 International license.

[29] Y. Qian and D. Del Vecchio. Realizing 'integral control' in living cells: how to overcome leaky integration due to dilution? *Royal Society Interface*, 15, 2018.

[30] C.C. Samaniego and E. Franco. Ultrasensitive molecular controllers for quasi-integral feedback. *Cell Systems*, In Press, 2021.

[31] M. Samoilov, S. Plyasunov, and A. P. Arkin. Stochastic amplification and signaling in enzymatic futile cycles through noise-induced bistability with oscillations. *Proceedings of the National Academy of Sciences of the United States of America*, 102(7):2310–5, feb 2005.

[32] L. Sherwood. *Human Physiology: From Cells to Systems*. Brooks Cole, 2013.

[33] M. K. Tonn, P. Thomas, M. Barahona, and D. A. Oyarzún. Stochastic modelling reveals mechanisms of metabolic heterogeneity. *Communications Biology*, 2(1):108, dec 2019.

[34] T. Wang, N. Tague, S.A. Whelan, and M.J. Dunlop. Programmable gene regulation for metabolic engineering using decoy transcription factor binding sites. *Nucleic Acids Research*, 49(2):1163–1172, 2021.

[35] M. Wehrs, D. Tanjore, T. Eng, J. Lievense, T.R. Pray, and A. Mukhopadhyay. Engineering robust production microbes for large-scale cultivation. *Trends in Microbiology*, 27(6), 2019.

[36] Andrea Y. Weisse, Diego A. Oyarzún, Vincent Danos, and Peter S. Swain. Mechanistic links between cellular trade-offs, gene expression, and growth. *Proceedings of the National Academy of Sciences*, 112(9):E1038–E1047, feb 2015.

bioRxiv preprint doi: https://doi.org/10.1101/2021.04.18.440372; this version posted September 29, 2021. The copyright holder for this preprint (which was not certified by peer review) is the author/funder, who has granted bioRxiv a license to display the preprint in perpetuity. It is made available under aCC-BY-NC-ND 4.0 International license.

Supplementary material

Stabilisation of Antithetic Control via Molecular Buffering

Edward J. Hancock [1,2], Diego A. Oyarzún[3,4]

[1] School of Mathematics and Statistics, The University of Sydney, NSW, 2006, Australia
[2] Charles Perkins Centre, The University of Sydney, NSW, 2006, Australia
[3] School of Biological Sciences, University of Edinburgh, UK
[4] School of Informatics, University of Edinburgh, UK

SI1. BUFFERING BACKGROUND

In this section, we provide a background on buffering[4], including methods for analysing models with buffering. We start with the simple model in the main section of a single regulated species that is being buffered, such that

$$\begin{aligned} \dot{x} &= \underbrace{p(x)}_{\substack{\text{production}\\ \text{with feedback}}} - \underbrace{\gamma_x x}_{\text{removal}} + \underbrace{g_w(w) - g_x(x)}_{\text{buffering}} \\ \dot{w} &= \underbrace{g_x(x) - g_w(w)}_{\text{buffering}} - \underbrace{\gamma_w w}_{\text{removal}} \end{aligned} \tag{S1}$$

where x is the output species being regulated, w is the buffering species, p is the production rate of x, γ_x is the removal kinetic rate of x, g_w is the forward buffering reaction rate and g_x is the reverse buffering reaction rate. Incorporation of feedback is represented by the x dependence of production. The steady state occurs when production matches degradation ($p(\bar{x}) = \gamma_x \bar{x} + \gamma_w \bar{w}$) and the buffer is at steady state ($g_w(\bar{w}) = g_x(\bar{x}) + \gamma_w \bar{w}$). To analyse (S1), we reduce the two state model to one state by assuming that the buffering reactions rapidly reach equilibrium (see[4] for more mathematically rigorous derivation). To carry this out, we first linearise (S1), which results in

$$\begin{aligned} \Delta\dot{x} &= \underbrace{-h\Delta x}_{\text{feedback}} - \underbrace{\gamma_x \Delta x}_{\text{removal}} + \underbrace{b_w \Delta w - b_x \Delta x}_{\text{buffering}} \\ \Delta\dot{w} &= \underbrace{-b_w \Delta w + b_x \Delta x}_{\text{buffering}} - \underbrace{\gamma_w \Delta w}_{\text{removal}} \end{aligned}$$

where $h = -\frac{\partial p}{\partial x}$ is the linearised feedback gain, and $b_w = \frac{\partial g_w}{\partial w}$ and $b_x = \frac{\partial g_x}{\partial x}$ are the linearised kinetic rates for the forward and reverse buffering reaction.
We introduce the variable $\Delta x_T = \Delta w + \Delta x$ to carry out a quasi-steady state approximation[2,4], where we have the transformed model

$$\begin{aligned} \Delta\dot{x}_T &= -h\Delta x - \gamma_x \Delta x - \gamma_w \Delta w \\ \Delta\dot{w} &= -b_w \Delta w + b_x \Delta x - \gamma_w \Delta w. \end{aligned}$$

We assume that the buffering species Δw rapidly reaches quasi-steady state due to large b_w and thus assume $\Delta\dot{w} = -(b_w + \gamma_w)\Delta w + b_x \Delta x = 0$, where x_T is a 'slow' variable as it is not a direct function of the buffering reactions. The quasi-steady state can be rewritten

$$\Delta w = B\Delta x, \quad B = \frac{b_x}{b_w + \gamma_w}. \tag{S2}$$

From this quasi-steady state, we have $\Delta x_T = (1+B)\Delta x$ and $\Delta\dot{x}_T = (1+B)\Delta\dot{x}$, resulting in

$$\boxed{(1+B)\Delta\dot{x} = -h\Delta x - (\gamma_x + B\gamma_w)\Delta x}$$

bioRxiv preprint doi: https://doi.org/10.1101/2021.04.18.440372; this version posted September 29, 2021. The copyright holder for this preprint (which was not certified by peer review) is the author/funder, who has granted bioRxiv a license to display the preprint in perpetuity. It is made available under aCC-BY-NC-ND 4.0 International license.

which is a reduced one state model, where the second state can be determined from $\Delta w = B\Delta x$.

In technology, integral feedback is often paired with proportional and derivative feedback (PID control)[1]. In biology, rapid buffering without degradation is equivalent to negative derivative feedback and rapid buffering with degradation is equivalent to PD feedback with degradation. These equivalences can be observed in[4]

$$\Delta\dot{x} = \underbrace{-B\Delta\dot{x} - \gamma_w B\Delta x}_{\substack{\text{proportional +}\\ \text{derivative}\\ \text{feedback}}} - \underbrace{h\Delta x}_{\substack{\text{proportional}\\ \text{feedback}}} - \gamma_x \Delta x$$

where the buffer equilibrium ratio B corresponds to the derivative feedback 'gain'.

To study the effect of buffering on stability, we can also modify the model in (S1) to include a delay of the production feedback term

$$\begin{aligned} \dot{x} &= \underbrace{p(x(t-\tau))}_{\substack{\text{production}\\ \text{with feedback}}} - \underbrace{\gamma_x x}_{\text{removal}} + \underbrace{g_w(w) - g_x(x)}_{\text{buffering}} \\ \dot{w} &= \underbrace{g_x(x) - g_w(w)}_{\text{buffering}} - \underbrace{\gamma_w w}_{\text{removal}} \end{aligned} \tag{S3}$$

where $p(x(t-\tau))$ represents the production feedback with a delay of time τ. The reduced model is

$$\boxed{(1+B)\Delta\dot{x} = -h\Delta x_\tau - (\gamma_x + B\gamma_w)\Delta x}$$

where $\Delta x_\tau = \Delta x(t-\tau)$.

It can be observed in Figure S2 that buffering can stabilise the oscillations that result from feedback delay. This stabilisation is a result of (a) the buffering reactions acting directly on the target molecular species (i.e. not being subject to delays) and (b) buffering having a 'derivative feedback' effect - known for its stabilising effects in control engineering[1].

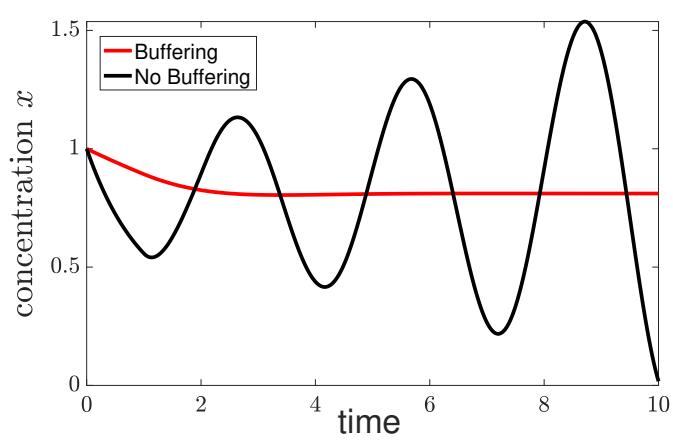

FIG. S1. The parameters are $B_x = 0$ and 5, $\tau = 1$ (delay), $\gamma_p = 1$, $\gamma_w = 0$ and $h = 2.7$.

bioRxiv preprint doi: https://doi.org/10.1101/2021.04.18.440372; this version posted September 29, 2021. The copyright holder for this preprint (which was not certified by peer review) is the author/funder, who has granted bioRxiv a license to display the preprint in perpetuity. It is made available under aCC-BY-NC-ND 4.0 International license.

SI2. STABILITY OF ANTITHETIC INTEGRAL FEEDBACK WITH BUFFERING

SI2.1. Stability of Antithetic Integral Feedback with Rapid Buffering: All Species

In this section, we analyse the stabilising effect of buffering (without degradation) on antithetic integral feedback. We base our studies on a simple model involving the antithetic integral feedback (without buffering)[5]. Consider

$$\begin{aligned} \dot{x}_1 &= \theta_1 z_1 - \gamma_p x_1 \\ \dot{x}_2 &= k x_1 - \gamma_p x_2 \\ \dot{z}_1 &= \mu - \eta z_1 z_2 \\ \dot{z}_2 &= \theta_2 x_2 - \eta z_1 z_2 \end{aligned} \tag{S4}$$

where x_2 is the output concentration being controlled, x_1 is another concentration in the process being controlled, and z_1 and z_2 represent the molecular species involved in the perfect adaptation mechanism.
We next introduce buffering to (S4). We show how the model reduction method described in SI1 can be used to simplify the model for one case. We then use the same method for all buffers.
As a first case, we introduce buffering at the controlled variable x_2 and simplify the model by assuming that the buffering reactions rapidly reach equilibrium. With buffering at x_2, we have

$$\begin{aligned} \dot{x}_1 &= \theta_1 z_1 - \gamma_p x_1 \\ \dot{x}_2 &= k x_1 - \gamma_p x - \gamma_p x_2 - b_x x + b_w w \\ \dot{z}_1 &= \mu - \eta z_1 z_2 \\ \dot{z}_2 &= \theta_2 x_2 - \eta z_1 z_2 \\ \dot{w}_x &= b_x x_2 - b_w w_x \end{aligned} \tag{S5}$$

where w_x is the buffering species at x_2 and b_x, b_w are the kinetic rate constants for the buffering reactions. Although the buffering equilibrium ratio is defined in terms of the linearised model and deviations from steady state, we can use the same notation here for the nonlinear model as the buffering reactions are linear. If the buffering reaction is at equilibrium then

$$b_x x_2 = b_w w_x.$$

If we assume that the buffer rapidly reaches equilibrium then w is at quasi-steady state and so

$$w_x = B_x x_2 \quad B_x = \frac{b_x}{b_w}.$$

We note that although the buffer equilibrium ratio is defined in (S2) in terms deviations from steady state, we can use the buffer equilibrium ratios in the nonlinear model as the reaction rates are linear.
We set $x_T = w_x + x$ as the slow variable and so $x_T = (1 + B_x)x_2$. Thus $\dot{x}_T = (1 + B_x)\dot{x}_2$ and so

$$(1 + B_x)\dot{x}_2 = k x_1 - \gamma_p x_2.$$

If we include buffering on z_1, z_2, x_2 and apply a similar model reduction by assuming rapid buffering, then we have

$$\begin{aligned} \dot{x}_1 &= \theta_1 z_1 - \gamma_p x_1 \\ (1 + B_x)\dot{x}_2 &= k x_1 - \gamma_p x_2 \\ (1 + B_1)\dot{z}_1 &= \mu - \eta z_1 z_2 \\ (1 + B_2)\dot{z}_2 &= \theta_2 x_2 - \eta z_1 z_2 \end{aligned} \tag{S6}$$

where B_1, B_2 are the buffer equilibrium ratios of the buffers at z_1 and z_2 respectively.

SI2.1.a. Steady State

We first determine the steady states of the system, which is useful both for determining perfect adaptation and as a prerequisite for stability analysis. Using

$$(1 + B_1)\dot{z}_1 - (1 + B_2)\dot{z}_2 = \mu - \theta_2 x_2 = 0$$

bioRxiv preprint doi: https://doi.org/10.1101/2021.04.18.440372; this version posted September 29, 2021. The copyright holder for this preprint (which was not certified by peer review) is the author/funder, who has granted bioRxiv a license to display the preprint in perpetuity. It is made available under aCC-BY-NC-ND 4.0 International license.

we can see that the steady state for the output is

$$\bar{x}_2 = \frac{\mu}{\theta_2}.$$

The correspondence of this steady state with perfect adaptation is discussed further in Section 2 & 3 of the paper. The species x_1, z_1 and z_2 have the corresponding steady states

$$\bar{x}_1 = \frac{\mu\gamma_p}{\theta_2 k}, \quad \bar{z}_1 = \frac{\gamma_p^2\mu}{\theta_1\theta_2 k}, \quad \bar{z}_2 = \frac{\theta_1\theta_2 k}{\eta\gamma_p^2}.$$

SI2.1.b. Linearised Model

We next determine the effect of buffering on the stability of the model. We follow the methodology used by Olsman and colleagues[5] to study the stability of antithetic integral feedback with the addition of buffering. Linearising the system (S6) about the steady states, we have

$$\begin{aligned}
\Delta\dot{x}_1 &= \theta_1\Delta z_1 - \gamma_p\Delta x_1 \\
(1+B_x)\Delta\dot{x}_2 &= k\Delta x_1 - \gamma_p\Delta x_2 \\
(1+B_1)\Delta\dot{z}_1 &= -\alpha\Delta z_1 - \frac{\beta}{\alpha}\Delta z_2 \\
(1+B_2)\Delta\dot{z}_2 &= \theta_2\Delta x_2 - \alpha\Delta z_1 - \frac{\beta}{\alpha}\Delta z_2
\end{aligned} \tag{S7}$$

where $\Delta z_1 = z_1 - \bar{z}_1$, $\Delta z_2 = z_2 - \bar{z}_2$, $\Delta x_1 = x_1 - \bar{x}_1$, $\Delta x_2 = x_2 - \bar{x}_2$ are the deviations from steady state and

$$\alpha = \frac{\theta_1\theta_2 k}{\gamma_p^2}, \quad \beta = \eta\mu.$$

Taking the Laplace transform of (S7), we have

$$\begin{aligned}
(s+\gamma_p)X_1 &= \theta_1 Z_1 \\
((1+B_x)s+\gamma_p)X_2 &= kX_1 \\
((1+B_1)s+\alpha)Z_1 &= -\frac{\beta}{\alpha}Z_2 \\
\left((1+B_2)s+\frac{\beta}{\alpha}\right)Z_2 &= \theta_2 X_2 - \alpha Z_1
\end{aligned} \tag{S8}$$

where $Z_1 = \mathcal{L}\{\Delta z_1\}$, $Z_2 = \mathcal{L}\{\Delta z_2\}$, $X_1 = \mathcal{L}\{\Delta x_1\}$, $X_2 = \mathcal{L}\{\Delta x_2\}$ are the Laplace transforms of the time-domain concentration deviations. Substituting, we have

$$\begin{aligned}
(s+\gamma_p)((1+B_x)s+\gamma_p)X_2 &= \theta_1 k Z_1 \\
\left((1+B_2)s+\frac{\beta}{\alpha}\right)((1+B_1)s+\alpha)Z_1 &= -\frac{\beta}{\alpha}(\theta_2 X_2 - \alpha Z_1).
\end{aligned} \tag{S9}$$

Simplifying, we have

$$(1+B_1)(1+B_2)\left(s^2 + \left(\frac{\beta}{\alpha(1+B_2)} + \frac{\alpha}{1+B_1}\right)s\right)Z_1 = -\frac{\beta}{\alpha}\theta_2 X_2.$$

Substituting from (S9), we have

$$\left[(1+B_1)(1+B_2)s((1+B_x)s+\gamma_p)(s+\gamma_p)\left(s+\frac{\beta}{\alpha(1+B_2)}+\frac{\alpha}{1+B_1}\right)+\frac{\beta}{\alpha}\theta_1\theta_2 k\right]X_2 = 0.$$

The characteristic equation used to analyse stability is thus

$$s((1+B_x)s+\gamma_p)(s+\gamma_p)\left(s+\frac{\beta}{\alpha(1+B_2)}+\frac{\alpha}{1+B_1}\right)+\frac{\beta\gamma_p^2}{(1+B_1)(1+B_2)} = 0. \tag{S10}$$

bioRxiv preprint doi: https://doi.org/10.1101/2021.04.18.440372; this version posted September 29, 2021. The copyright holder for this preprint (which was not certified by peer review) is the author/funder, who has granted bioRxiv a license to display the preprint in perpetuity. It is made available under aCC-BY-NC-ND 4.0 International license.

SI2.1.c. Characterisation of roots

Following the methodology used by Olsman and colleagues[5], we first characterise the roots of (S10). If we substitute $s = \gamma_p \sigma$ then

$$\sigma(1+\sigma)\left(1+(1+B_x)\sigma\right)\left(\sigma + \frac{\beta}{\gamma_p \alpha(1+B_2)} + \frac{\alpha}{\gamma_p(1+B_1)}\right) = -\frac{\beta}{\gamma_p^2(1+B_1)(1+B_2)}. \tag{S11}$$

Taking the limit of strong binding for the sequestration process in antithetic integral feedback $\left(\beta \gg \max\left\{\alpha^2 \frac{(1+B_2)}{(1+B_1)}, \alpha\gamma_p(1+B_2)\right\}\right)$ then

$$\sigma(1+\sigma)\left(1+(1+B_x)\sigma\right)\left(1+\sigma\frac{\gamma_p\alpha(1+B_2)}{\beta}\right) = -\frac{\alpha}{\gamma_p(1+B_1)}.$$

It can be observed that there is a large, real root at $\sigma \approx -\frac{\beta}{\gamma_p\alpha(1+B_2)}$. We next examine the region $|\sigma| \ll \frac{\beta}{\gamma_p\alpha(1+B_2)}$, where we have

$$\sigma(1+\sigma)\left(1+(1+B_x)\sigma\right) = -\frac{\alpha}{\gamma_p(1+B_1)}.$$

The magnitude and phase constraints are

$$|\sigma||1+\sigma||1+(1+B_x)\sigma| = \frac{\alpha}{\gamma_p(1+B_1)}$$
$$\arg\sigma + \arg(1+\sigma) + \arg\left(1+(1+B_x)\sigma\right) = (1+2k)\pi.$$

If we assume that σ is real and positive, then the LHS of the phase constraint is

$$\arg\sigma + \arg(1+\sigma) + \arg\left(1+(1+B_x)\sigma\right) = 0$$

which contradicts. Thus unstable roots are not purely real.
If we assume that σ is real and $-1/(1+B_x) < \sigma < 0$ then the LHS of the phase constraint is

$$\arg\sigma + \arg(1+\sigma) + \arg\left(1+(1+B_x)\sigma\right) = \pi$$

and so it is possible to have stable real roots. If we set $f = |\sigma||1+\sigma||1+(1+B_x)\sigma|$ from the magnitude constraint, then there is a local maxim of f at

$$\sigma_{max} = \frac{-(2+B_x) + \sqrt{1+B_x+B_x^2}}{3(1+B_x)}.$$

Thus there are two stable real roots between $-1/(1+B_x) < \sigma < 0$ if

$$f(\sigma_{max}) > \frac{\alpha}{\gamma_p(1+B_1)}$$

as $f(\sigma_{max})$ is larger than the RHS of the magnitude constraint. There is a bifurcation at the boundary $f(\sigma_{max}) = \frac{\alpha}{\gamma_p(1+B_1)}$ resulting in a pair of complex conjugate roots if

$$f(\sigma_{max}) < \frac{\alpha}{\gamma_p(1+B_1)}.$$

For $-1 < \sigma < -1/(1+B_x)$ then

$$\arg\sigma + \arg(1+\sigma) + \arg\left(1+(1+B_x)\sigma\right) = 2\pi$$

which violates the phase constraints. For $\sigma < -1$ then

$$\arg\sigma + \arg(1+\sigma) + \arg\left(1+(1+B_x)\sigma\right) = 3\pi$$

which meets the phase constraints. Thus for the stability boundary with strong binding there is a negative real root and a complex pair of roots in the region $|\sigma| \ll \frac{\beta}{\gamma_p\alpha(1+B_2)}$, as well as one large negative root.

bioRxiv preprint doi: https://doi.org/10.1101/2021.04.18.440372; this version posted September 29, 2021. The copyright holder for this preprint (which was not certified by peer review) is the author/funder, who has granted bioRxiv a license to display the preprint in perpetuity. It is made available under aCC-BY-NC-ND 4.0 International license.

SI2.1.d. Stability Conditions

We next determine the stability boundary, where roots of the characteristic equation have zero real parts. Substituting $s = i\omega\gamma_p$, we have

$$\gamma_p^4 i\omega(1+i\omega)(1+(1+B_x)i\omega)\left(i\omega+\left(\frac{\beta}{\alpha\gamma_p(1+B_2)}+\frac{\alpha}{\gamma_p(1+B_1)}\right)\right) = -\frac{\beta\gamma_p^2}{(1+B_1)(1+B_2)}.$$

From these equations, the magnitude and phase constraint are

$$\begin{aligned}
&\omega(1+\omega^2)^{0.5}(1+(1+B_x)^2\omega^2)^{0.5}\left(\omega^2+\phi^2\right)^{0.5} = \frac{\beta}{\gamma_p^2(1+B_1)(1+B_2)}\\
&\tan^{-1}(\omega)+\tan^{-1}((1+B_x)\omega)+\tan^{-1}\left(\frac{\omega}{\phi}\right) = \frac{\pi}{2}+2k\pi\\
&\phi = \frac{\beta}{\alpha\gamma_p(1+B_2)}+\frac{\alpha}{\gamma_p(1+B_1)}
\end{aligned}$$

for some integer k. Using the strong binding assumption $\left(\beta \gg \max\left\{\alpha^2\frac{(1+B_2)}{(1+B_1)}, \alpha\gamma_p(1+B_2)\right\}\right)$ then from above $|\omega| \ll \frac{\beta(1+B_1)}{\gamma_p\alpha(1+B_2)}$ and so

$$\begin{aligned}
\omega(1+\omega^2)^{0.5}(1+(1+B_x)^2\omega^2)^{0.5} &= \frac{\alpha}{\gamma_p(1+B_1)}\\
\tan^{-1}(\omega)+\tan^{-1}((1+B_x)\omega) &= \frac{\pi}{2}+2k\pi.
\end{aligned}$$

Rewriting the phase constraint, we have

$$\tan^{-1}(\omega)-\frac{\pi}{4} = \frac{\pi}{4}-\tan^{-1}((1+B_x)\omega).$$

Applying $\tan(\cdot)$ and trigonometric identities to both sides, we have

$$\frac{\omega-1}{\omega+1} = \frac{1-(1+B_x)\omega}{1+(1+B_x)\omega}.$$

Solving, we have

$$\omega = \frac{1}{\sqrt{1+B_x}}.$$

Thus the stability boundary occurs at

$$\gamma_p = \frac{\alpha}{(1+B_1)}\frac{1+B_x}{2+B_x}.$$

From above, we know that all roots are real and stable if $\alpha/(\gamma_p(1+B_1))$ is sufficiently small, and so the stability condition is

$$\gamma_p > \frac{\alpha}{(1+B_1)}\frac{1+B_x}{2+B_x}$$

or

$$\boxed{\gamma_p^3 > \frac{\theta_1\theta_2 k}{(1+B_1)}\frac{1+B_x}{2+B_x}}. \tag{S12}$$

Thus increasing B_1 improves stability and increasing B_2 has no effect on stability. Further, increasing B_x worsens stability, although this effect saturates as B_x increases.

bioRxiv preprint doi: https://doi.org/10.1101/2021.04.18.440372; this version posted September 29, 2021. The copyright holder for this preprint (which was not certified by peer review) is the author/funder, who has granted bioRxiv a license to display the preprint in perpetuity. It is made available under aCC-BY-NC-ND 4.0 International license.

SI2.2. Stability of Antithetic Feedback with Non-Rapid Buffering at z_1

In this section, we analyse the ability of non-rapid buffering at z_1 to stabilise antithetic integral feedback. We use the model

$$\begin{aligned}
\dot{x}_1 &= \theta_1 z_1 - \gamma_p x_1 \\
\dot{x}_2 &= k x_1 - \gamma_p x_2 \\
\dot{z}_1 &= \mu - \eta z_1 z_2 - b_z z_1 + b_w w \\
\dot{z}_2 &= \theta_2 x_2 - \eta z_1 z_2 \\
\dot{w} &= b_z z_1 - b_w w.
\end{aligned} \tag{S13}$$

where the buffer w is not assumed to rapidly reach equilbrium. As a result, the model cannot be reduced in a similar manner to SI2.1. The steady state for (S13) is identical to the rapid case in SI2.1. The linearisation is

$$\begin{aligned}
\Delta\dot{x}_1 &= \theta_1 \Delta z_1 - \gamma_p \Delta x_1 \\
\Delta\dot{x}_2 &= k \Delta x_1 - \gamma_p \Delta x_2 \\
\Delta\dot{z}_1 &= -\eta \bar{z}_2 \Delta z_1 - \eta \bar{z}_1 \Delta z_2 - b_z \Delta z_1 + b_w \Delta w \\
\Delta\dot{z}_2 &= \theta_2 \Delta x_2 - \eta \bar{z}_2 \Delta z_1 - \eta \bar{z}_1 \Delta z_2 \\
\Delta\dot{w} &= b_z \Delta z_1 - b_w \Delta w.
\end{aligned}$$

This system can be rewritten

$$\begin{aligned}
\Delta\dot{x}_1 &= \theta_1 \Delta z_1 - \gamma_p \Delta x_1 \\
\Delta\dot{x}_2 &= k \Delta x_1 - \gamma_p \Delta x_2 \\
\Delta\dot{z}_1 &= -\alpha \Delta z_1 - \frac{\beta}{\alpha} \Delta z_2 - b_z \Delta z_1 + b_w \Delta w \\
\Delta\dot{z}_2 &= \theta_2 \Delta x_2 - \alpha \Delta z_1 - \frac{\beta}{\alpha} \Delta z_2 \\
\Delta\dot{w} &= b_z \Delta z_1 - b_w \Delta w
\end{aligned} \tag{S14}$$

where

$$\alpha = \frac{\theta_1 \theta_2 k}{\gamma_p^2}, \quad \beta = \eta \mu.$$

Taking the Laplace transform of $\Delta\dot{w} = b_z \Delta z_1 - b_w \Delta w$, we have

$$W = \frac{b_z}{s + b_w} Z_1$$

where W and Z_1 are the Laplace transforms of w and z_1. We have

$$\begin{aligned}
-b_z Z_1 + b_w W &= -b_z Z_1 + b_w \frac{b_z}{s + b_w} Z_1 \\
&= -B_1 \frac{s}{1 + \frac{s}{b_w}} Z_1 \\
&= -C_b(s) Z_1
\end{aligned}$$

where

$$C_b = B_1 \frac{s}{1 + \frac{s}{b_w}}.$$

Taking the Laplace transform of (S14), we have

$$\begin{aligned}
(s + \gamma_p) X_1 &= \theta_1 Z_1 \\
(s + \gamma_p) X_2 &= k X_1 \\
(s + \alpha + C_b) Z_1 &= -\frac{\beta}{\alpha} Z_2 \\
\left(s + \frac{\beta}{\alpha}\right) Z_2 &= \theta_2 X_2 - \alpha Z_1.
\end{aligned}$$

bioRxiv preprint doi: https://doi.org/10.1101/2021.04.18.440372; this version posted September 29, 2021. The copyright holder for this preprint (which was not certified by peer review) is the author/funder, who has granted bioRxiv a license to display the preprint in perpetuity. It is made available under aCC-BY-NC-ND 4.0 International license.

Combining, we have

$$(s+\gamma_p)^2 X_2 = \theta_1 k Z_1$$
$$(s+\alpha+C_b)\left(s+\frac{\beta}{\alpha}\right) Z_1 = -\frac{\beta}{\alpha}(\theta_2 X_2 - \alpha Z_1).$$

Simplifying, we have

$$\left[s\left(s+\alpha+\frac{\beta}{\alpha}\right)+C_b\left(s+\frac{\beta}{\alpha}\right)\right] Z_1 = -\frac{\beta}{\alpha}\theta_2 X_2.$$

Taking the strong antithetic binding limit of the sequestration mechanism $(\beta \gg \max\{\alpha^2, \gamma_p\alpha\})$, we have

$$(s+C_b)\left(s+\frac{\beta}{\alpha}\right) Z_1 = -\frac{\beta}{\alpha}\theta_2 X_2$$

and so

$$(s+\gamma_p)^2\left[(s+C_b)\left(s+\frac{\beta}{\alpha}\right)\right] X_2 = -\beta\gamma_p^2 X_2.$$

Rewriting C_b, we have

$$\left[(s+\gamma_p)^2 s\frac{1+B_1+\frac{s}{b_w}}{1+\frac{s}{b_w}}\left(s+\frac{\beta}{\alpha}\right)+\beta\gamma_p^2\right] X_2 = 0$$

and so the characteristic equation is

$$(s+\gamma_p)^2 s\left(1+B_1+\frac{s}{b_w}\right)\left(s+\frac{\beta}{\alpha}\right)+\beta\gamma_p^2\left(1+\frac{s}{b_w}\right) = 0.$$

Substituting $s = i\omega\gamma_p$, we have

$$\left(1+B_1+i\omega\frac{\gamma_p}{b_w}\right)(1+i\omega)^2 i\omega\left(i\omega+\frac{\beta}{\gamma_p\alpha}\right)+\frac{\beta}{\gamma_p^2}\left(1+i\omega\frac{\gamma_p}{b_w}\right) = 0.$$

Taking the strong antithetic binding limit where $|i\omega| \ll \frac{\beta}{\gamma_p\alpha}$, we have

$$\left(1+B_1+i\omega\frac{\gamma_p}{b_w}\right)(1+i\omega)^2 i\omega = -\frac{\alpha}{\gamma_p}\left(1+i\omega\frac{\gamma_p}{b_w}\right).$$

The magnitude constraint is

$$(1+B_1)\left(1+\frac{\gamma_p^2}{b_w^2}\frac{\omega^2}{(1+B_1)^2}\right)^{0.5}(1+\omega^2)\omega = \frac{\alpha}{\gamma_p}\left(1+\frac{\gamma_p^2}{b_w^2}\omega^2\right)^{0.5} \tag{S15}$$

and the phase constraint is

$$\tan^{-1}\left(\frac{\gamma_p}{b_w}\frac{\omega}{1+B_1}\right)+2\tan^{-1}(\omega)+\frac{\pi}{2} = \tan^{-1}\left(\frac{\gamma_p}{b_w}\omega\right)+\pi+2k\pi.$$

for some integer k. Using trigonometric identities, we have

$$\tan^{-1}\left(\frac{2\omega}{1-\omega^2}\right)-\frac{\pi}{4} = \tan^{-1}\left(\frac{\frac{B_1}{1+B_1}\frac{\gamma_p}{b_w}\omega}{1+\frac{1}{1+B_1}\frac{\gamma_p^2}{b_w^2}\omega^2}\right)+\frac{\pi}{4}+2k\pi.$$

bioRxiv preprint doi: https://doi.org/10.1101/2021.04.18.440372; this version posted September 29, 2021. The copyright holder for this preprint (which was not certified by peer review) is the author/funder, who has granted bioRxiv a license to display the preprint in perpetuity. It is made available under aCC-BY-NC-ND 4.0 International license.

This can be simplified to

$$\frac{\frac{2\omega}{1-\omega^2}-1}{1+\frac{2\omega}{1-\omega^2}} = \frac{\frac{\frac{B_1}{1+B_1}\frac{\gamma_p}{b_w}\omega}{1+\frac{1}{1+B_1}\frac{\gamma_p^2}{b_w^2}\omega^2}+1}{1-\frac{\frac{B_1}{1+B_1}\frac{\gamma_p}{b_w}\omega}{1+\frac{1}{1+B_1}\frac{\gamma_p^2}{b_w^2}\omega^2}}$$

or

$$\frac{2\omega-1+\omega^2}{1-\omega^2+2\omega} = \frac{1+\frac{1}{1+B_1}\frac{\gamma_p^2}{b_w^2}\omega^2+\frac{B_1}{1+B_1}\frac{\gamma_p}{b_w}\omega}{1+\frac{1}{1+B_1}\frac{\gamma_p^2}{b_w^2}\omega^2-\frac{B_1}{1+B_1}\frac{\gamma_p}{b_w}\omega}.$$

We have

$$\begin{aligned}&\left(2\omega-1+\omega^2\right)\left(1+\frac{1}{1+B_1}\frac{\gamma_p^2}{b_w^2}\omega^2-\frac{B_1}{1+B_1}\frac{\gamma_p}{b_w}\omega\right)\\ &=\left(1+\frac{1}{1+B_1}\frac{\gamma_p^2}{b_w^2}\omega^2+\frac{B_1}{1+B_1}\frac{\gamma_p}{b_w}\omega\right)\left(1-\omega^2+2\omega\right).\end{aligned}$$

Setting

$$\begin{aligned}a_1 &= \frac{B_1}{1+B_1}\frac{\gamma_p}{b_w}\\ a_2 &= \frac{1}{1+B_1}\frac{\gamma_p^2}{b_w^2}\end{aligned}$$

we have

$$\left(2\omega-1+\omega^2\right)\left(1+a_2\omega^2-a_1\omega\right) = \left(1+a_2\omega^2+a_1\omega\right)\left(1-\omega^2+2\omega\right).$$

Matching coefficients, we have

$$2a_1\omega^2+(1-\omega^2)(1+a_2\omega^2)=0.$$

and thus

$$a_2\omega^4+(1-2a_1-a_2)\omega^2-1=0 \tag{S16}$$

Solving for ω^2, we have the stability constraint

$$\gamma_p > \frac{\alpha}{(1+B_1)}\frac{1}{(1+\omega^2)\omega}\left(\frac{1+\frac{\gamma_p^2}{b_w^2}\omega^2}{1+\frac{\gamma_p^2}{b_w^2}\frac{\omega^2}{(1+B_1)^2}}\right)^{0.5} \tag{S17}$$

where

$$\omega^2=\sqrt{\left(\frac{1}{2a_2}-\frac{a_1}{a_2}-\frac{1}{2}\right)^2+\frac{1}{a_2}}-\left(\frac{1}{2a_2}-\frac{a_1}{a_2}-\frac{1}{2}\right)$$

which can be rewritten as

$$\gamma_p^3 > \frac{\theta_1\theta_2 k}{(1+B_1)}\underbrace{\frac{1}{(1+\omega^2)\omega}\left(\frac{1+\frac{\gamma_p^2}{b_w^2}\omega^2}{1+\frac{\gamma_p^2}{b_w^2}\frac{\omega^2}{(1+B_1)^2}}\right)^{0.5}}_{\mathrm{F}} \tag{S18}$$

bioRxiv preprint doi: https://doi.org/10.1101/2021.04.18.440372; this version posted September 29, 2021. The copyright holder for this preprint (which was not certified by peer review) is the author/funder, who has granted bioRxiv a license to display the preprint in perpetuity. It is made available under aCC-BY-NC-ND 4.0 International license.

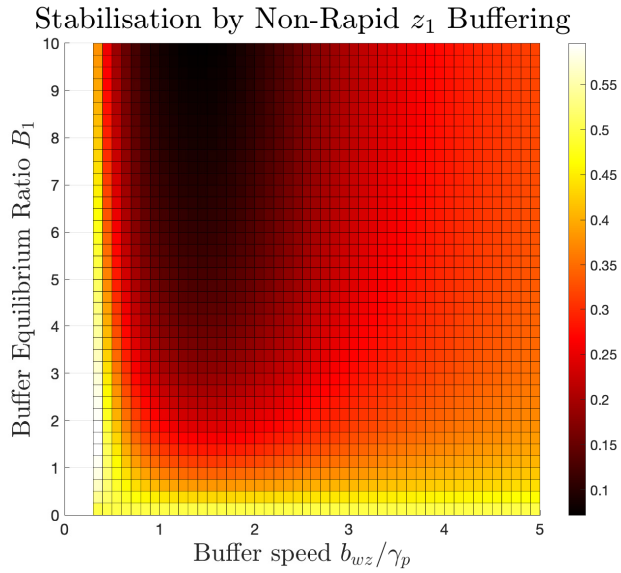

FIG. S2. Stabilisation effect F in (S18) where smaller implies improved stability.

$$\omega^2 = \sqrt{\left((1+B_1)\frac{b_w^2}{2\gamma_p^2} - B_1\frac{b_w}{\gamma_p} - \frac{1}{2}\right)^2 + (1+B_1)\frac{b_w^2}{\gamma_p^2}} - \left((1+B_1)\frac{b_w^2}{2\gamma_p^2} - B_1\frac{b_w}{\gamma_p} - \frac{1}{2}\right)$$

where F, which is the stabilisation effect independent of the integral gain, can be seen as a function of B_1 and $\frac{b_w}{\gamma_p}$ in Figure S2.
For the special case that $b_w = \gamma_p$ then we have

$$\omega^2 = 1 + B_1$$

and so

$$\gamma_p^3 > \frac{\theta_1\theta_2 k}{(1+B_1)}\frac{1}{(2+B_1)}.$$

SI2.3. Stability of Antithetic Feedback with Non-Rapid Buffering at x_2

In this section, we analyse the ability of non-rapid buffering at x_2 to stabilise antithetic integral feedback. We use the model

$$\begin{aligned}
\dot{x}_1 &= \theta_1 z_1 - \gamma_p x_1 \\
\dot{x}_2 &= k x_1 - \gamma_p x_2 - b_x x_2 + b_w w \\
\dot{w} &= b_x x_2 - b_w w \\
\dot{z}_1 &= \mu - \eta z_1 z_2 \\
\dot{z}_2 &= \theta_2 x_2 - \eta z_1 z_2.
\end{aligned} \tag{S19}$$

where the buffer w is not assumed to rapidly reach equilbrium. As a result, the model cannot be reduced in a similar manner to SI2.1. The steady state for (S19) is identical to the rapid case in SI2.1. The linearisation is

$$\begin{aligned}
\Delta\dot{x}_1 &= \theta_1 \Delta z_1 - \gamma_p \Delta x_1 \\
\Delta\dot{x}_2 &= k\Delta x_1 - \gamma_p \Delta x_2 - b_x \Delta x_2 + b_w \Delta w \\
\Delta\dot{w} &= b_x \Delta x_2 - b_w \Delta w \\
\Delta\dot{z}_1 &= -\eta \bar{z}_2 \Delta z_1 - \eta \bar{z}_1 \Delta z_2 \\
\Delta\dot{z}_2 &= \theta_2 \Delta x_2 - \eta \bar{z}_2 \Delta z_1 - \eta \bar{z}_1 \Delta z_2.
\end{aligned}$$

bioRxiv preprint doi: https://doi.org/10.1101/2021.04.18.440372; this version posted September 29, 2021. The copyright holder for this preprint (which was not certified by peer review) is the author/funder, who has granted bioRxiv a license to display the preprint in perpetuity. It is made available under aCC-BY-NC-ND 4.0 International license.

This system can be rewritten

$$\begin{aligned}
\Delta\dot{x}_1 &= \theta_1\Delta z_1 - \gamma_p\Delta x_1 \\
\Delta\dot{x}_2 &= k\Delta x_1 - \gamma_p\Delta x_2 - b_x\Delta x_2 + b_w\Delta w \\
\Delta\dot{w} &= b_x\Delta x_2 - b_w\Delta w \\
\Delta\dot{z}_1 &= -\alpha\Delta z_1 - \frac{\beta}{\alpha}\Delta z_2 \\
\Delta\dot{z}_2 &= \theta_2\Delta x_2 - \alpha\Delta z_1 - \frac{\beta}{\alpha}\Delta z_2
\end{aligned} \tag{S20}$$

where

$$\alpha = \frac{\theta_1\theta_2 k}{\gamma_p^2}, \quad \beta = \eta\mu.$$

Taking the Laplace transform of $\Delta\dot{w} = b_z\Delta z_1 - b_w\Delta w$, we have

$$W = \frac{b_z}{s + b_w} Z_1$$

where W and Z_1 are the Laplace transforms of w and z_1. We have

$$-b_x X_2 + b_w W = -B_x \frac{s}{1 + \frac{s}{b_w}} X_2 = -C_b(s) X_2$$

where

$$C_b = B_x \frac{s}{1 + \frac{s}{b_w}}.$$

Taking the Laplace transform of (S20), we have

$$\begin{aligned}
(s + \gamma_p)X_1 &= \theta_1 Z_1 \\
(s + \gamma_p + C_b)X_2 &= kX_1 \\
(s + \alpha)Z_1 &= -\frac{\beta}{\alpha} Z_2 \\
\left(s + \frac{\beta}{\alpha}\right) Z_2 &= \theta_2 X_2 - \alpha Z_1.
\end{aligned}$$

Combining, we have

$$\begin{aligned}
(s + \gamma_p)(s + \gamma_p + C_b)X_2 &= \theta_1 k Z_1 \\
(s + \alpha)\left(s + \frac{\beta}{\alpha}\right) Z_1 &= -\frac{\beta}{\alpha}(\theta_2 X_2 - \alpha Z_1).
\end{aligned}$$

Simplifying, we have

$$s\left(s + \alpha + \frac{\beta}{\alpha}\right) Z_1 = -\frac{\beta}{\alpha}\theta_2 X_2.$$

Taking the strong antithetic binding limit of the sequestration mechanism $\left(\beta \gg \max\left\{\alpha^2, \gamma_p\alpha\right\}\right)$, we have

$$s\left(s + \frac{\beta}{\alpha}\right) Z_1 = -\frac{\beta}{\alpha}\theta_2 X_2$$

and so

$$(s + \gamma_p)(s + \gamma_p + C_b)s\left(s + \frac{\beta}{\alpha}\right) X_2 = -\beta\gamma_p^2 X_2.$$

bioRxiv preprint doi: https://doi.org/10.1101/2021.04.18.440372; this version posted September 29, 2021. The copyright holder for this preprint (which was not certified by peer review) is the author/funder, who has granted bioRxiv a license to display the preprint in perpetuity. It is made available under aCC-BY-NC-ND 4.0 International license.

Rewriting C_b, we have

$$(s+\gamma_p)\left(s+\gamma_p+B_x\frac{s}{1+\frac{s}{b_w}}\right)s\left(s+\frac{\beta}{\alpha}\right)X_2=-\beta\gamma_p^2X_2.$$

and so the characteristic equation is

$$(s+\gamma_p)\left((s+\gamma_p)\left(1+\frac{s}{b_w}\right)+B_xs\right)s\left(s+\frac{\beta}{\alpha}\right)=-\beta\gamma_p^2\left(1+\frac{s}{b_w}\right).$$

Substituting $s=i\omega\gamma_p$, we have

$$(1+i\omega)\left((1+i\omega)\left(1+i\omega\frac{\gamma_p}{b_w}\right)+i\omega B_x\right)i\omega\left(i\omega+\frac{\beta}{\gamma_p\alpha}\right)=-\frac{\beta}{\gamma_p^2}\left(1+i\omega\frac{\gamma_p}{b_w}\right).$$

Taking the strong antithetic binding limit where $|i\omega|\ll\frac{\beta}{\gamma_p\alpha}$, we have

$$\left(1-\frac{\gamma_p}{b_w}\omega^2+i\omega\left(1+B_x+\frac{\gamma_p}{b_w}\right)\right)(1+i\omega)i\omega=-\frac{\alpha}{\gamma_p}\left(1+i\omega\frac{\gamma_p}{b_w}\right).$$

The magnitude constraint is

$$\left(\left(\left(1-\frac{\gamma_p}{b_w}\omega^2\right)^2+\omega^2\left(1+B_x+\frac{\gamma_p}{b_w}\right)^2\right)^{0.5}(1+\omega^2)^{0.5}\omega=\frac{\alpha}{\gamma_p}\left(1+\frac{\gamma_p^2}{b_w^2}\omega^2\right)^{0.5}\tag{S21}$$

and the phase constraint is

$$\tan^{-1}\left(\frac{\omega\left(1+B_x+\frac{\gamma_p}{b_w}\right)}{1-\frac{\gamma_p}{b_w}\omega^2}\right)+\tan^{-1}(\omega)+\frac{\pi}{2}=\tan^{-1}\left(\frac{\gamma_p}{b_w}\omega\right)+\pi+2k\pi.$$

for some integer k. Using trigonometric identities and rearranging, we have

$$\tan^{-1}\left(\frac{\omega\left(1+B_x+\frac{\gamma_p}{b_w}\right)}{1-\frac{\gamma_p}{b_w}\omega^2}\right)-\frac{\pi}{4}=\tan^{-1}\left(\frac{\left(\frac{\gamma_p}{b_w}-1\right)\omega}{1+\frac{\gamma_p}{b_w}\omega^2}\right)+\frac{\pi}{4}+2k\pi.$$

Taking the tangent of both sides, we have

$$\frac{\frac{\omega\left(1+B_x+\frac{\gamma_p}{b_w}\right)}{1-\frac{\gamma_p}{b_w}\omega^2}-1}{1+\frac{\omega\left(1+B_x+\frac{\gamma_p}{b_w}\right)}{1-\frac{\gamma_p}{b_w}\omega^2}}=\frac{\frac{\left(\frac{\gamma_p}{b_w}-1\right)\omega}{1+\frac{\gamma_p}{b_w}\omega^2}+1}{1-\frac{\left(\frac{\gamma_p}{b_w}-1\right)\omega}{1+\frac{\gamma_p}{b_w}\omega^2}}.$$

Multiplying out fractions, we have

$$\frac{\omega\left(1+B_x+\frac{\gamma_p}{b_w}\right)-\left(1-\frac{\gamma_p}{b_w}\omega^2\right)}{1-\frac{\gamma_p}{b_w}\omega^2+\omega\left(1+B_x+\frac{\gamma_p}{b_w}\right)}=\frac{\left(\frac{\gamma_p}{b_w}-1\right)\omega+1+\frac{\gamma_p}{b_w}\omega^2}{1+\frac{\gamma_p}{b_w}\omega^2-\left(\frac{\gamma_p}{b_w}-1\right)\omega}.$$

Simplifying, we have

$$\frac{\gamma_p^2}{b_w^2}\omega^4+\left(1+B_x+\frac{\gamma_p}{b_w}\right)\left(1-\frac{\gamma_p}{b_w}\right)\omega^2-1=0$$

bioRxiv preprint doi: https://doi.org/10.1101/2021.04.18.440372; this version posted September 29, 2021. The copyright holder for this preprint (which was not certified by peer review) is the author/funder, who has granted bioRxiv a license to display the preprint in perpetuity. It is made available under aCC-BY-NC-ND 4.0 International license.

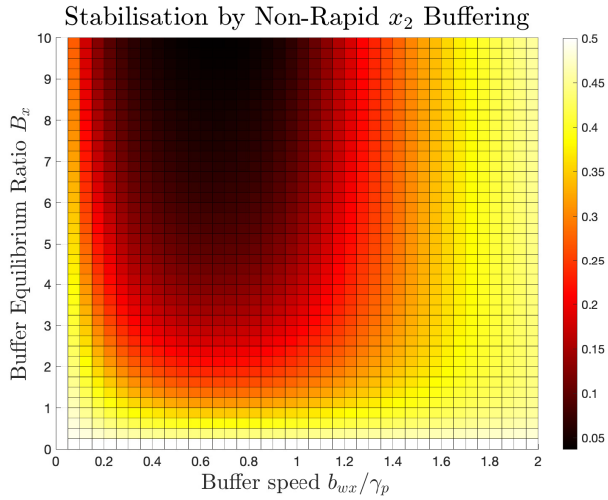

FIG. S3. Stabilisation effect F in (S22) where smaller implies improved stability.

Solving for ω^2 and using the same approach as in previous sections, the magnitude constraint leads to the stability

$$\gamma_p^3 > \theta_1\theta_2 k \underbrace{\frac{1}{(1+\omega^2)^{0.5}\omega}\left(\frac{1+\frac{\gamma_p^2}{b_w^2}\omega^2}{\left(\left(1-\frac{\gamma_p}{b_w}\omega^2\right)^2+\omega^2\left(1+B_x+\frac{\gamma_p}{b_w}\right)^2\right)}\right)^{0.5}}_{\mathrm{F}} \tag{S22}$$

$$\omega^2 = \frac{b_w^2}{2\gamma_p^2}\left[\sqrt{\left(1+B_x+\frac{\gamma_p}{b_w}\right)^2\left(1-\frac{\gamma_p}{b_w}\right)^2+4\frac{\gamma_p^2}{b_w^2}}-\left(1+B_x+\frac{\gamma_p}{b_w}\right)\left(1-\frac{\gamma_p}{b_w}\right)\right].$$

where F, which is the stabilisation effect independent of the integral gain, can be seen as a function of B_x and $\frac{b_w}{\gamma_p}$ in Figure S3.

For the special case where we set $b_w = \gamma_p$ then we have $\omega^2 = 1$ and so the stability constraint is

$$\gamma_p^3 > \frac{\theta_1\theta_2 k}{2+B_x}. \tag{S23}$$

SI2.4. Stability of Antithetic Feedback: Rapid x_2 Buffering with Degradation

In this section, we analyse the stabilising effect of buffering at the output species x_2 on antithetic integral feedback, where the buffering can be degraded. Consider the model (S5) with buffering at x_2 that is degraded

$$\begin{aligned}
\dot{x}_1 &= \theta_1 z_1 - \gamma_p x_1 \\
\dot{x}_2 &= k x_1 - \gamma_p x_2 - b_x x_2 + b_w w_x \\
\dot{w}_x &= b_x x_2 - b_w w_x - \gamma_x w_x \\
\dot{z}_1 &= \mu - \eta z_1 z_2 \\
\dot{z}_2 &= \theta_2 x_2 - \eta z_1 z_2
\end{aligned}$$

where w_x is the buffering species of x_2, and b_x, b_w are the kinetic rates for the buffering reactions. If we assume rapid buffering such that $w_x + x_2$ is the slow variable, $w_x = B_x x_2$ and $B_x = \frac{b_x}{b_w+\gamma_x}$, and use the methodology from

bioRxiv preprint doi: https://doi.org/10.1101/2021.04.18.440372; this version posted September 29, 2021. The copyright holder for this preprint (which was not certified by peer review) is the author/funder, who has granted bioRxiv a license to display the preprint in perpetuity. It is made available under aCC-BY-NC-ND 4.0 International license.

SI1 and SI2.1 then we have the reduced model

$$\begin{aligned}\dot{x}_1 &= \theta_1 z_1 - \gamma_p x_1\\ (1+B_x)\dot{x}_2 &= k x_1 - (\gamma_p + B_x\gamma_x)x_2\\ \dot{z}_1 &= \mu - \eta z_1 z_2\\ \dot{z}_2 &= \theta_2 x_2 - \eta z_1 z_2.\end{aligned}$$

SI2.4.a. Steady State Analysis

We next analyse the steady state. We have

$$\dot{z}_1 - \dot{z}_2 = \mu - \theta_2 x_2$$

and so the steady state of the output is

$$x_2 = \frac{\mu}{\theta_2}.$$

We also have corresponding steady states

$$\begin{aligned}x_1 &= \frac{\gamma_p}{k}\left(1 + B_x\frac{\gamma_x}{\gamma_p}\right)\frac{\mu}{\theta_2}\\ z_1 &= \frac{\gamma_p}{\theta_1}x_1 = \frac{\gamma_p^2\mu}{\theta_1 k\theta_2}\left(1+B_x\frac{\gamma_x}{\gamma_p}\right) = \frac{\mu}{\alpha}\left(1+B_x\frac{\gamma_x}{\gamma_p}\right)\\ z_2 &= \frac{1}{\eta}\frac{\mu}{z_1} = \frac{\alpha}{\eta\left(1+B_x\frac{\gamma_x}{\gamma_p}\right)}\end{aligned}$$

where $\alpha = \frac{\theta_1\theta_2 k}{\gamma_p^2}$.

SI2.4.b. Linearised Model

We next analyse the stability of the system. If we linearise about the steady states, we have

$$\begin{aligned}\Delta\dot{x}_1 &= \theta_1\Delta z_1 - \gamma_p\Delta x_1\\ (1+B_x)\Delta\dot{x}_2 &= k\Delta x_1 - \gamma_p\left(1+B_x\frac{\gamma_x}{\gamma_p}\right)\Delta x_2\\ \Delta\dot{z}_1 &= -\eta\bar{z}_2\Delta z_1 - \eta\bar{z}_1\Delta z_2\\ \Delta\dot{z}_2 &= \theta_2\Delta x_2 - \eta\bar{z}_2\Delta z_1 - \eta\bar{z}_1\Delta z_2.\end{aligned}$$

This system can be rewritten as

$$\begin{aligned}\Delta\dot{x}_1 &= \theta_1\Delta z_1 - \gamma_p\Delta x_1\\ (1+B_x)\Delta\dot{x}_2 &= k\Delta x_1 - \gamma_p\left(1+B_x\frac{\gamma_x}{\gamma_p}\right)\Delta x_2\\ \Delta\dot{z}_1 &= -\frac{\alpha}{\left(1+B_x\frac{\gamma_x}{\gamma_p}\right)}\Delta z_1 - \frac{\beta\left(1+B_x\frac{\gamma_x}{\gamma_p}\right)}{\alpha}\Delta z_2\\ \Delta\dot{z}_2 &= \theta_2\Delta x_2 - \frac{\alpha}{\left(1+B_x\frac{\gamma_x}{\gamma_p}\right)}\Delta z_1 - \frac{\beta\left(1+B_x\frac{\gamma_x}{\gamma_p}\right)}{\alpha}\Delta z_2.\end{aligned}$$

bioRxiv preprint doi: https://doi.org/10.1101/2021.04.18.440372; this version posted September 29, 2021. The copyright holder for this preprint (which was not certified by peer review) is the author/funder, who has granted bioRxiv a license to display the preprint in perpetuity. It is made available under aCC-BY-NC-ND 4.0 International license.

where $\alpha = \frac{\theta_1\theta_2 k}{\gamma_p^2}$ and $\beta = \eta\mu$. Taking the Laplace transforms, we have

$$
\begin{aligned}
&(s+\gamma_p)X_1 = \theta_1 Z_1 \\
&(1+B_x)\left(s+\frac{\gamma_p+B_x\gamma_x}{1+B_x}\right)X_2 = kX_1 \\
&\left(s+\frac{\alpha}{\left(1+B_x\frac{\gamma_x}{\gamma_p}\right)}\right)Z_1 = -\frac{\beta\left(1+B_x\frac{\gamma_x}{\gamma_p}\right)}{\alpha}Z_2 \\
&\left(s+\frac{\beta\left(1+B_x\frac{\gamma_x}{\gamma_p}\right)}{\alpha}\right)Z_2 = \theta_2 X_2 - \frac{\alpha}{\left(1+B_x\frac{\gamma_x}{\gamma_p}\right)}Z_1
\end{aligned}
$$

where $Z_1 = \mathcal{L}\{\Delta z_1\}$, $Z_2 = \mathcal{L}\{\Delta z_2\}$, $X_1 = \mathcal{L}\{\Delta x_1\}$, $X_2 = \mathcal{L}\{\Delta x_2\}$ are the Laplace transforms of the time-domain concentration deviations. Substituting, we have

$$
\begin{aligned}
&(1+B_x)(s+\gamma_p)\left(s+\frac{\gamma_p+B_x\gamma_x}{1+B_x}\right)X_2 = \theta_1 k Z_1 \\
&\left(s+\frac{\alpha}{\left(1+B_x\frac{\gamma_x}{\gamma_p}\right)}\right)\left(s+\frac{\beta\left(1+B_x\frac{\gamma_x}{\gamma_p}\right)}{\alpha}\right)Z_1 \\
&= -\frac{\beta\left(1+B_x\frac{\gamma_x}{\gamma_p}\right)}{\alpha}\left(\theta_2 X_2 - \frac{\alpha}{\left(1+B_x\frac{\gamma_x}{\gamma_p}\right)}Z_1\right).
\end{aligned}
$$

Rewriting and substituting, we have

$$
\begin{aligned}
&(1+B_x)(s+\gamma_p)\left(s+\frac{\gamma_p+B_x\gamma_x}{1+B_x}\right)s\left(s+\frac{\alpha}{\left(1+B_x\frac{\gamma_x}{\gamma_p}\right)}+\frac{\beta\left(1+B_x\frac{\gamma_x}{\gamma_p}\right)}{\alpha}\right)X_2 \\
&= -\frac{\beta\left(1+B_x\frac{\gamma_x}{\gamma_p}\right)}{\alpha}\theta_1\theta_2 k X_2.
\end{aligned}
$$

Simplifying and taking the limit of strong binding for the sequestration process in the antithetic integral feedback $\left(\beta \gg \frac{\alpha^2}{\left(1+B_x\frac{\gamma_x}{\gamma_p}\right)^2}, \frac{\alpha\gamma_p}{\left(1+B_x\frac{\gamma_x}{\gamma_p}\right)}\right)$ then

$$
(1+B_x)(s+\gamma_p)\left(s+\frac{\gamma_p+B_x\gamma_x}{1+B_x}\right)s\left(s+\frac{\beta\left(1+B_x\frac{\gamma_x}{\gamma_p}\right)}{\alpha}\right)X_2 = -\frac{\beta\left(1+B_x\frac{\gamma_x}{\gamma_p}\right)}{\alpha}\theta_1\theta_2 k X_2.
$$

Thus we have the characteristic equation

$$
(1+B_x)(s+\gamma_p)\left(s+\frac{\gamma_p+B_x\gamma_x}{1+B_x}\right)s\left(s+\frac{\beta\left(1+B_x\frac{\gamma_x}{\gamma_p}\right)}{\alpha}\right)+\beta\gamma_p^2\left(1+B_x\frac{\gamma_x}{\gamma_p}\right)=0.
$$

Substituting $s = \gamma_p\sigma$, we have

$$
(1+B_x)(1+\sigma)\left(\sigma+\frac{1+B_x\frac{\gamma_x}{\gamma_p}}{1+B_x}\right)\sigma\left(\sigma+\frac{\beta\left(1+B_x\frac{\gamma_x}{\gamma_p}\right)}{\gamma_p\alpha}\right) = -\frac{\beta}{\gamma_p^2}\left(1+B_x\frac{\gamma_x}{\gamma_p}\right).
$$

Using the same argument as that in SI2.1, for the stability boundary with strong binding there is a negative real and complex pair of roots in the region $|\sigma| \ll \frac{\beta\left(1+B_x\frac{\gamma_x}{\gamma_y}\right)}{\gamma_p\alpha}$, as well as one large negative root.

bioRxiv preprint doi: https://doi.org/10.1101/2021.04.18.440372; this version posted September 29, 2021. The copyright holder for this preprint (which was not certified by peer review) is the author/funder, who has granted bioRxiv a license to display the preprint in perpetuity. It is made available under aCC-BY-NC-ND 4.0 International license.

To determine the boundary of stability, we next determine the conditions for which the roots are purely imaginary. Substituting $s = i\omega\gamma_p$, we have

$$(1+B_x)(1+i\omega)\left(i\omega + \frac{1+B_x\frac{\gamma_x}{\gamma_p}}{1+B_x}\right) i\omega \left(i\omega + \frac{\beta\left(1+B_x\frac{\gamma_x}{\gamma_p}\right)}{\gamma_p\alpha}\right) = -\frac{\beta}{\gamma_p^2}\left(1+B_x\frac{\gamma_x}{\gamma_p}\right).$$

Taking the strong antithetic binding limit where $|i\omega| \ll \frac{\beta\left(1+B_x\frac{\gamma_x}{\gamma_y}\right)}{\gamma_p\alpha}$, we have

$$(1+i\omega)\left(i\omega + \frac{1+B_x\frac{\gamma_x}{\gamma_p}}{1+B_x}\right) i\omega = -\frac{\alpha}{\gamma_p(1+B_x)}.$$

The phase and magnitude constraints are

$$(1+\omega^2)^{0.5}\left(\omega^2 + \left(\frac{1+B_x\frac{\gamma_x}{\gamma_p}}{1+B_x}\right)^2\right)^{0.5}\omega = \frac{\alpha}{\gamma_p(1+B_x)}$$

$$\tan^{-1}(\omega) + \tan^{-1}\left(\frac{1+B_x}{1+B_x\frac{\gamma_x}{\gamma_p}}\omega\right) = \frac{\pi}{2} + 2k\pi$$

for some integer k. Solving the phase constraint, we have

$$\frac{\omega-1}{1+\omega} = \frac{1-C\omega}{1+C\omega}$$
$$C = \frac{1+B_x}{1+B_x\frac{\gamma_x}{\gamma_p}}.$$

For this constraint we require

$$C\omega^2 = 1$$

which reduces to

$$\omega^2 = \frac{1+B_x\frac{\gamma_x}{\gamma_p}}{1+B_x}.$$

Substituting into the magnitude equation, we have

$$\frac{\alpha}{\gamma_p(1+B_x)} = (1+C)^{0.5}\left(C+C^{-2}\right)^{0.5}C^{-0.5}$$
$$= (1+C)C.$$

Rearranging, we have the stability condition

$$\boxed{\gamma_p^3 > \frac{\theta_1\theta_2 k}{2+\left(1+\frac{\gamma_x}{\gamma_p}\right)B_x}\frac{1+B_x}{1+\frac{\gamma_x}{\gamma_p}B_x}}.$$

We can differentiate the right hand side with respect to B_x to determine whether increasing B_x has a stabilising effect. If we set

$$f(B_x) = \frac{1+B_x}{\left(2+\left(1+\frac{\gamma_x}{\gamma_p}\right)B_x\right)\left(1+\frac{\gamma_x}{\gamma_p}B_x\right)}.$$

then

$$\frac{\partial f}{\partial B_x} = \frac{1-3\frac{\gamma_x}{\gamma_p}-2\frac{\gamma_x}{\gamma_p}\left(1+\frac{\gamma_x}{\gamma_p}\right)B_x-(1+\frac{\gamma_x}{\gamma_p})\frac{\gamma_x}{\gamma_p}B_x^2}{\left(2+\left(1+\frac{\gamma_x}{\gamma_p}\right)B_x\right)^2\left(1+\frac{\gamma_x}{\gamma_p}B_x\right)^2}.$$

Thus for small B_x then buffering stabilises antithetic integral feedback if $\gamma_x > \frac{1}{3}\gamma_p$. For large B_x then increasing B_x improves stability if $\gamma_x > 0$.

bioRxiv preprint doi: https://doi.org/10.1101/2021.04.18.440372; this version posted September 29, 2021. The copyright holder for this preprint (which was not certified by peer review) is the author/funder, who has granted bioRxiv a license to display the preprint in perpetuity. It is made available under aCC-BY-NC-ND 4.0 International license.

SI2.5. Stability of Antithetic Feedback: Rapid x_1 Buffering with Degradation

In this section, we analyse the stabilising effect of buffering at the intermediate species x_1 on antithetic integral feedback, where the buffering can be degraded. This section uses identical methodology and obtains equivalent results to SI2.4.
Consider the model (S4) with buffering at x_1 that is degraded

$$\begin{aligned}
\dot{x}_1 &= \theta_1 z_1 - \gamma_p x_1 - b_i x_1 + b_w w_i \\
\dot{x}_2 &= k x_1 - \gamma_p x_2 \\
\dot{w}_i &= b_i x_1 - b_w w_i - \gamma_i w_x \\
\dot{z}_1 &= \mu - \eta z_1 z_2 \\
\dot{z}_2 &= \theta_2 x_2 - \eta z_1 z_2
\end{aligned}$$

where w_i is the buffering species of x_1, and b_i, b_w are the kinetic rates for the buffering reactions. If we assume rapid buffering such that $w_i + x_1$ is the slow variable, $w_i = B_i x_1$ and $B_i = \frac{b_i}{b_w + \gamma_i}$, and use the methodology from SI2.4 then

$$\begin{aligned}
(1 + B_i)\dot{x}_1 &= \theta_1 z_1 - (\gamma_p + B_x \gamma_i) x_1 \\
\dot{x}_2 &= k x_1 - \gamma_p x_2 \\
\dot{z}_1 &= \mu - \eta z_1 z_2 \\
\dot{z}_2 &= \theta_2 x_2 - \eta z_1 z_2.
\end{aligned}$$

SI2.5.a. Steady State Analysis

We next analyse the steady state. We have

$$\dot{z}_1 - \dot{z}_2 = \mu - \theta_2 x_2$$

and so the steady state of the output is

$$x_2 = \frac{\mu}{\theta_2}.$$

The corresponding steady states of the other species are

$$\begin{aligned}
x_1 &= \frac{\gamma_p}{k} x_2 = \frac{\gamma_p}{k} \frac{\mu}{\theta_2} \\
z_1 &= \frac{(\gamma_p + B_i \gamma_i)}{\theta_1} x_1 = \frac{\gamma_p^2 \mu}{\theta_1 \theta_2 k} \left(1 + B_i \frac{\gamma_i}{\gamma_p}\right) = \frac{\mu}{\alpha} \left(1 + B_i \frac{\gamma_i}{\gamma_p}\right) \\
z_2 &= \frac{1}{\eta} \frac{\mu}{z_1} = \frac{\alpha}{\eta \left(1 + B_i \frac{\gamma_i}{\gamma_p}\right)}
\end{aligned}$$

where $\alpha = \frac{\theta_1 \theta_2 k}{\gamma_p^2}$.

SI2.5.b. Stability Analysis

We next study the stability of the system. If we linearise about the steady states, we have

$$\begin{aligned}
(1 + B_i)\Delta\dot{x}_1 &= \theta_1 \Delta z_1 - \gamma_p \left(1 + B_i \frac{\gamma_i}{\gamma_p}\right) \Delta x_1 \\
\Delta\dot{x}_2 &= k \Delta x_1 - \gamma_p \Delta x_2 \\
\Delta\dot{z}_1 &= -\eta \bar{z}_2 \Delta z_1 - \eta \bar{z}_1 \Delta z_2 \\
\Delta\dot{z}_2 &= \theta_2 \Delta x_2 - \eta \bar{z}_2 \Delta z_1 - \eta \bar{z}_1 \Delta z_2.
\end{aligned}$$

bioRxiv preprint doi: https://doi.org/10.1101/2021.04.18.440372; this version posted September 29, 2021. The copyright holder for this preprint (which was not certified by peer review) is the author/funder, who has granted bioRxiv a license to display the preprint in perpetuity. It is made available under aCC-BY-NC-ND 4.0 International license.

This system can be rewritten as

$$
\begin{aligned}
(1+B_i)\Delta\dot{x}_1 &= \theta_1\Delta z_1 - \gamma_p\left(1+B_i\frac{\gamma_i}{\gamma_p}\right)\Delta x_1 \\
\Delta\dot{x}_2 &= k\Delta x_1 - \gamma_p\Delta x_2 \\
\Delta\dot{z}_1 &= -\frac{\alpha}{\left(1+B_i\frac{\gamma_i}{\gamma_p}\right)}\Delta z_1 - \frac{\beta\left(1+B_i\frac{\gamma_i}{\gamma_p}\right)}{\alpha}\Delta z_2 \\
\Delta\dot{z}_2 &= \theta_2\Delta x_2 - \frac{\alpha}{\left(1+B_i\frac{\gamma_i}{\gamma_p}\right)}\Delta z_1 - \frac{\beta\left(1+B_i\frac{\gamma_i}{\gamma_p}\right)}{\alpha}\Delta z_2.
\end{aligned}
$$

where $\alpha = \frac{\theta_1\theta_2 k}{\gamma_p^2}$ and $\beta = \eta\mu$. Taking the Laplace transforms, we have

$$
\begin{aligned}
&(1+B_i)\left(s+\frac{\gamma_p+B_i\gamma_i}{1+B_i}\right)X_1 = \theta_1 Z_1 \\
&(s+\gamma_p)X_2 = kX_1 \\
&\left(s+\frac{\alpha}{\left(1+B_i\frac{\gamma_i}{\gamma_p}\right)}\right)Z_1 = -\frac{\beta\left(1+B_i\frac{\gamma_i}{\gamma_p}\right)}{\alpha}Z_2 \\
&\left(s+\frac{\beta\left(1+B_i\frac{\gamma_i}{\gamma_p}\right)}{\alpha}\right)Z_2 = \theta_2 X_2 - \frac{\alpha}{\left(1+B_i\frac{\gamma_i}{\gamma_p}\right)}Z_1
\end{aligned}
$$

where $Z_1 = \mathcal{L}\{\Delta z_1\}$, $Z_2 = \mathcal{L}\{\Delta z_2\}$, $X_1 = \mathcal{L}\{\Delta x_1\}$, $X_2 = \mathcal{L}\{\Delta x_2\}$ are the Laplace transforms of the time-domain concentration deviations. Substituting, we have

$$
\begin{aligned}
&(1+B_i)(s+\gamma_p)\left(s+\frac{\gamma_p+B_i\gamma_i}{1+B_i}\right)X_2 = \theta_1 k Z_1 \\
&\left(s+\frac{\alpha}{\left(1+B_i\frac{\gamma_i}{\gamma_p}\right)}\right)\left(s+\frac{\beta\left(1+B_i\frac{\gamma_i}{\gamma_p}\right)}{\alpha}\right)Z_1 = -\frac{\beta\left(1+B_i\frac{\gamma_i}{\gamma_p}\right)}{\alpha}\left(\theta_2 X_2 - \frac{\alpha}{\left(1+B_i\frac{\gamma_i}{\gamma_p}\right)}Z_1\right).
\end{aligned}
$$

Rewriting and substituting, we have

$$
(1+B_i)(s+\gamma_p)\left(s+\frac{\gamma_p+B_i\gamma_i}{1+B_i}\right)s\left(s+\frac{\alpha}{\left(1+B_i\frac{\gamma_i}{\gamma_p}\right)}+\frac{\beta\left(1+B_i\frac{\gamma_i}{\gamma_p}\right)}{\alpha}\right)X_2 = -\frac{\beta\left(1+B_i\frac{\gamma_i}{\gamma_p}\right)}{\alpha}\theta_1\theta_2 k X_2.
$$

The above equation is equivalent to x_2 buffering (see SI2.5), and so for strong integral binding we have the stability condition

$$
\gamma_p^3 > \frac{\theta_1\theta_2 k}{2+\left(1+\frac{\gamma_i}{\gamma_p}\right)B_i}\frac{1+B_i}{1+\frac{\gamma_i}{\gamma_p}B_i}
$$

which is equivalent to the case of x_2 buffering.

bioRxiv preprint doi: https://doi.org/10.1101/2021.04.18.440372; this version posted September 29, 2021. The copyright holder for this preprint (which was not certified by peer review) is the author/funder, who has granted bioRxiv a license to display the preprint in perpetuity. It is made available under aCC-BY-NC-ND 4.0 International license.

SI3. BUFFERING CAN ENABLE NEAR-PERFECT ADAPTATION DESPITE LEAKY INTEGRATION

SI3.1. Rapid x_2 Buffering with Degradation can Enable Near-Perfect Adaptation

In this section, we analyse the ability of buffering at x_2 to enable near perfect adaptation by stabilising antithetic integral feedback. Consider the model (S5) with buffering at x_2 that is degraded

$$\begin{aligned}
\dot{x}_1 &= \theta_1 z_1 - \gamma_p x_1 \\
\dot{x}_2 &= k x_1 - \gamma_p x_2 - b_x x_2 + b_w w_x \\
\dot{w}_x &= b_x x_2 - b_w w_x - \gamma_x w_x \\
\dot{z}_1 &= \mu - \eta z_1 z_2 - \gamma_c z_1 \\
\dot{z}_2 &= \theta_2 x_2 - \eta z_1 z_2 - \gamma_c z_2
\end{aligned}$$

where w_x is the buffering species of x_2, and b_x, b_w are the kinetic rates for the buffering reactions. Assuming that the buffer rapidly reaches equilibrium then using the methodology from SI1 and SI2.1, we have the reduced model

$$\begin{aligned}
\dot{x}_1 &= \theta_1 z_1 - \gamma_p x_1 \\
(1 + B_x)\dot{x}_2 &= k x_1 - (\gamma_p + B_x \gamma_x) x_2 \\
\dot{z}_1 &= \mu - \eta z_1 z_2 - \gamma_c z_1 \\
\dot{z}_2 &= \theta_2 x_2 - \eta z_1 z_2 - \gamma_c z_2.
\end{aligned} \tag{S24}$$

where

$$\begin{aligned}
B_x &= \frac{b_x}{b_w + \gamma_c} \\
w_x &= B_x x_2.
\end{aligned}$$

SI3.1.a. Steady State Analysis

We next analyse the steady state. We have

$$\dot{z}_1 - \dot{z}_2 = \mu - \theta_2 x_2 - \gamma_c z_1 + \gamma_c z_2$$

and so the steady state of the output is

$$x_2 = \frac{\mu}{\theta_2} - \frac{\gamma_c}{\theta_2} z_1 + \frac{\gamma_c}{\theta_2} z_2.$$

We also have the steady state

$$z_2 = \frac{1}{\eta}\left(\frac{\mu}{z_1} - \gamma_c\right)$$

and so

$$x_2 = \frac{\mu}{\theta_2} - \frac{\gamma_c^2}{\theta_2 \eta} - \frac{\gamma_c}{\theta_2} z_1 + \frac{\gamma_c \mu}{\theta_2 \eta} \frac{1}{z_1}.$$

The other species have the steady states

$$\begin{aligned}
x_1 &= \frac{\gamma_p}{k}\left(1 + B_x \frac{\gamma_x}{\gamma_p}\right) x_2 \\
z_1 &= \frac{\gamma_p}{\theta_1} x_1 = \frac{\gamma_p^2}{\theta_1 k}\left(1 + B_x \frac{\gamma_x}{\gamma_p}\right) x_2 = \frac{\theta_2}{\alpha}\left(1 + B_x \frac{\gamma_x}{\gamma_p}\right) x_2
\end{aligned}$$

bioRxiv preprint doi: https://doi.org/10.1101/2021.04.18.440372; this version posted September 29, 2021. The copyright holder for this preprint (which was not certified by peer review) is the author/funder, who has granted bioRxiv a license to display the preprint in perpetuity. It is made available under aCC-BY-NC-ND 4.0 International license.

where $\alpha = \frac{\theta_1\theta_2 k}{\gamma_p^2}$. Substituting, we have

$$\left(1+\frac{\gamma_c}{\alpha}\left(1+B_x\frac{\gamma_x}{\gamma_p}\right)\right)x_2^2 = \left(\frac{\mu}{\theta_2}-\frac{\gamma_c^2}{\theta_2\eta}\right)x_2 + \frac{\gamma_c\mu\alpha}{\theta_2^2\eta\left(1+B_x\frac{\gamma_x}{\gamma_p}\right)}. \tag{S25}$$

We assume strong binding of the sequestration mechanism in antithetic integral feedback (η large), which for steady state is the condition

$$\beta \gg \frac{\gamma_c^2}{\mu}, \frac{\gamma_c\mu\alpha}{\theta_2^2\left(1+B_x\frac{\gamma_x}{\gamma_p}\right)}.$$

With this assumption, we have

$$\left(1+\frac{\gamma_c}{\alpha}\left(1+B_x\frac{\gamma_x}{\gamma_p}\right)\right)x_2^2 = \frac{\mu}{\theta_2}x_2.$$

We ignore the zero solution, which corresponds to a negative solution in (S25), and so the steady state concentrations are

$$\boxed{x_2 = \frac{\mu}{\theta_2}\frac{1}{1+\frac{\gamma_c}{\alpha}\left(1+B_x\frac{\gamma_x}{\gamma_p}\right)}}$$

$$x_1 = \frac{\gamma_p}{k}\frac{\mu}{\theta_2}\frac{\left(1+B_x\frac{\gamma_x}{\gamma_p}\right)}{1+\frac{\gamma_c}{\alpha}\left(1+B_x\frac{\gamma_x}{\gamma_p}\right)}, \quad z_1 = \frac{\mu\left(1+B_x\frac{\gamma_x}{\gamma_p}\right)}{\alpha+\gamma_c\left(1+B_x\frac{\gamma_x}{\gamma_p}\right)}, \quad z_2 = \frac{\alpha}{\eta\left(1+B_x\frac{\gamma_x}{\gamma_p}\right)}.$$

The steady state error of x_2 is

$$\boxed{\frac{x_{2n}-x_2}{x_{2n}} = \frac{1}{1+\Omega_x}, \quad \Omega_x = \frac{\alpha}{\gamma_c\left(1+B_x\frac{\gamma_x}{\gamma_p}\right)}}.$$

SI3.1.b. Stability Analysis

We next study the stability of the system. If we linearise (S24) about the steady state, we have

$$\begin{aligned}
\Delta\dot{x}_1 &= \theta_1\Delta z_1 - \gamma_p\Delta x_1 \\
(1+B_x)\Delta\dot{x}_2 &= k\Delta x_1 - \gamma_p\left(1+B_x\frac{\gamma_x}{\gamma_p}\right)\Delta x_2 \\
\Delta\dot{z}_1 &= -\eta\bar{z}_2\Delta z_1 - \eta\bar{z}_1\Delta z_2 - \gamma_c\Delta z_1 \\
\Delta\dot{z}_2 &= \theta_2\Delta x_2 - \eta\bar{z}_2\Delta z_1 - \eta\bar{z}_1\Delta z_2 - \gamma_c\Delta z_2.
\end{aligned}$$

This system can be rewritten as

$$\begin{aligned}
\Delta\dot{x}_1 &= \theta_1\Delta z_1 - \gamma_p\Delta x_1 \\
(1+B_x)\Delta\dot{x}_2 &= k\Delta x_1 - \gamma_p\left(1+B_x\frac{\gamma_x}{\gamma_p}\right)\Delta x_2 \\
\Delta\dot{z}_1 &= -\left(\frac{\alpha}{\left(1+B_x\frac{\gamma_x}{\gamma_p}\right)}+\gamma_c\right)\Delta z_1 - \frac{\beta\left(1+B_x\frac{\gamma_x}{\gamma_p}\right)}{\alpha+\gamma_c\left(1+B_x\frac{\gamma_x}{\gamma_p}\right)}\Delta z_2 \\
\Delta\dot{z}_2 &= \theta_2\Delta x_2 - \frac{\alpha}{\left(1+B_x\frac{\gamma_x}{\gamma_p}\right)}\Delta z_1 - \left(\frac{\beta\left(1+B_x\frac{\gamma_x}{\gamma_p}\right)}{\alpha+\gamma_c\left(1+B_x\frac{\gamma_x}{\gamma_p}\right)}+\gamma_c\right)\Delta z_2
\end{aligned}$$

bioRxiv preprint doi: https://doi.org/10.1101/2021.04.18.440372; this version posted September 29, 2021. The copyright holder for this preprint (which was not certified by peer review) is the author/funder, who has granted bioRxiv a license to display the preprint in perpetuity. It is made available under aCC-BY-NC-ND 4.0 International license.

where $\alpha = \frac{\theta_1\theta_2 k}{\gamma_p^2}$ and $\beta = \eta\mu$. Taking the Laplace transforms, we have

$$
\begin{aligned}
&(s+\gamma_p)X_1 = \theta_1 Z_1 \\
&(1+B_x)\left(s+\frac{\gamma_p+B_x\gamma_x}{1+B_x}\right)X_2 = kX_1 \\
&\left(s+\frac{\alpha}{\left(1+B_x\frac{\gamma_x}{\gamma_p}\right)}+\gamma_c\right)Z_1 = -\frac{\beta\left(1+B_x\frac{\gamma_x}{\gamma_p}\right)}{\alpha+\gamma_c\left(1+B_x\frac{\gamma_x}{\gamma_p}\right)}Z_2 \\
&\left(s+\frac{\beta\left(1+B_x\frac{\gamma_x}{\gamma_p}\right)}{\alpha+\gamma_c\left(1+B_x\frac{\gamma_x}{\gamma_p}\right)}+\gamma_c\right)Z_2 = \theta_2 X_2 - \frac{\alpha}{\left(1+B_x\frac{\gamma_x}{\gamma_p}\right)}Z_1
\end{aligned}
$$

where X_1, X_1, Z_1 andZ_2 are the Laplace transforms of $\Delta x_1, \Delta x_2, \Delta z_1$ andΔz_2. Substituting, we have

$$
\begin{aligned}
&(1+B_x)(s+\gamma_p)\left(s+\frac{\gamma_p+B_x\gamma_x}{1+B_x}\right)X_2 = \theta_1 k Z_1 \\
&\left(s+\frac{\alpha}{\left(1+B_x\frac{\gamma_x}{\gamma_p}\right)}+\gamma_c\right)\left(s+\frac{\beta\left(1+B_x\frac{\gamma_x}{\gamma_p}\right)}{\alpha+\gamma_c\left(1+B_x\frac{\gamma_x}{\gamma_p}\right)}+\gamma_c\right)Z_1 \\
&= -\frac{\beta\left(1+B_x\frac{\gamma_x}{\gamma_p}\right)}{\alpha+\gamma_c\left(1+B_x\frac{\gamma_x}{\gamma_p}\right)}\left(\theta_2 X_2 - \frac{\alpha}{\left(1+B_x\frac{\gamma_x}{\gamma_p}\right)}Z_1\right).
\end{aligned}
$$

Rewriting and substituting, we have

$$
\begin{aligned}
&(1+B_x)(s+\gamma_p)\left(s+\frac{\gamma_p+B_x\gamma_x}{1+B_x}\right)\left[(s+\gamma_c)\left(s+\frac{\alpha}{\left(1+B_x\frac{\gamma_x}{\gamma_p}\right)}+\frac{\beta\left(1+B_x\frac{\gamma_x}{\gamma_p}\right)}{\alpha+\gamma_c\left(1+B_x\frac{\gamma_x}{\gamma_p}\right)}+\gamma_c\right)\right]X_2 \\
&= -\frac{\beta\left(1+B_x\frac{\gamma_x}{\gamma_p}\right)}{\alpha+\gamma_c\left(1+B_x\frac{\gamma_x}{\gamma_p}\right)}\theta_1\theta_2 k X_2.
\end{aligned}
$$

Simplifying and taking the limit of strong binding of the sequestration mechanism in antithetic integral feedback

$$
\beta \gg \frac{\left(\alpha+\gamma_c\left(1+B_x\frac{\gamma_x}{\gamma_p}\right)\right)^2}{\left(1+B_x\frac{\gamma_x}{\gamma_p}\right)^2}, \frac{(\alpha+\gamma_c(1+B_x\frac{\gamma_x}{\gamma_p}))\gamma_p}{\left(1+B_x\frac{\gamma_x}{\gamma_p}\right)}
$$

then

$$
\begin{aligned}
&(1+B_x)(s+\gamma_p)\left(s+\frac{\gamma_p+B_x\gamma_x}{1+B_x}\right)(s+\gamma_c)\left(s+\frac{\beta\left(1+B_x\frac{\gamma_x}{\gamma_p}\right)}{\alpha+\gamma_c\left(1+B_x\frac{\gamma_x}{\gamma_p}\right)}\right)X_2 \\
&= -\frac{\beta\left(1+B_x\frac{\gamma_x}{\gamma_p}\right)}{\alpha+\gamma_c\left(1+B_x\frac{\gamma_x}{\gamma_p}\right)}\theta_1\theta_2 k X_2.
\end{aligned}
$$

Thus we have the characteristic equation

$$
(1+B_x)(s+\gamma_p)\left(s+\frac{\gamma_p+B_x\gamma_x}{1+B_x}\right)(s+\gamma_c)\left(s+\frac{\beta\left(1+B_x\frac{\gamma_x}{\gamma_p}\right)}{\alpha+\gamma_c\left(1+B_x\frac{\gamma_x}{\gamma_p}\right)}\right)+\beta\gamma_p^2\frac{\alpha\left(1+B_x\frac{\gamma_x}{\gamma_p}\right)}{\alpha+\gamma_c\left(1+B_x\frac{\gamma_x}{\gamma_p}\right)} = 0.
$$

bioRxiv preprint doi: https://doi.org/10.1101/2021.04.18.440372; this version posted September 29, 2021. The copyright holder for this preprint (which was not certified by peer review) is the author/funder, who has granted bioRxiv a license to display the preprint in perpetuity. It is made available under aCC-BY-NC-ND 4.0 International license.

Substituting $s = \gamma_p \sigma$, we have

$$(1+B_x)(1+\sigma)\left(\sigma + \frac{1+B_x\frac{\gamma_x}{\gamma_p}}{1+B_x}\right)\left(\sigma+\frac{\gamma_c}{\gamma_p}\right)\left(\sigma + \frac{\beta\left(1+B_x\frac{\gamma_x}{\gamma_p}\right)}{\gamma_p\left(\alpha+\gamma_c\left(1+B_x\frac{\gamma_x}{\gamma_p}\right)\right)}\right) = -\frac{\beta}{\gamma_p^2}\frac{\alpha\left(1+B_x\frac{\gamma_x}{\gamma_p}\right)}{\alpha+\gamma_c\left(1+B_x\frac{\gamma_x}{\gamma_p}\right)}.$$

Using the same argument as that used in SI2.1, for the stability boundary with strong binding there is a negative real and complex pair of roots in the region $|\sigma| \ll \frac{\beta\left(1+B_x\frac{\gamma_x}{\gamma_p}\right)}{\gamma_p\left(\alpha+\gamma_c\left(1+B_x\frac{\gamma_x}{\gamma_p}\right)\right)}$, as well as one large negative root.

To determine the boundary of stability, we next determine the conditions for which the roots are purely imaginary. Substituting $s = i\omega\gamma_p$, we have

$$(1+B_x)(1+i\omega)\left(i\omega + \frac{1+B_x\frac{\gamma_x}{\gamma_p}}{1+B_x}\right)\left(i\omega+\frac{\gamma_c}{\gamma_p}\right)\left(i\omega + \frac{\beta\left(1+B_x\frac{\gamma_x}{\gamma_p}\right)}{\gamma_p\left(\alpha+\gamma_c\left(1+B_x\frac{\gamma_x}{\gamma_p}\right)\right)}\right) = -\frac{\beta}{\gamma_p^2}\frac{\alpha\left(1+B_x\frac{\gamma_x}{\gamma_p}\right)}{\alpha+\gamma_c\left(1+B_x\frac{\gamma_x}{\gamma_p}\right)}.$$

Taking the strong antithetic binding limit where $|i\omega| \ll \frac{\beta\left(1+B_x\frac{\gamma_x}{\gamma_p}\right)}{\gamma_p\left(\alpha+\gamma_c\left(1+B_x\frac{\gamma_x}{\gamma_p}\right)\right)}$, we have

$$(1+i\omega)\left(i\omega + \frac{1+B_x\frac{\gamma_x}{\gamma_p}}{1+B_x}\right)\left(i\omega+\frac{\gamma_c}{\gamma_p}\right) = -\frac{\alpha}{\gamma_p(1+B_x)}.$$

The phase and magnitude constraints are

$$(1+\omega^2)^{0.5}\left(\omega^2 + \left(\frac{1+B_x\frac{\gamma_x}{\gamma_p}}{1+B_x}\right)^2\right)^{0.5}\left(\omega^2+\frac{\gamma_c^2}{\gamma_p^2}\right)^{0.5} = \frac{\alpha}{\gamma_p(1+B_x)}$$

$$\tan^{-1}(\omega) + \tan^{-1}\left(\frac{1+B_x}{1+B_x\frac{\gamma_x}{\gamma_p}}\omega\right) + \tan^{-1}\left(\frac{\gamma_p}{\gamma_c}\omega\right) = \pi + 2k\pi$$

for some integer k. Solving the phase constraint, we have

$$\tan^{-1}\left(\frac{(1+A^{-1})\omega + \frac{\gamma_p}{\gamma_c}\omega(1-A^{-1}\omega^2)}{1-\left(A^{-1}+(1+A^{-1})\frac{\gamma_p}{\gamma_c}\right)\omega^2}\right) = \pi + 2k\pi$$

$$A = \frac{1+B_x\frac{\gamma_x}{\gamma_p}}{1+B_x}.$$

For this we require

$$(1+A^{-1})\omega + \frac{\gamma_p}{\gamma_c}\omega(1-A^{-1}\omega^2) = 0$$

which reduces to

$$\omega^2 = \frac{\gamma_c}{\gamma_p}(1+A) + A.$$

Substituting into the magnitude equation, we have

$$\begin{aligned}
&\left(\left(1+\frac{\gamma_c}{\gamma_p}\right)(1+A)\right)^{0.5}\left(\left(\frac{\gamma_c}{\gamma_p}+A\right)(1+A)\right)^{0.5}\left(\left(\frac{\gamma_c}{\gamma_p}+1\right)\left(\frac{\gamma_c}{\gamma_p}+A\right)\right)^{0.5} \\
&= \left(1+\frac{\gamma_c}{\gamma_p}\right)(1+A)\left(\frac{\gamma_c}{\gamma_p}+A\right) \\
&= \frac{\alpha}{\gamma_p(1+B_x)}.
\end{aligned}$$

bioRxiv preprint doi: https://doi.org/10.1101/2021.04.18.440372; this version posted September 29, 2021. The copyright holder for this preprint (which was not certified by peer review) is the author/funder, who has granted bioRxiv a license to display the preprint in perpetuity. It is made available under aCC-BY-NC-ND 4.0 International license.

Simplifying, we have

$$\frac{\alpha}{\gamma_p(1+B_x)} = \left(1+\frac{\gamma_c}{\gamma_p}\right)(1+A)\left(\frac{\gamma_c}{\gamma_p}+A\right).$$

Multiplying by $A^{-1}\frac{\gamma_p}{\gamma_c}$, we have

$$\frac{\alpha}{\gamma_c\left(1+B_x\frac{\gamma_x}{\gamma_p}\right)} = A^{-1}\frac{\gamma_p}{\gamma_c}\left(1+\frac{\gamma_c}{\gamma_p}\right)(1+A)\left(\frac{\gamma_c}{\gamma_p}+A\right)$$
$$A = \frac{1+B_x\frac{\gamma_x}{\gamma_p}}{1+B_x}.$$

and so the stability condition is

$$\boxed{\Omega_x < \left(1+\frac{\gamma_c}{\gamma_p}\right)(1+A)\left(\frac{\gamma_p}{\gamma_c}+A^{-1}\right)}$$
$$\boxed{A = \frac{1+B_x\frac{\gamma_x}{\gamma_p}}{1+B_x}}$$

where

$$\Omega_x = \frac{\alpha}{\gamma_c\left(1+B_x\frac{\gamma_x}{\gamma_p}\right)}.$$

From earlier, we know that the steady state error of x_2 is

$$\frac{x_{2n}-x_2}{x_{2n}} = \frac{1}{1+\Omega_x}.$$

SI3.2. Non-Rapid x_2 Buffering can enable Near Perfect Adaptation

In this section, we analyse the ability of non-rapid buffering at z_1 to enable near perfect adaptation by stabilising antithetic integral feedback. We use the model

$$\begin{aligned}
\dot{x}_1 &= \theta_1 z_1 - \gamma_p x_1 \\
\dot{x}_2 &= k x_1 - \gamma_p x_2 - b_x x_2 + b_w w \\
\dot{z}_1 &= \mu - \eta z_1 z_2 - \gamma_c z_1 \\
\dot{z}_2 &= \theta_2 x_2 - \eta z_1 z_2 - \gamma_c z_2 \\
\dot{w} &= b_x x_2 - b_w w - \gamma_c w.
\end{aligned} \tag{S26}$$

where the buffer w is not assumed to rapidly reach equilbrium. The steady state for (S26) is identical to the rapid case in SI3.1 if we replace γ_x by γ_c. The linearisation is

$$\begin{aligned}
\Delta\dot{x}_1 &= \theta_1 \Delta z_1 - \gamma_p \Delta x_1 \\
\Delta\dot{x}_2 &= k\Delta x_1 - \gamma_p \Delta x_2 - b_x \Delta x_2 + b_w \Delta w \\
\Delta\dot{z}_1 &= -\eta \bar{z}_2 \Delta z_1 - \eta \bar{z}_1 \Delta z_2 - \gamma_c \Delta z_1 \\
\Delta\dot{z}_2 &= \theta_2 \Delta x_2 - \eta \bar{z}_2 \Delta z_1 - \eta \bar{z}_1 \Delta z_2 - \gamma_c \Delta z_2 \\
\Delta\dot{w} &= b_x \Delta x_2 - (b_w + \gamma_c)\Delta w.
\end{aligned}$$

bioRxiv preprint doi: https://doi.org/10.1101/2021.04.18.440372; this version posted September 29, 2021. The copyright holder for this preprint (which was not certified by peer review) is the author/funder, who has granted bioRxiv a license to display the preprint in perpetuity. It is made available under aCC-BY-NC-ND 4.0 International license.

From SI3.1, the steady states are

$$
\begin{aligned}
z_1 &= \frac{\gamma_p}{\theta_1} x_1 = \frac{\gamma_p^2}{\theta_1 k}\left(1 + B_x \frac{\gamma_c}{\gamma_p}\right) x_2 = \frac{\theta_2}{\alpha}\left(1 + B_x \frac{\gamma_c}{\gamma_p}\right) x_2 \\
z_2 &= \frac{1}{\eta}\left(\frac{\mu}{z_1} - \gamma_c\right) \\
x_2 &= \frac{\mu}{\theta_2} \frac{1}{1 + \frac{\gamma_c}{\alpha}\left(1 + B_x \frac{\gamma_c}{\gamma_p}\right)}
\end{aligned}
$$

where

$$
\alpha = \frac{\theta_1 \theta_2 k}{\gamma_p^2}, \quad \beta = \eta\mu, \quad B_x = \frac{b_x}{b_w + \gamma_c}.
$$

This system can be rewritten

$$
\begin{aligned}
\Delta\dot{x}_1 &= \theta_1 \Delta z_1 - \gamma_p \Delta x_1 \\
\Delta\dot{x}_2 &= k\Delta x_1 - \gamma_p \Delta x_2 - b_x \Delta x_2 + b_w \Delta w \\
\Delta\dot{w} &= b_x \Delta x_2 - (b_w + \gamma_c)\Delta w \\
\Delta\dot{z}_1 &= -\left(\frac{\alpha}{\left(1 + B_x \frac{\gamma_c}{\gamma_p}\right)} + \gamma_c\right)\Delta z_1 - \frac{\beta\left(1 + B_x \frac{\gamma_c}{\gamma_p}\right)}{\alpha + \gamma_c\left(1 + B_x \frac{\gamma_c}{\gamma_p}\right)}\Delta z_2 \\
\Delta\dot{z}_2 &= \theta_2 \Delta x_2 - \frac{\alpha}{\left(1 + B_x \frac{\gamma_c}{\gamma_p}\right)}\Delta z_1 - \left(\frac{\beta\left(1 + B_x \frac{\gamma_c}{\gamma_p}\right)}{\alpha + \gamma_c\left(1 + B_x \frac{\gamma_c}{\gamma_p}\right)} + \gamma_c\right)\Delta z_2.
\end{aligned}
$$

Taking the Laplace transform of $\Delta\dot{w} = b_x \Delta x_2 - (b_w + \gamma_c)\Delta w$, we have

$$
W = \frac{b_x}{s + b_w + \gamma_c} X_2
$$

where W and Z_1 are the Laplace transforms of w and x_2. We have

$$
\begin{aligned}
-b_x X_2 + b_w W &= -b_x X_2 + b_w \frac{b_x}{s + b_w + \gamma_c} X_2 \\
&= -B_x \frac{s + \gamma_c}{1 + \frac{s}{b_w + \gamma_c}} X_2 \\
&= -C_b(s) X_2
\end{aligned}
$$

where

$$
C_b = B_x \frac{s + \gamma_c}{1 + \frac{s}{\hat{b}_w}}, \quad \hat{b}_w = b_w + \gamma_c.
$$

Taking the Laplace transforms, we have

$$
\begin{aligned}
(s + \gamma_p) X_1 &= \theta_1 Z_1 \\
(s + \gamma_p + C_b) X_2 &= k X_1 \\
\left(s + \frac{\alpha}{\left(1 + B_x \frac{\gamma_c}{\gamma_p}\right)} + \gamma_c\right) Z_1 &= -\frac{\beta\left(1 + B_x \frac{\gamma_c}{\gamma_p}\right)}{\alpha + \gamma_c\left(1 + B_x \frac{\gamma_c}{\gamma_p}\right)} Z_2 \\
\left(s + \frac{\beta\left(1 + B_x \frac{\gamma_c}{\gamma_p}\right)}{\alpha + \gamma_c\left(1 + B_x \frac{\gamma_c}{\gamma_p}\right)} + \gamma_c\right) Z_2 &= \theta_2 X_2 - \frac{\alpha}{\left(1 + B_x \frac{\gamma_c}{\gamma_p}\right)} Z_1
\end{aligned}
$$

bioRxiv preprint doi: https://doi.org/10.1101/2021.04.18.440372; this version posted September 29, 2021. The copyright holder for this preprint (which was not certified by peer review) is the author/funder, who has granted bioRxiv a license to display the preprint in perpetuity. It is made available under aCC-BY-NC-ND 4.0 International license.

where X_1, X_1, Z_1 andZ_2 are the Laplace transforms of $\Delta x_1, \Delta x_2, \Delta z_1$ andΔz_2. Substituting, we have

$$(s+\gamma_p)(s+\gamma_p+C_b)X_2 = \theta_1 k Z_1$$
$$\left(s+\frac{\alpha}{\left(1+B_x\frac{\gamma_c}{\gamma_p}\right)}+\gamma_c\right)\left(s+\frac{\beta\left(1+B_x\frac{\gamma_c}{\gamma_p}\right)}{\alpha+\gamma_c\left(1+B_x\frac{\gamma_c}{\gamma_p}\right)}+\gamma_c\right)Z_1$$
$$=-\frac{\beta\left(1+B_x\frac{\gamma_c}{\gamma_p}\right)}{\alpha+\gamma_c\left(1+B_x\frac{\gamma_c}{\gamma_p}\right)}\left(\theta_2 X_2-\frac{\alpha}{\left(1+B_x\frac{\gamma_c}{\gamma_p}\right)}Z_1\right).$$

Rewriting and substituting, we have

$$(s+\gamma_p)(s+\gamma_p+C_b)(s+\gamma_c)\left(s+\frac{\alpha}{\left(1+B_x\frac{\gamma_c}{\gamma_p}\right)}+\frac{\beta\left(1+B_x\frac{\gamma_c}{\gamma_p}\right)}{\alpha+\gamma_c\left(1+B_x\frac{\gamma_c}{\gamma_p}\right)}+\gamma_c\right)X_2=-\beta\gamma_p^2\frac{\alpha\left(1+B_x\frac{\gamma_c}{\gamma_p}\right)}{\alpha+\gamma_c\left(1+B_x\frac{\gamma_c}{\gamma_p}\right)}X_2.$$

Simplifying and taking the limit of strong binding of the sequestration mechanism in antithetic integral feedback

$$\beta \gg \frac{\left(\alpha+\gamma_c\left(1+B_x\frac{\gamma_c}{\gamma_p}\right)\right)^2}{\left(1+B_x\frac{\gamma_c}{\gamma_p}\right)^2}, \frac{(\alpha+\gamma_c(1+B_x\frac{\gamma_c}{\gamma_p}))\gamma_p}{\left(1+B_x\frac{\gamma_c}{\gamma_p}\right)}$$

then

$$(s+\gamma_p)(s+\gamma_p+C_b)(s+\gamma_c)\left(s+\frac{\beta\left(1+B_x\frac{\gamma_c}{\gamma_p}\right)}{\alpha+\gamma_c\left(1+B_x\frac{\gamma_c}{\gamma_p}\right)}\right)X_2=-\beta\gamma_p^2\frac{\alpha\left(1+B_x\frac{\gamma_c}{\gamma_p}\right)}{\alpha+\gamma_c\left(1+B_x\frac{\gamma_c}{\gamma_p}\right)}X_2.$$

Rewriting C_b, we have

$$(s+\gamma_p)\left(s+\gamma_p+B_x\frac{s+\gamma_c}{1+\frac{s}{\hat{b}_w}}\right)(s+\gamma_c)\left(s+\frac{\beta\left(1+B_x\frac{\gamma_c}{\gamma_p}\right)}{\alpha+\gamma_c\left(1+B_x\frac{\gamma_c}{\gamma_p}\right)}\right)X_2=-\beta\gamma_p^2\frac{\alpha\left(1+B_x\frac{\gamma_c}{\gamma_p}\right)}{\alpha+\gamma_c\left(1+B_x\frac{\gamma_c}{\gamma_p}\right)}X_2.$$

and so we have the characteristic equation

$$(s+\gamma_p)\left((s+\gamma_p)\left(1+\frac{s}{\hat{b}_w}\right)+B_x(s+\gamma_c)\right)(s+\gamma_c)\left(s+\frac{\beta\left(1+B_x\frac{\gamma_c}{\gamma_p}\right)}{\alpha+\gamma_c\left(1+B_x\frac{\gamma_c}{\gamma_p}\right)}\right)$$
$$=-\beta\gamma_p^2\frac{\alpha\left(1+B_x\frac{\gamma_c}{\gamma_p}\right)}{\alpha+\gamma_c\left(1+B_x\frac{\gamma_c}{\gamma_p}\right)}\left(1+\frac{s}{\hat{b}_w}\right).$$

Substituting $s = i\omega\gamma_p$, we have

$$(1+i\omega)\left(1+B_x\frac{\gamma_c}{\gamma_p}-\frac{\gamma_p}{\hat{b}_w}\omega^2+i\omega\left(1+B_x+\frac{\gamma_p}{\hat{b}_w}\right)\right)\left(i\omega+\frac{\gamma_c}{\gamma_p}\right)\left(i\omega+\frac{\beta\left(1+B_x\frac{\gamma_c}{\gamma_p}\right)}{\gamma_p\left(\alpha+\gamma_c\left(1+B_x\frac{\gamma_c}{\gamma_p}\right)\right)}\right)$$
$$=-\frac{\beta}{\gamma_p^2}\frac{\alpha\left(1+B_x\frac{\gamma_c}{\gamma_p}\right)}{\left(\alpha+\gamma_c\left(1+B_x\frac{\gamma_c}{\gamma_p}\right)\right)}\left(1+i\omega\frac{\gamma_p}{\hat{b}_w}\right).$$

Taking the strong antithetic binding limit where $|i\omega| \ll \frac{\beta\left(1+B_x\frac{\gamma_c}{\gamma_p}\right)}{\gamma_p\left(\alpha+\gamma_c\left(1+B_x\frac{\gamma_c}{\gamma_p}\right)\right)}$, we have

$$\left(1+B_x\frac{\gamma_c}{\gamma_p}-\frac{\gamma_p}{\hat{b}_w}\omega^2+i\omega\left(1+B_x+\frac{\gamma_p}{\hat{b}_w}\right)\right)(1+i\omega)\left(i\omega+\frac{\gamma_c}{\gamma_p}\right)=-\frac{\alpha}{\gamma_p}\left(1+i\omega\frac{\gamma_p}{\hat{b}_w}\right).$$

bioRxiv preprint doi: https://doi.org/10.1101/2021.04.18.440372; this version posted September 29, 2021. The copyright holder for this preprint (which was not certified by peer review) is the author/funder, who has granted bioRxiv a license to display the preprint in perpetuity. It is made available under aCC-BY-NC-ND 4.0 International license.

The magnitude constraint is

$$\left(\left(\left(1+B_x\frac{\gamma_c}{\gamma_p}-\frac{\gamma_p}{\hat{b}_w}\omega^2\right)^2+\omega^2\left(1+B_x+\frac{\gamma_p}{\hat{b}_w}\right)^2\right)^{0.5}(1+\omega^2)^{0.5}\left(\omega^2+\frac{\gamma_c^2}{\gamma_p^2}\right)^{0.5}=\frac{\alpha}{\gamma_p}\left(1+\frac{\gamma_p^2}{\hat{b}_w^2}\omega^2\right)^{0.5} \tag{S27}$$

and the phase constraint is

$$\tan^{-1}\left(\frac{\omega\left(1+B_x+\frac{\gamma_p}{\hat{b}_w}\right)}{1+B_x\frac{\gamma_c}{\gamma_p}-\frac{\gamma_p}{\hat{b}_w}\omega^2}\right)+\tan^{-1}(\omega)+\tan^{-1}\left(\frac{\gamma_p}{\gamma_c}\omega\right)=\tan^{-1}\left(\frac{\gamma_p}{\hat{b}_w}\omega\right)+\pi+2k\pi.$$

for some integer k. Rearranging, we have

$$\tan^{-1}\left(\frac{\omega\left(1+B_x+\frac{\gamma_p}{\hat{b}_w}\right)}{1+B_x\frac{\gamma_c}{\gamma_p}-\frac{\gamma_p}{\hat{b}_w}\omega^2}\right)=\tan^{-1}\left(\frac{\frac{\gamma_p}{\hat{b}_w}\omega\left(1-\frac{\gamma_p}{\gamma_c}\omega^2\right)-\left(1+\frac{\gamma_p}{\gamma_c}\right)\omega}{1-\frac{\gamma_p}{\gamma_c}\omega^2+\left(1+\frac{\gamma_p}{\gamma_c}\right)\frac{\gamma_p}{\hat{b}_w}\omega^2}\right)+\pi+2k\pi.$$

Taking the tangent of both sides and ignoring the trivial solution, we have

$$\frac{\left(1+B_x+\frac{\gamma_p}{\hat{b}_w}\right)}{1+B_x\frac{\gamma_c}{\gamma_p}-\frac{\gamma_p}{\hat{b}_w}\omega^2}=\frac{\frac{\gamma_p}{\hat{b}_w}\left(1-\frac{\gamma_p}{\gamma_c}\omega^2\right)-\left(1+\frac{\gamma_p}{\gamma_c}\right)}{1-\frac{\gamma_p}{\gamma_c}\omega^2+\left(1+\frac{\gamma_p}{\gamma_c}\right)\frac{\gamma_p}{\hat{b}_w}\omega^2}$$

Multiplying out fractions, we have

$$\left(1+B_x+\frac{\gamma_p}{\hat{b}_w}\right)\left(1-\frac{\gamma_p}{\gamma_c}\omega^2+\left(1+\frac{\gamma_p}{\gamma_c}\right)\frac{\gamma_p}{\hat{b}_w}\omega^2\right)=\left(\frac{\gamma_p}{\hat{b}_w}\left(1-\frac{\gamma_p}{\gamma_c}\omega^2\right)-\left(1+\frac{\gamma_p}{\gamma_c}\right)\right)\left(1+B_x\frac{\gamma_c}{\gamma_p}-\frac{\gamma_p}{\hat{b}_w}\omega^2\right).$$

Expanding, we have

$$\begin{aligned}&\left(1+B_x+\frac{\gamma_p}{\hat{b}_w}\right)+\left(1+B_x+\frac{\gamma_p}{\hat{b}_w}\right)\left(\frac{\gamma_p}{\hat{b}_w}+\frac{\gamma_p}{\gamma_c}\frac{\gamma_p}{\hat{b}_w}-\frac{\gamma_p}{\gamma_c}\right)\omega^2\\&=-\left(1+\frac{\gamma_p}{\gamma_c}-\frac{\gamma_p}{\hat{b}_w}\right)\left(1+B_x\frac{\gamma_c}{\gamma_p}\right)+\left(1+\frac{\gamma_p}{\gamma_c}-\frac{\gamma_p}{\hat{b}_w}\right)\frac{\gamma_p}{\hat{b}_w}\omega^2-\left(1+B_x\frac{\gamma_c}{\gamma_p}\right)\frac{\gamma_p}{\hat{b}_w}\frac{\gamma_p}{\gamma_c}\omega^2+\frac{\gamma_p^2}{\hat{b}_w^2}\frac{\gamma_p}{\gamma_c}\omega^4\end{aligned}$$

Simplifying, we have

$$-\frac{\gamma_p^2}{\hat{b}_w^2}\omega^4+\left[\left(1+B_x+\frac{\gamma_p}{\hat{b}_w}\right)\left(\frac{\gamma_c}{\hat{b}_w}+\frac{\gamma_p}{\hat{b}_w}-1\right)+\left(B_x-1+\frac{\gamma_p}{\hat{b}_w}\right)\frac{\gamma_c}{\hat{b}_w}\right]\omega^2+\left[2+2B_x+\frac{\gamma_p}{\gamma_c}+B_x\frac{\gamma_c}{\gamma_p}-B_x\frac{\gamma_c}{b_w}\right]\frac{\gamma_c}{\gamma_p}=0$$

Solving, we have

$$\begin{aligned}\omega^2&=\frac{\hat{b}_w^2}{2\gamma_p^2}\left[A+\sqrt{A^2+4\frac{\gamma_p^2}{\hat{b}_w^2}\frac{\gamma_c}{\gamma_p}\left[2+2B_x+\frac{\gamma_p}{\gamma_c}+B_x\frac{\gamma_c}{\gamma_p}-B_x\frac{\gamma_c}{b_w}\right]}\right]\\A&=\left[\left(1+B_x+\frac{\gamma_p}{\hat{b}_w}\right)\left(\frac{\gamma_c}{\hat{b}_w}+\frac{\gamma_p}{\hat{b}_w}-1\right)+\left(B_x-1+\frac{\gamma_p}{\hat{b}_w}\right)\frac{\gamma_c}{\hat{b}_w}\right]\end{aligned} \tag{S28}$$

Using the same approach as in previous sections, the magnitude constraint leads to the stability constraint

$$\gamma_p^3>\frac{\theta_1\theta_2k}{(1+\omega^2)^{0.5}\left(\omega^2+\frac{\gamma_c^2}{\gamma_p^2}\right)^{0.5}}\left(\frac{1+\frac{\gamma_p^2}{b_w^2}\omega^2}{\left(\left(1+B_x\frac{\gamma_c}{\gamma_p}-\frac{\gamma_p}{\hat{b}_w}\omega^2\right)^2+\omega^2\left(1+B_x+\frac{\gamma_p}{\hat{b}_w}\right)^2\right)}\right)^{0.5} \tag{S29}$$

using ω from (S28). This can be rewritten

$$\frac{\alpha}{\gamma_p}<(1+\omega^2)^{0.5}\left(\omega^2+\frac{\gamma_c^2}{\gamma_p^2}\right)^{0.5}\left(\frac{\left(\left(1+B_x\frac{\gamma_c}{\gamma_p}-\frac{\gamma_p}{\hat{b}_w}\omega^2\right)^2+\omega^2\left(1+B_x+\frac{\gamma_p}{\hat{b}_w}\right)^2\right)}{1+\frac{\gamma_p^2}{b_w^2}\omega^2}\right)^{0.5} \tag{S30}$$

bioRxiv preprint doi: https://doi.org/10.1101/2021.04.18.440372; this version posted September 29, 2021. The copyright holder for this preprint (which was not certified by peer review) is the author/funder, who has granted bioRxiv a license to display the preprint in perpetuity. It is made available under aCC-BY-NC-ND 4.0 International license.

From SI3.1, we have there steady state error

$$\frac{x_{2n} - x_2}{x_{2n}} = \frac{1}{1 + \Omega_x}.$$

where

$$\Omega_x = \frac{\alpha}{\gamma_c \left(1 + B_x \frac{\gamma_c}{\gamma_p}\right)}$$

and so the steady state error constraint is

$$\Omega_x < \frac{\gamma_p}{\gamma_c} \frac{(1+\omega^2)^{0.5}}{\left(1 + B_x \frac{\gamma_c}{\gamma_p}\right)} \left(\omega^2 + \frac{\gamma_c^2}{\gamma_p^2}\right)^{0.5} \left(\frac{\left((1 + B_x \frac{\gamma_c}{\gamma_p} - \frac{\gamma_p}{\hat{b}_w}\omega^2\right)^2 + \omega^2 \left(1 + B_x + \frac{\gamma_p}{\hat{b}_w}\right)^2}{1 + \frac{\gamma_p^2}{\hat{b}_w^2}\omega^2}\right)^{0.5}.$$

where ω is given in (S28).
If we set $\hat{b}_w = \gamma_p$ for simplicity then $\omega^2 = 1 + 2(1 + B_x)\frac{\gamma_c}{\gamma_p}$ and

$$\Omega_x < \frac{\gamma_p}{\gamma_c} \frac{2 + B_x}{1 + B_x \frac{\gamma_c}{\gamma_p}} \left(1 + \frac{\gamma_c^2}{\gamma_p^2} + 2(1 + B_x)\frac{\gamma_c}{\gamma_p}\right).$$

This equation can be rewritten

$$\Omega_x < \frac{\gamma_p}{\gamma_c} \frac{2 + B_x}{1 + B_x \frac{\gamma_c}{\gamma_p}} \left(\left(1 + \frac{\gamma_c}{\gamma_p}\right)^2 + 2B_x \frac{\gamma_c}{\gamma_p}\right).$$

SI3.3. Rapid x_1 Buffering with Degradation can enable near-perfect adaptation

In this section, we analyse the ability of buffering at x_1 to enable near perfect adaptation by stabilising antithetic integral feedback. This section uses identical methodology and obtains equivalent results to SI3.1.
Consider the model with x_1 buffering and dilution

$$\begin{aligned}
\dot{x}_1 &= \theta_1 z_1 - \gamma_p x_1 - b_i x_1 + b_w w_x \\
\dot{x}_2 &= k x_1 - \gamma_p x_2 \\
\dot{w}_x &= b_i x_1 - b_w w_x - \gamma_i w_x \\
\dot{z}_1 &= \mu - \eta z_1 z_2 \\
\dot{z}_2 &= \theta_2 x_2 - \eta z_1 z_2
\end{aligned}$$

where w_x is the buffering species of x_1, and b_i, b_w are the kinetic rates for the buffering reactions. Assuming rapid buffering and using the same methodology as previous sections, the reduced model is

$$\begin{aligned}
(1 + B_i)\dot{x}_1 &= \theta_1 z_1 - (\gamma_p + B_i \gamma_i) x_1 \\
\dot{x}_2 &= k x_1 - \gamma_p x_2 \\
\dot{z}_1 &= \mu - \eta z_1 z_2 - \gamma_c z_1 \\
\dot{z}_2 &= \theta_2 x_2 - \eta z_1 z_2 - \gamma_c z_2.
\end{aligned}$$

where $B_i = \frac{b_i}{b_w + \gamma_i}$ is the buffer equilibrium ratio.

SI3.3.a. Steady State Analysis

We next analyse the steady state of the system. We have

$$\dot{z}_1 - \dot{z}_2 = \mu - \theta_2 x_2 - \gamma_c z_1 + \gamma_c z_2$$

bioRxiv preprint doi: https://doi.org/10.1101/2021.04.18.440372; this version posted September 29, 2021. The copyright holder for this preprint (which was not certified by peer review) is the author/funder, who has granted bioRxiv a license to display the preprint in perpetuity. It is made available under aCC-BY-NC-ND 4.0 International license.

and so the steady state of the output is

$$x_2 = \frac{\mu}{\theta_2} - \frac{\gamma_c}{\theta_2} z_1 + \frac{\gamma_c}{\theta_2} z_2.$$

We also have the steady state

$$z_2 = \frac{1}{\eta}\left(\frac{\mu}{z_1} - \gamma_c\right)$$

and so

$$x_2 = \frac{\mu}{\theta_2} - \frac{\gamma_c^2}{\theta_2 \eta} - \frac{\gamma_c}{\theta_2} z_1 + \frac{\gamma_c \mu}{\theta_2 \eta}\frac{1}{z_1}.$$

Now at steady state we have

$$\begin{aligned} x_1 &= \frac{\gamma_p}{k} x_2 \\ z_1 &= \frac{\gamma_p}{\theta_1}\left(1 + B_i \frac{\gamma_i}{\gamma_p}\right) x_1 = \frac{\gamma_p^2}{\theta_1 k}\left(1 + B_i \frac{\gamma_i}{\gamma_p}\right) x_2 = \frac{\theta_2}{\alpha}\left(1 + B_i \frac{\gamma_i}{\gamma_p}\right) x_2 \end{aligned}$$

where $\alpha = \frac{\theta_1 \theta_2 k}{\gamma_p^2}$. Substituting, we have

$$\left(1 + \frac{\gamma_c}{\alpha}\left(1 + B_i \frac{\gamma_i}{\gamma_p}\right)\right) x_2^2 = \left(\frac{\mu}{\theta_2} - \frac{\gamma_c^2}{\theta_2 \eta}\right) x_2 + \frac{\gamma_c \mu \alpha}{\theta_2^2 \eta \left(1 + B_i \frac{\gamma_i}{\gamma_p}\right)}.$$

Assuming strong binding

$$\eta \gg \frac{\gamma_c^2}{\mu}, \frac{\gamma_c \mu \alpha}{\theta_2^2 \left(1 + B_i \frac{\gamma_i}{\gamma_p}\right)}$$

we have

$$\left(1 + \frac{\gamma_c}{\alpha}\left(1 + B_i \frac{\gamma_i}{\gamma_p}\right)\right) x_2^2 = \frac{\mu}{\theta_2} x_2$$

and so, ignoring the solution $x_1 = 0$, the steady state is

$$\begin{aligned} x_2 &= \frac{\mu}{\theta_2} \frac{1}{1 + \frac{\gamma_c}{\alpha}\left(1 + B_i \frac{\gamma_i}{\gamma_p}\right)} \\ x_1 &= \frac{\gamma_p}{k}\frac{\mu}{\theta_2} \frac{1}{1 + \frac{\gamma_c}{\alpha}\left(1 + B_i \frac{\gamma_i}{\gamma_p}\right)}, \quad z_1 = \frac{\mu\left(1 + B_i \frac{\gamma_i}{\gamma_p}\right)}{\alpha + \gamma_c\left(1 + B_i \frac{\gamma_i}{\gamma_p}\right)}, \quad z_2 = \frac{\alpha}{\eta\left(1 + B_i \frac{\gamma_i}{\gamma_p}\right)}. \end{aligned}$$

The steady state error of x_2 is

$$\frac{x_{2n} - x_2}{x_{2n}} = \frac{1}{1 + \frac{\alpha}{\gamma_c\left(1 + B_i \frac{\gamma_i}{\gamma_p}\right)}}.$$

SI3.3.b. Stability Analysis

We next study the stability of the system. If we linearise about the steady state, we have

$$\begin{aligned} (1 + B_i)\Delta \dot{x}_1 &= \theta_1 \Delta z_1 - \gamma_p\left(1 + B_i \frac{\gamma_i}{\gamma_p}\right)\Delta x_1 \\ \Delta \dot{x}_2 &= k \Delta x_1 - \gamma_p \Delta x_2 \\ \Delta \dot{z}_1 &= -\eta \bar{z}_2 \Delta z_1 - \eta \bar{z}_1 \Delta z_2 - \gamma_c \Delta z_1 \\ \Delta \dot{z}_2 &= \theta_2 \Delta x_2 - \eta \bar{z}_2 \Delta z_1 - \eta \bar{z}_1 \Delta z_2 - \gamma_c \Delta z_2. \end{aligned}$$

bioRxiv preprint doi: https://doi.org/10.1101/2021.04.18.440372; this version posted September 29, 2021. The copyright holder for this preprint (which was not certified by peer review) is the author/funder, who has granted bioRxiv a license to display the preprint in perpetuity. It is made available under aCC-BY-NC-ND 4.0 International license.

This system can be rewritten as

$$\begin{aligned}
\Delta\dot{x}_1 &= \theta_1\Delta z_1 - \gamma_p\Delta x_1 \\
(1+B_i)\Delta\dot{x}_2 &= k\Delta x_1 - \gamma_p\left(1+B_i\frac{\gamma_i}{\gamma_p}\right)\Delta x_2 \\
\Delta\dot{z}_1 &= -\left(\frac{\alpha}{\left(1+B_i\frac{\gamma_i}{\gamma_p}\right)}+\gamma_c\right)\Delta z_1 - \frac{\beta\left(1+B_i\frac{\gamma_i}{\gamma_p}\right)}{\alpha+\gamma_c\left(1+B_i\frac{\gamma_i}{\gamma_p}\right)}\Delta z_2 \\
\Delta\dot{z}_2 &= \theta_2\Delta x_2 - \frac{\alpha}{\left(1+B_i\frac{\gamma_i}{\gamma_p}\right)}\Delta z_1 - \left(\frac{\beta\left(1+B_i\frac{\gamma_i}{\gamma_p}\right)}{\alpha+\gamma_c\left(1+B_i\frac{\gamma_i}{\gamma_p}\right)}+\gamma_c\right)\Delta z_2.
\end{aligned}$$

where $\alpha = \frac{\theta_1\theta_2 k}{\gamma_p^2}$ and $\beta = \eta\mu$. Taking the Laplace transforms, we have

$$\begin{aligned}
&(1+B_i)\left(s+\frac{\gamma_p+B_i\gamma_i}{1+B_i}\right)X_1 = \theta_1 Z_1 \\
&(s+\gamma_p)X_2 = kX_1 \\
&\left(s+\frac{\alpha}{\left(1+B_i\frac{\gamma_i}{\gamma_p}\right)}+\gamma_c\right)Z_1 = -\frac{\beta\left(1+B_i\frac{\gamma_i}{\gamma_p}\right)}{\alpha+\gamma_c\left(1+B_i\frac{\gamma_i}{\gamma_p}\right)}Z_2 \\
&\left(s+\frac{\beta\left(1+B_i\frac{\gamma_i}{\gamma_p}\right)}{\alpha+\gamma_c\left(1+B_i\frac{\gamma_i}{\gamma_p}\right)}+\gamma_c\right)Z_2 = \theta_2 X_2 - \frac{\alpha}{\left(1+B_i\frac{\gamma_i}{\gamma_p}\right)}Z_1.
\end{aligned}$$

where X_1, X_2, Z_1 and Z_2 are the Laplace transforms for $\Delta x_1, \Delta x_2, \Delta z_1$ and Δz_2. Substituting, we have

$$\begin{aligned}
&(1+B_i)(s+\gamma_p)\left(s+\frac{\gamma_p+B_i\gamma_i}{1+B_i}\right)X_2 = \theta_1 k Z_1 \\
&\left(s+\frac{\alpha}{\left(1+B_i\frac{\gamma_i}{\gamma_p}\right)}+\gamma_c\right)\left(s+\frac{\beta\left(1+B_i\frac{\gamma_i}{\gamma_p}\right)}{\alpha+\gamma_c\left(1+B_i\frac{\gamma_i}{\gamma_p}\right)}+\gamma_c\right)Z_1 \\
&= -\frac{\beta\left(1+B_i\frac{\gamma_i}{\gamma_p}\right)}{\alpha+\gamma_c\left(1+B_i\frac{\gamma_i}{\gamma_p}\right)}\left(\theta_2 X_2 - \frac{\alpha}{\left(1+B_i\frac{\gamma_i}{\gamma_p}\right)}Z_1\right).
\end{aligned}$$

Rewriting and substituting, we have

$$\begin{aligned}
&(1+B_i)(s+\gamma_p)\left(s+\frac{\gamma_p+B_i\gamma_i}{1+B_i}\right)\left[(s+\gamma_c)\left(s+\frac{\alpha}{\left(1+B_i\frac{\gamma_i}{\gamma_p}\right)}+\frac{\beta\left(1+B_i\frac{\gamma_i}{\gamma_p}\right)}{\alpha+\gamma_c\left(1+B_i\frac{\gamma_i}{\gamma_p}\right)}+\gamma_c\right)\right]X_2 \\
&= -\frac{\beta\left(1+B_i\frac{\gamma_i}{\gamma_p}\right)}{\alpha+\gamma_c\left(1+B_i\frac{\gamma_i}{\gamma_p}\right)}\theta_1\theta_2 k X_2
\end{aligned}$$

The above equation is equivalent to that for x_2 buffering (see SI3.1), and so for strong integral binding we have the equivalent stability constraint and steady state error

$$\begin{aligned}
\frac{x_{2n}-x_2}{x_{2n}} &= \frac{1}{1+\Omega_i} \\
\Omega_i &< \left(1+\frac{\gamma_c}{\gamma_p}\right)(1+A)\left(\frac{\gamma_p}{\gamma_c}+A^{-1}\right) \\
A &= \frac{1+\frac{\gamma_i}{\gamma_p}B_i}{1+B_i}.
\end{aligned}$$

bioRxiv preprint doi: https://doi.org/10.1101/2021.04.18.440372; this version posted September 29, 2021. The copyright holder for this preprint (which was not certified by peer review) is the author/funder, who has granted bioRxiv a license to display the preprint in perpetuity. It is made available under aCC-BY-NC-ND 4.0 International license.

SI3.4. Rapid z_1 Buffering with Degradation has a trade-off due to leaky integration

In this section, we analyse the trade-offs for rapid buffering at z_1 on stability and the steady state error from perfect adaptation. For buffering at z_1 with dilution, we use the model

$$\begin{aligned}
\dot{x}_1 &= \theta_1 z_1 - \gamma_p x_1 \\
\dot{x}_2 &= k x_1 - \gamma_p x - \gamma_p x_2 \\
\dot{z}_1 &= \mu - \eta z_1 z_2 - \gamma_c z_1 - b_z z_1 + b_w w \\
\dot{z}_2 &= \theta_2 x_2 - \eta z_1 z_2 - \gamma_c z_2 \\
\dot{w} &= b_z z_1 - b_w w - \gamma_c w
\end{aligned}$$

where x_2 is the output concentration being controlled, x_1 is another concentration in the process being controlled, and z_1 and z_2 represent the molecular species involved in the perfect adaptation mechanism. Assuming that the buffer is rapid then w is at quasi-steady state then

$$w = B_1 z_1 \quad B_1 = \frac{b_z}{b_w + \gamma_c}.$$

If $x_T = w + z_1$ is the slow variable then $x_T = (1 + B_1) z_1$. Thus $\dot{x}_T = (1 + B_1)\dot{z}_1$ and so

$$(1 + B_1)\dot{z}_1 = \mu - \eta z_1 z_2 - \gamma_c (1 + B_1) z_1.$$

Thus we have

$$\begin{aligned}
\dot{x}_1 &= \theta_1 z_1 - \gamma_p x_1 \\
\dot{x}_2 &= k x_1 - \gamma_p x_2 \\
(1 + B_1)\dot{z}_1 &= \mu - \eta z_1 z_2 - \gamma_c (1 + B_1) z_1 \\
\dot{z}_2 &= \theta_2 x_2 - \eta z_1 z_2 - \gamma_c z_2.
\end{aligned}$$

SI3.4.a. Steady State Analysis

We next determine the steady state and and any error from perfect adaptation. For the case of dilution, we have

$$(1 + B_1)\dot{z}_1 - \dot{z}_2 = \mu - \theta_2 x_2 - \gamma_c((1 + B_1) z_1 - z_2) = 0$$

resulting in

$$x_2 = \frac{\mu}{\theta_2} - \frac{\gamma_c}{\theta_2}(1 + B_1) z_1 + \frac{\gamma_c}{\theta_2} z_2.$$

We also have

$$z_2 = \frac{1}{\eta}\left(\frac{\mu}{z_1} - \gamma_c (1 + B_1)\right)$$

and so

$$x_2 = \frac{\mu}{\theta_2} - \frac{\gamma_c^2}{\theta_2 \eta}(1 + B_1) - \frac{\gamma_c}{\theta_2}(1 + B_1) z_1 + \frac{\gamma_c \mu}{\theta_2 \eta}\frac{1}{z_1}.$$

Now at steady state we have

$$\begin{aligned}
x_1 &= \frac{\gamma_p}{k} x_2 \\
z_1 &= \frac{\gamma_p}{\theta_1} x_1 = \frac{\gamma_p^2}{\theta_1 k} x_2 = \frac{\theta_2}{\alpha} x_2.
\end{aligned}$$

bioRxiv preprint doi: https://doi.org/10.1101/2021.04.18.440372; this version posted September 29, 2021. The copyright holder for this preprint (which was not certified by peer review) is the author/funder, who has granted bioRxiv a license to display the preprint in perpetuity. It is made available under aCC-BY-NC-ND 4.0 International license.

where $\alpha = \frac{\theta_1\theta_2 k}{\gamma_p^2}$. Substituting, we have

$$\left(1 + \frac{\gamma_c}{\alpha}(1+B_1)\right) x_2^2 = \left(\frac{\mu}{\theta_2} - \frac{\gamma_c^2}{\theta_2\eta}(1+B_1)\right) x_2 + \frac{\gamma_c\mu\alpha}{\theta_2^2\eta}.$$

Assuming strong binding of the sequestration mechanism

$$\eta \gg \frac{\gamma_c^2(1+B_1)}{\mu}, \frac{\gamma_c\mu\alpha}{\theta_2^2}$$

we have

$$\left(1 + \frac{\gamma_c}{\alpha}(1+B_1)\right) x_2^2 = \frac{\mu}{\theta_2} x_2$$

and so, ignoring the zero solution, the steady state is

$$\boxed{x_2 = \frac{\mu}{\theta_2}\frac{1}{1+\frac{\gamma_c}{\alpha}(1+B_1)}} \tag{S31}$$

$$x_1 = \frac{\gamma_p}{k}\frac{\mu}{\theta_2}\frac{1}{1+\frac{\gamma_c}{\alpha}(1+B_1)}, \quad z_1 = \frac{\mu}{\alpha+\gamma_c(1+B_1)}, \quad z_2 = \frac{\alpha}{\eta}. \tag{S32}$$

The steady state error of x_2 is

$$\boxed{\frac{x_{2n} - x_2}{x_{2n}} = \frac{1}{1+\Omega_1}, \quad \Omega_1 = \frac{\alpha}{\gamma_c(1+B_1)}}.$$

We can see that increasing B_1 increases the steady state error of x_2 when there is degradation/dilution of z_1 and z_2.

SI3.4.b. Stability Analysis

We next study the stability of the system with degradation. If we linearise about the steady states, we have

$$\begin{aligned}
\Delta\dot{x}_1 &= \theta_1\Delta z_1 - \gamma_p\Delta x_1 \\
\Delta\dot{x}_2 &= k\Delta x_1 - \gamma_p\Delta x_2 \\
(1+B_1)\Delta\dot{z}_1 &= -\eta\bar{z}_2\Delta z_1 - \eta\bar{z}_1\Delta z_2 - \gamma_c(1+B_1)\Delta z_1 \\
\Delta\dot{z}_2 &= \theta_2\Delta x_2 - \eta\bar{z}_2\Delta z_1 - \eta\bar{z}_1\Delta z_2 - \gamma_c\Delta z_2.
\end{aligned}$$

This system can be rewritten as

$$\begin{aligned}
\Delta\dot{x}_1 &= \theta_1\Delta z_1 - \gamma_p\Delta x_1 \\
\Delta\dot{x}_2 &= k\Delta x_1 - \gamma_p\Delta x_2 \\
(1+B_1)\Delta\dot{z}_1 &= -(\alpha+\gamma_c(1+B_1))\Delta z_1 - \frac{\beta}{\alpha+\gamma_c(1+B_1)}\Delta z_2 \\
\Delta\dot{z}_2 &= \theta_2\Delta x_2 - \alpha\Delta z_1 - \left(\frac{\beta}{\alpha+\gamma_c(1+B_1)} + \gamma_c\right)\Delta z_2
\end{aligned}$$

where

$$\alpha = \frac{\theta_1\theta_2 k}{\gamma_p^2}, \quad \beta = \eta\mu.$$

bioRxiv preprint doi: https://doi.org/10.1101/2021.04.18.440372; this version posted September 29, 2021. The copyright holder for this preprint (which was not certified by peer review) is the author/funder, who has granted bioRxiv a license to display the preprint in perpetuity. It is made available under aCC-BY-NC-ND 4.0 International license.

Taking the Laplace transforms, we have

$$
\begin{aligned}
&(s+\gamma_p)X_1 = \theta_1 Z_1 \\
&(s+\gamma_p)X_2 = kX_1 \\
&((1+B_1)s+\alpha+\gamma_c(1+B_1))Z_1 = -\frac{\beta}{\alpha+\gamma_c(1+B_1)}Z_2 \\
&\left(s+\frac{\beta}{\alpha+\gamma_c(1+B_1)}+\gamma_c\right)Z_2 = \theta_2 X_2 - \alpha Z_1.
\end{aligned}
$$

where X_1, X_2, Z_1 and Z_2 are the laplace transforms for $\Delta x_1, \Delta x_2, \Delta z_1$ and Δz_2. Substituting, we have

$$
\begin{aligned}
&(s+\gamma_p)^2 X_2 = \theta_1 k Z_1 \\
&((1+B_1)s+\alpha+\gamma_c(1+B_1))\left(s+\frac{\beta}{\alpha+\gamma_c(1+B_1)}+\gamma_c\right)Z_1 \\
&= -\frac{\beta}{\alpha+\gamma_c(1+B_1)}(\theta_2 X_2 - \alpha Z_1).
\end{aligned}
$$

Rewriting and substituting, we have

$$
\begin{aligned}
&(s+\gamma_p)^2\left[(s+\gamma_c)\left((1+B_1)s+\alpha+\frac{\beta(1+B_1)}{\alpha+\gamma_c(1+B_1)}+\gamma_c(1+B_1)\right)\right]X_2 \\
&= -\frac{\beta}{\alpha+\gamma_c(1+B_1)}\theta_1\theta_2 k X_2.
\end{aligned}
$$

Taking the limit of strong binding $\left(\beta \gg \max\left\{\frac{(\alpha+\gamma_c(1+B_1))^2}{1+B_1}, \frac{\gamma_p(\alpha+\gamma_c(1+B_1))}{1+B_1}\right\}\right)$ then

$$
(1+B_1)(s+\gamma_p)^2(s+\gamma_c)\left(s+\frac{\beta}{\alpha+\gamma_c(1+B_1)}\right)X_2 = -\frac{\beta}{\alpha+\gamma_c(1+B_1)}\theta_1\theta_2 k X_2.
$$

Thus we have the characteristic equation

$$
(s+\gamma_p)^2(s+\gamma_c)\left(s+\frac{\beta}{\alpha+\gamma_c(1+B_1)}\right)+\frac{\beta\gamma_p^2}{(1+B_1)}\frac{\alpha}{\alpha+\gamma_c(1+B_1)} = 0.
$$

Substituting $s = \gamma_p\sigma$, we have

$$
(1+\sigma)^2\left(\sigma+\frac{\gamma_c}{\gamma_p}\right)\left(\sigma+\frac{\beta}{\gamma_p(\alpha+\gamma_c(1+B_1))}\right) = -\frac{\beta}{\gamma_p^2(1+B_1)}\frac{\alpha}{\alpha+\gamma_c(1+B_1)}.
$$

Using the same argument as above, for the stability boundary with strong binding there is a negative real and complex pair of roots in the region $|\sigma| \ll \frac{\beta}{\gamma_p(\alpha+\gamma_c(1+B_1))}$, as well as one large negative root.
To determine the boundary of stability, we next determine the conditions for which the roots are purely imaginary. Substituting $s = i\omega\gamma_p$, we have

$$
(1+i\omega)^2\left(i\omega+\frac{\gamma_c}{\gamma_p}\right)\left(i\omega+\frac{\beta}{\gamma_p(\alpha+\gamma_c(1+B_1))}\right) = -\frac{\beta}{\gamma_p^2(1+B_1)}\frac{\alpha}{\alpha+\gamma_c(1+B_1)}.
$$

Taking the strong antithetic binding limit where $|i\omega| \ll \frac{\beta}{\gamma_p(\alpha+\gamma_c(1+B_1))}$, we have

$$
(1+i\omega)^2\left(i\omega+\frac{\gamma_c}{\gamma_p}\right) = -\frac{\alpha}{\gamma_p(1+B_1)}.
$$

The phase and magnitude constraints are

$$
\begin{aligned}
&(1+\omega^2)\left(\omega^2+\frac{\gamma_c^2}{\gamma_p^2}\right)^{0.5} = \frac{\alpha}{\gamma_p(1+B_1)} \\
&2\tan^{-1}(\omega)+\tan^{-1}\left(\frac{\gamma_p}{\gamma_c}\omega\right) = \pi + 2k\pi.
\end{aligned}
$$

bioRxiv preprint doi: https://doi.org/10.1101/2021.04.18.440372; this version posted September 29, 2021. The copyright holder for this preprint (which was not certified by peer review) is the author/funder, who has granted bioRxiv a license to display the preprint in perpetuity. It is made available under aCC-BY-NC-ND 4.0 International license.

for some integer k. Solving the phase constraint, we have

$$\tan^{-1}\left(\frac{2\omega + \frac{\gamma_p}{\gamma_c}\omega(1-\omega^2)}{1-\left(1+2\frac{\gamma_p}{\gamma_c}\right)\omega^2}\right) = \pi + 2k\pi.$$

For this, we require

$$2\omega + \frac{\gamma_p}{\gamma_c}\omega(1-\omega^2)$$

which reduces to

$$\omega = \sqrt{2\frac{\gamma_c}{\gamma_p}+1}.$$

Substituting into the magnitude equation, we have

$$\frac{\alpha}{\gamma_p(1+B_1)} = 2\left(1+\frac{\gamma_c}{\gamma_p}\right)^2.$$

As a consequence, the stability constraint is

$$\Omega_1 = \frac{\alpha}{\gamma_c(1+B_1)} < 2\frac{\gamma_p}{\gamma_c}\left(1+\frac{\gamma_c}{\gamma_p}\right)^2.$$

We can observe that increasing B_1 improves the stability constraint. However, the steady state error of x_2 is

$$\frac{x_{2n}-x_2}{x_{2n}} = \frac{1}{1+\Omega_1}$$
$$\Omega_1 = \frac{\alpha}{\gamma_c(1+B_1)}$$

$$\boxed{\Omega_1 < 2\frac{\gamma_p}{\gamma_c}\left(1+\frac{\gamma_c}{\gamma_p}\right)^2}$$

Thus there is a steady state error constraint that is independent of B_1, and so increasing B_1 does not enable the removal of leaky integration.

SI3.5. Non-Rapid z_1 Buffering can allow Near Perfect Adaptation

In this section, we analyse the ability of non-rapid buffering at z_1 to enable near perfect adaptation by stabilising antithetic integral feedback. We use the model

$$\begin{aligned}
\dot{x}_1 &= \theta_1 z_1 - \gamma_p x_1 \\
\dot{x}_2 &= k x_1 - \gamma_p x_2 \\
\dot{z}_1 &= \mu - \eta z_1 z_2 - \gamma_c z_1 - b_z z_1 + b_w w \\
\dot{z}_2 &= \theta_2 x_2 - \eta z_1 z_2 - \gamma_c z_2 \\
\dot{w} &= b_z z_1 - b_w w - \gamma_c w.
\end{aligned} \tag{S33}$$

where the buffer w is not assumed to rapidly reach equilibrium. The steady state for (S33) is identical to the rapid case in SI3.4. The linearisation is

$$\begin{aligned}
\Delta\dot{x}_1 &= \theta_1 \Delta z_1 - \gamma_p \Delta x_1 \\
\Delta\dot{x}_2 &= k\Delta x_1 - \gamma_p \Delta x_2 \\
\Delta\dot{z}_1 &= -\eta\bar{z}_2\Delta z_1 - \eta\bar{z}_1\Delta z_2 - \gamma_c\Delta z_1 - b_z\Delta z_1 + b_w\Delta w \\
\Delta\dot{z}_2 &= \theta_2\Delta x_2 - \eta\bar{z}_2\Delta z_1 - \eta\bar{z}_1\Delta z_2 - \gamma_c\Delta z_2 \\
\Delta\dot{w} &= b_z\Delta z_1 - (b_w+\gamma_c)\Delta w.
\end{aligned}$$

bioRxiv preprint doi: https://doi.org/10.1101/2021.04.18.440372; this version posted September 29, 2021. The copyright holder for this preprint (which was not certified by peer review) is the author/funder, who has granted bioRxiv a license to display the preprint in perpetuity. It is made available under aCC-BY-NC-ND 4.0 International license.

This system can be rewritten

$$\begin{aligned}
\Delta\dot{x}_1 &= \theta_1\Delta z_1 - \gamma_p\Delta x_1 \\
\Delta\dot{x}_2 &= k\Delta x_1 - \gamma_p\Delta x_2 \\
\Delta\dot{z}_1 &= -(\alpha+\gamma_c)\Delta z_1 - \frac{\beta}{\alpha+\gamma_c(1+B_1)}\Delta z_2 - b_z\Delta z_1 + b_w\Delta w \\
\Delta\dot{z}_2 &= \theta_2\Delta x_2 - \alpha\Delta z_1 - \left(\frac{\beta}{\alpha+\gamma_c(1+B_1)} + \gamma_c\right)\Delta z_2 \\
\Delta\dot{w} &= b_z\Delta z_1 - (b_w+\gamma_c)\Delta w.
\end{aligned}$$

where

$$\alpha = \frac{\theta_1\theta_2 k}{\gamma_p^2}, \quad \beta = \eta\mu.$$

Taking the Laplace transform of $\Delta\dot{w} = b_z\Delta z_1 - (b_w+\gamma_c)\Delta w$, we have

$$W = \frac{b_z}{s+b_w+\gamma_c}Z_1$$

where W and Z_1 are the Laplace transforms of w and z_1. We have

$$\begin{aligned}
-b_zZ_1 + b_wW &= -b_zZ_1 + b_w\frac{b_z}{s+b_w+\gamma_c}Z_1 \\
&= -B_1\frac{s+\gamma_c}{1+\frac{s}{b_w+\gamma_c}}Z_1 \\
&= -C_b(s)Z_1
\end{aligned}$$

where

$$C_b = B_1\frac{s+\gamma_c}{1+\frac{s}{\hat{b}_w}}, \quad \hat{b}_w = b_w+\gamma_c.$$

Thus

$$\begin{aligned}
(s+\gamma_p)X_1 &= \theta_1 Z_1 \\
(s+\gamma_p)X_2 &= kX_1 \\
(s+\alpha+\gamma_c+C_b)Z_1 &= -\frac{\beta}{\alpha+\gamma_c(1+B_1)}Z_2 \\
\left(s+\frac{\beta}{\alpha+\gamma_c(1+B_1)}+\gamma_c\right)Z_2 &= \theta_2X_2 - \alpha Z_1.
\end{aligned}$$

Combining, we have

$$\begin{aligned}
&(s+\gamma_p)^2X_2 = \theta_1 kZ_1 \\
&(s+\alpha+\gamma_c+C_b)\left(s+\frac{\beta}{\alpha+\gamma_c(1+B_1)}+\gamma_c\right)Z_1 = -\frac{\beta}{\alpha+\gamma_c(1+B_1)}(\theta_2X_2-\alpha Z_1).
\end{aligned}$$

Simplifying, we have

$$\begin{aligned}
&\left[(s+\gamma_c)\left(s+\alpha+\frac{\beta}{\alpha+\gamma_c(1+B_1)}+\gamma_c\right) + C_b\left(s+\frac{\beta}{\alpha+\gamma_c(1+B_1)}+\gamma_c\right)\right]Z_1 \\
&= -\frac{\beta}{\alpha+\gamma_c(1+B_1)}\theta_2X_2.
\end{aligned}$$

Taking the strong antithetic binding limit of the sequestration mechanism ($\beta \gg \max\{(\alpha+\gamma_c)(\alpha+\gamma_c(1+B_1)), \gamma_p(\alpha+\gamma_c(1+B_1))\}$), we have

$$(s+\gamma_c+C_b)\left(s+\frac{\beta}{\alpha+\gamma_c(1+B_1)}\right)Z_1 = -\frac{\beta}{\alpha+\gamma_c(1+B_1)}\theta_2X_2$$

bioRxiv preprint doi: https://doi.org/10.1101/2021.04.18.440372; this version posted September 29, 2021. The copyright holder for this preprint (which was not certified by peer review) is the author/funder, who has granted bioRxiv a license to display the preprint in perpetuity. It is made available under aCC-BY-NC-ND 4.0 International license.

and so

$$(s+\gamma_p)^2\left[(s+\gamma_c+C_b)\left(s+\frac{\beta}{\alpha+\gamma_c(1+B_1)}\right)\right]X_2=-\beta\gamma_p^2\frac{\alpha}{\alpha+\gamma_c(1+B_1)}X_2.$$

Rewriting C_b, we have

$$\left[(s+\gamma_p)^2(s+\gamma_c)\frac{1+B_1+\frac{s}{\hat{b}_w}}{1+\frac{s}{\hat{b}_w}}\left(s+\frac{\beta}{\alpha+\gamma_c(1+B_1)}\right)+\beta\gamma_p^2\frac{\alpha}{\alpha+\gamma_c(1+B_1)}\right]X_2=0$$

or

$$\left[(s+\gamma_p)^2(s+\gamma_c)(1+B_1+\frac{s}{\hat{b}_w})\left(s+\frac{\beta}{\alpha+\gamma_c(1+B_1)}\right)+\beta\gamma_p^2\frac{\alpha(1+\frac{s}{\hat{b}_w})}{\alpha+\gamma_c(1+B_1)}\right]X_2=0.$$

Substituting $s=i\omega\gamma_p$, we have

$$(1+B_1+i\omega\frac{\gamma_p}{\hat{b}_w})(1+i\omega)^2\left(\frac{\gamma_c}{\gamma_p}+i\omega\right)\left(i\omega+\frac{\beta}{\gamma_p(\alpha+\gamma_c(1+B_1))}\right)+\frac{\beta}{\gamma_p^2}\frac{\alpha\left(1+i\omega\frac{\gamma_p}{\hat{b}_w}\right)}{\alpha+\gamma_c(1+B_1)}=0.$$

Taking the strong antithetic binding limit where $|i\omega|\ll\frac{\beta}{\gamma_p(\alpha+\gamma_c(1+B_1))}$, we have

$$\left(1+B_1+i\omega\frac{\gamma_p}{\hat{b}_w}\right)(1+i\omega)^2\left(\frac{\gamma_c}{\gamma_p}+i\omega\right)=-\frac{\alpha}{\gamma_p}\left(1+i\omega\frac{\gamma_p}{\hat{b}_w}\right).$$

The magnitude constraint is

$$(1+B_1)\left(1+\frac{\gamma_p^2}{\hat{b}_w^2}\frac{\omega^2}{(1+B_1)^2}\right)^{0.5}(1+\omega^2)\left(\frac{\gamma_c^2}{\gamma_p^2}+\omega^2\right)^{0.5}=\frac{\alpha}{\gamma_p}\left(1+\omega^2\frac{\gamma_p^2}{\hat{b}_w^2}\right)^{0.5} \tag{S34}$$

and the phase constraint is

$$2\tan^{-1}(\omega)+\tan^{-1}\left(\frac{\gamma_p}{\gamma_c}\omega\right)+\tan^{-1}\left(\frac{\gamma_p}{\hat{b}_w}\frac{1}{1+B_1}\omega\right)=\pi+\tan^{-1}\left(\frac{\gamma_p}{\hat{b}_w}\omega\right)+2k\pi.$$

for some integer k. Using trigonometric identities, we have

$$\tan^{-1}\left(\frac{2\omega+\frac{\gamma_p}{\gamma_c}\omega(1-\omega^2)}{1-\left(1+2\frac{\gamma_p}{\gamma_c}\right)\omega^2}\right)=\pi+2k\pi+\tan^{-1}\left(\frac{\frac{B_1}{1+B_1}\frac{\gamma_p}{\hat{b}_w}\omega}{1+\frac{1}{1+B_1}\frac{\gamma_p^2}{\hat{b}_w^2}\omega^2}\right).$$

This can be simplified to

$$\frac{2\omega+\frac{\gamma_p}{\gamma_c}\omega(1-\omega^2)}{1-\left(1+2\frac{\gamma_p}{\gamma_c}\right)\omega^2}=\frac{\frac{B_1}{1+B_1}\frac{\gamma_p}{\hat{b}_w}\omega}{1+\frac{1}{1+B_1}\frac{\gamma_p^2}{\hat{b}_w^2}\omega^2}.$$

Ignoring the trivial solution $\omega=0$, we have

$$\left(2+\frac{\gamma_p}{\gamma_c}-\frac{\gamma_p}{\gamma_c}\omega^2\right)\left(1+\frac{1}{1+B_1}\frac{\gamma_p^2}{\hat{b}_w^2}\omega^2\right)=\frac{B_1}{1+B_1}\frac{\gamma_p}{\hat{b}_w}\left(1-\left(1+2\frac{\gamma_p}{\gamma_c}\right)\omega^2\right).$$

Rewriting, we have

$$-\frac{1}{1+B_1}\frac{\gamma_p^2}{\hat{b}_w^2}\frac{\gamma_p}{\gamma_c}\omega^4+\left[-\frac{\gamma_p}{\gamma_c}+\left(2+\frac{\gamma_p}{\gamma_c}\right)\frac{1}{1+B_1}\frac{\gamma_p^2}{\hat{b}_w^2}+\frac{B_1}{1+B_1}\frac{\gamma_p}{\hat{b}_w}\left(1+2\frac{\gamma_p}{\gamma_c}\right)\right]\omega^2+\left(2+\frac{\gamma_p}{\gamma_c}\right)-\frac{B_1}{1+B_1}\frac{\gamma_p}{\hat{b}_w}=0.$$

bioRxiv preprint doi: https://doi.org/10.1101/2021.04.18.440372; this version posted September 29, 2021. The copyright holder for this preprint (which was not certified by peer review) is the author/funder, who has granted bioRxiv a license to display the preprint in perpetuity. It is made available under aCC-BY-NC-ND 4.0 International license.

Simplifying, we have

$$-\frac{\gamma_p^2}{\hat{b}_w^2}\omega^4 + \left[-(1+B_1) + \left(2\frac{\gamma_c}{\gamma_p}+1\right)\frac{\gamma_p^2}{\hat{b}_w^2} + B_1\frac{\gamma_p}{\hat{b}_w}\left(\frac{\gamma_c}{\gamma_p}+2\right)\right]\omega^2 + \left(2\frac{\gamma_c}{\gamma_p}+1\right)(1+B_1) - B_1\frac{\gamma_p}{\hat{b}_w}\frac{\gamma_c}{\gamma_p} = 0.$$

Solving, we have

$$\omega^2 = \frac{\hat{b}_w^2}{2\gamma_p^2}\left[A + \sqrt{A^2 + 4\frac{\gamma_p^2}{\hat{b}_w^2}\left(\left(2\frac{\gamma_c}{\gamma_p}+1\right)(1+B_1) - B_1\frac{\gamma_c}{\hat{b}_w}\right)}\right]$$
$$A = -(1+B_1) + \left(2\frac{\gamma_c}{\gamma_p}+1\right)\frac{\gamma_p^2}{\hat{b}_w^2} + B_1\frac{\gamma_p}{\hat{b}_w}\left(\frac{\gamma_c}{\gamma_p}+2\right).$$

From the magnitude constraint S34, we have the stability constraint

$$(1+B_1)\left(\frac{1+\frac{\gamma_p^2}{\hat{b}_w^2}\frac{\omega^2}{(1+B_1)^2}}{1+\omega^2\frac{\gamma_p^2}{\hat{b}_w^2}}\right)^{0.5}(1+\omega^2)\left(\frac{\gamma_c^2}{\gamma_p^2}+\omega^2\right)^{0.5} > \frac{\alpha}{\gamma_p} \tag{S35}$$

which can be rewritten in terms of steady state error $\Omega_1 = \frac{\alpha}{\gamma_c(1+B_1)}$ as

$$\Omega_1 < \frac{\gamma_p}{\gamma_c}(1+\omega^2)\left(\frac{\gamma_c^2}{\gamma_p^2}+\omega^2\right)^{0.5}\left(\frac{1+\frac{\gamma_p^2}{\hat{b}_w^2}\frac{\omega^2}{(1+B_1)^2}}{1+\omega^2\frac{\gamma_p^2}{\hat{b}_w^2}}\right)^{0.5}.$$

For $\hat{b}_w = \gamma_p$, we have

$$A = \left(1+\frac{\gamma_c}{\gamma_p}\right)B_1 + 2\frac{\gamma_c}{\gamma_p}.$$

$$\omega^2 = \left(1+\frac{\gamma_c}{\gamma_p}\right)B_1 + 1 + 2\frac{\gamma_c}{\gamma_p}$$

and the stability constraint

$$\Omega_1 < \frac{\gamma_p}{\gamma_c}\frac{(2+B_1)}{(1+B_1)}\left(1+B_1+\frac{\gamma_c}{\gamma_p}\right)\left(1+\frac{\gamma_c}{\gamma_p}\right).$$

SI4. CHARACTERISATION OF ANTITHETIC FEEDBACK WITH BUFFERING

In this section we characterise the feedback in the system with antithetic feedback and buffering of the control species z_1, z_2.

SI4.1. Characterisation with Rapid Buffering

We first characterise antithetic feedback with rapid buffering. We use the model

$$\begin{aligned}\dot{x}_1 &= \theta_1 z_1 - \gamma_p x_1\\ (1+B_x)\dot{x}_2 &= k x_1 - (\gamma_p + B_x\gamma_x)x_2\\ (1+B_1)\dot{z}_1 &= \mu - \eta z_1 z_2\\ (1+B_2)\dot{z}_2 &= \theta_2 x_2 - \eta z_1 z_2.\end{aligned} \tag{S36}$$

bioRxiv preprint doi: https://doi.org/10.1101/2021.04.18.440372; this version posted September 29, 2021. The copyright holder for this preprint (which was not certified by peer review) is the author/funder, who has granted bioRxiv a license to display the preprint in perpetuity. It is made available under aCC-BY-NC-ND 4.0 International license.

It can be observed that rapid buffers of the controller change the time-scale for z_1 and z_2. In integral feedback, the time-scale is inversely proportional to gain, and this relationship can be observed in the following characterisation of integral gain. We have

$$(1+B_1)\dot{z}_1(t) - (1+B_2)\dot{z}_2(t) = \mu - \theta_2 x_2.$$

Integrating, we have

$$(1+B_1)z_1(t) - (1+B_2)z_2(t) = \theta_2 \int_0^t \left(\frac{\mu}{\theta_2} - x_2(t')\right) dt'.$$

Rearranging, we can observe that the feedback control input u into the plant (i.e. (x_1, x_2) subsystem) is

$$u = \theta_1 z_1 = \underbrace{\frac{\theta_1\theta_2}{(1+B_1)}}_{\substack{\text{integral}\\ \text{feedback gain}}} \underbrace{\int_0^t \left(\frac{\mu}{\theta_2} - x_2(t')\right) dt'}_{\substack{\text{negative}\\ \text{integral feedback}}} + \underbrace{\frac{1+B_2}{1+B_1}\theta_1 z_2}_{\substack{\text{other}\\ \text{feedback}}}.$$

We can observe an integral feedback term and a second feedback term that is dependent upon z_2. The other feedback term becomes negligible and the integral term dominates the overall feedback if

$$\frac{1+B_2}{1+B_1}\theta_1 z_2 \ll \theta_1 z_1$$

which can occurs if $1+B_1$ is sufficiently large or if z_2 is sufficiently small. The latter can be achieved via large η, which drives z_2 to a much lower concentration than z_1. For this case

$$u = \theta_1 z_1 = \underbrace{\frac{\theta_1\theta_2}{(1+B_1)}}_{\substack{\text{integral}\\ \text{feedback gain}}} \underbrace{\int_0^t \left(\frac{\mu}{\theta_2} - x_2(t')\right) dt'}_{\substack{\text{negative}\\ \text{integral feedback}}}$$

where we can observe that the feedback gain is dependent on B_1.

SI4.2. Characterisation with Non-rapid z_1 Buffering

For the case of non-rapid z_1 buffering, we have

$$\begin{aligned}
\dot{x}_1 &= \theta_1 z_1 - \gamma_p x_1 \\
\dot{x}_2 &= k x_1 - (\gamma_p + B_x\gamma_x) x_2 \\
\dot{z}_1 &= \mu - \eta z_1 z_2 - b_z z_1 + b_w w \\
\dot{z}_2 &= \theta_2 x_2 - \eta z_1 z_2 \\
\dot{w} &= b_z z_1 - b_w w
\end{aligned} \tag{S37}$$

We have

$$\dot{z}_1(t) + \dot{w}(t) - \dot{z}_2(t) = \mu - \theta_2 x_2$$

where the integral is

$$z_1(t) + w(t) - z_2(t) = \theta_2 \int_0^t \left(\frac{\mu}{\theta_2} - x_2(t')\right) dt'$$

and so perfect adaptation occurs. Rearranging, we have the feedback

$$u = \theta_1 z_1 = -\theta_1 w(t) + \theta_1 z_2(t) + \theta_1\theta_2 \int_0^t \left(\frac{\mu}{\theta_2} - x_2(t')\right) dt'.$$

bioRxiv preprint doi: https://doi.org/10.1101/2021.04.18.440372; this version posted September 29, 2021. The copyright holder for this preprint (which was not certified by peer review) is the author/funder, who has granted bioRxiv a license to display the preprint in perpetuity. It is made available under aCC-BY-NC-ND 4.0 International license.

Taking Laplace transforms, we have

$$U = \theta_1 Z_1 = -\theta_1 W + \theta_1 Z_2 + \theta_1\theta_2 \frac{1}{s}\left(\frac{\mu}{\theta_2} - X_2\right)$$

where Z_1, W, Z_2, X_2 are the Laplace transforms of z_1, w, z_2, x_2. Taking the Laplace transforms of (S37), we also have

$$sW = b_z Z_1 - b_w W \tag{S38}$$

and so

$$W = \frac{b_z}{s + b_w} Z_1. \tag{S39}$$

Substituting, we have

$$\theta_1 Z_1 = -\theta_1 \frac{b_z}{s + b_w} Z_1 + \theta_1 Z_2 + \theta_1\theta_2 \frac{1}{s}\left(\frac{\mu}{\theta_2} - X_2\right)$$

and so the control input is

$$U = \theta_1 Z_1 = \theta_1 \frac{s + b_w}{s + b_z + b_w} Z_2 + \theta_1\theta_2 \frac{s + b_w}{s + b_z + b_w} \frac{1}{s}\left(\frac{\mu}{\theta_2} - X_2\right)$$

If Z_2 is small due to large η, then we have

$$U = \theta_1 Z_1 = \theta_1\theta_2 \frac{s + b_w}{s + b_z + b_w} \frac{1}{s}\left(\frac{\mu}{\theta_2} - X_2\right)$$

Thus for non-rapid buffering (small b_w) we are able to add a zero and pole and zero to the controller, where the zero is small than the pole. This result is equivalent to the integral controller in series with a lead controller, where the latter is know to help stabilise systems[1].
We can see the effect of non-rapid buffering on the integral component of feedback gain separately by determining the gain of the control input in the asymptote as $s \to 0$, where we have

$$\theta_1\theta_2 \frac{s + b_w}{s + b_z + b_w} \frac{1}{s} = \frac{\theta_1\theta_2}{1 + B_1} \frac{1}{s}.$$

Thus the integral component of feedback gain is $\frac{\theta_1\theta_2}{1+B_1}$, which is identical to the rapid case.

SI4.3. Bode Integral of Buffering and Antithetic Integral Feedback

Feedback is a highly effective method of robust regulation, but this mechanism is subject to fundamental limits. The Bode integral describes one of these fundamental limit, where improving the regulation at one frequency of a disturbance will worsen regulation of disturbances at other frequencies. Here, we show that topology 3 has the ability to reduce the fundamental limit on feedback and thus uniformly improve output regulation at all frequencies, while topology 1 does not. While we show the two state example from above to illustrate the concept, the Fourier transform description below is written generally as the Bode Integral holds for more general processes controlled by antithetic feedback and buffering.
We use the example model of the system

$$\begin{aligned}
\dot{x}_1 &= \theta_1 z_1 - \gamma_p x_1 \\
\dot{x}_2 &= k x_1 - \gamma_p x_2 - b_x w + b_x w_x \\
\dot{w}_x &= b_x x - b_w w_x - \gamma_x w \\
\dot{z}_1 &= \mu - \eta z_1 z_2 - \gamma_c z_1 - b_z z_1 + b_w w_1 \\
\dot{w}_1 &= b_z z_1 - b_w w_1 - \gamma_c w_1 \\
\dot{z}_2 &= \theta_2 x_2 - \eta z_1 z_2 - \gamma_c z_2.
\end{aligned}$$

bioRxiv preprint doi: https://doi.org/10.1101/2021.04.18.440372; this version posted September 29, 2021. The copyright holder for this preprint (which was not certified by peer review) is the author/funder, who has granted bioRxiv a license to display the preprint in perpetuity. It is made available under aCC-BY-NC-ND 4.0 International license.

We can write the linearised model in an open-loop form with the two states

$$\Delta\dot{x}_1 = \theta_1 u_h - \gamma_p \Delta x_1$$
$$\Delta\dot{x}_2 = k\Delta x_1 - \gamma_p \Delta x_2 + u_b$$

where $\Delta x_i = x_i - \bar{x}_i$ for $i = 1, 2$, $\bar{x}_i$ is the steady state of x_i for the closed loop system, u_h is the process input for antithetic integral feedback and u_b is the input for buffering at x_2. Buffering at z_1 and antithetic integral feedback act through the input u_a while buffering at x_2 acts through u_b.
If we take the Fourier transform, we can describe the open loop model in general terms by[3]

$$X_2 = G(i\omega)U_h + G_b(i\omega)U_b$$

where X_2, U_h, U_b are the Fourier transforms of x_2, u_h, u_b respectively, G is the transfer function from U_h to the output X_1 and G_b is the transfer function from U_h to X_1. With two control inputs we have the loop transfer function[3]

$$L(i\omega) = G(i\omega)C_h(i\omega) + G_b(i\omega)C_b(i\omega)$$

where C_h is the transfer function for the antithetic feedback controller (i.e. from X_2 to U_h) and C_b is the transfer function for the output buffer (i.e. from X_2 to U_b). The sensitivity function quantifies the improvement or worsening in regulation at each frequency for the 'closed-loop' system, where a smaller magnitude implies improved regulation, and can be described by

$$S(i\omega) = \frac{1}{1 + L(i\omega)}$$

In this case the sensitivity function incorporates the regulatory effect of both feedback and buffering[3].
The Bode integral is a fundamental constraint on the effectiveness of feedback in any system. It provides a constraint on the overall regulatory effectiveness in terms of the sensitivity function. If the system without feedback is stable then Bode's integral with output buffering (Topology 3) is[3]

$$\int_0^\infty \log\left(|S(i\omega)|\right) d\omega = -\frac{\pi}{2} b_x$$

where the integral of $S(i\omega)$ represents an overall measure of regulation and b_x is the kinetic rate of the forward buffering reaction. The integral of $S(i\omega)$ sums the effect of oscillating disturbances at different frequencies ω. Without buffering, if regulation is improved at one frequency of regulation, it worsens at other frequencies. However, increasing b_x reduces the whole integral. Thus buffering can uniformly improve regulation and thus improve the trade-off.
In contrast, control species buffering (Topology 1) is part of the feedback regulation mechanism using the same control input and so Bode's integral is[3]

$$\int_0^\infty \log\left(|S(i\omega)|\right) d\omega = 0.$$

Thus control buffering does not remove fundamental constraints, despite stabilising buffering. The tradeoff remains such that improving regulation at one frequency will worsen regulation of disturbances at other frequencies.

References

[1] K. J. Aström and R. M. Murray. *Feedback Systems*. Princeton University Press, 2008.
[2] J. A. M. Borghans, R. J. De Boer, and L.A. Segel. Extending the quasi-steady state approximation by changing variables. *Bull. Math. Biol.*, 58(1):43–63, 1996.
[3] E.J. Hancock and J.Ang. Frequency domain properties and fundamental limits of buffer–feedback regulation in biochemical systems. *Automatica*, 103:330–336, 2019.
[4] E.J. Hancock, J.Ang, A.Papachristodoulou, and G-B.Stan. The interplay between feedback and buffering in cellular homeostasis. *Cell Systems*, 5(5):498–508, 2017.
[5] N. Olsman, A-A. Baetica, F. Xiao, Y.P. Leong, R.M. Murray, and J.C. Doyle. Hard limits and performance tradeoffs in a class of antithetic integral feedback networks. *Cell Systems*, 9, 2019.